Lecture 2

Nominal or local design for fatigue assessment?

An introduction of local approaches

Contents of the lecture

Section 1: Neuber's procedure of fictitious notch rounding and recent developments

Section 2: Notch Stress Intensity Factors

Section 3: Strain Energy Density Approach

SECTION 1

Neuber's procedure of fictitious notch rounding and recent developments

Neuber's notch stress theory, starting situation

Situation in 1930 with regard to leight-weight designs:

- Problems with stress concentration in fatigue

Experimental methods:

- Brittle surface coatings (Maybach Comp. 1926)
- Photo-elastic models (Coker and Filon, 1931)

Theoretical solutions:

- Circular hole in tensile loaded infinite plate (Kirsch, 1898)
- Pointed wedge subjected to splitting force (Wieghardt 1907)
- Spherical hole in tensile loaded infinite body (Leon 1908)
- Elliptical hole in tensile loaded infinite plate (Inglis 1913)

Neuber's 'Three Function Approach' (1934) allowed application-relevant closed-form solutions for engineers:

- Neuber's book 'Theory of Notch Stresses' (1937)

Neuber's procedure of fictitious notch rounding

The averaged notch stresses $\bar{\sigma}$ at the real notch with radius ρ can directly be determined without an averaging procedure by analysing a substitute notch with fictitiously enlarged notch radius ρ_f :

$$\rho_f = \rho + s\rho^*$$

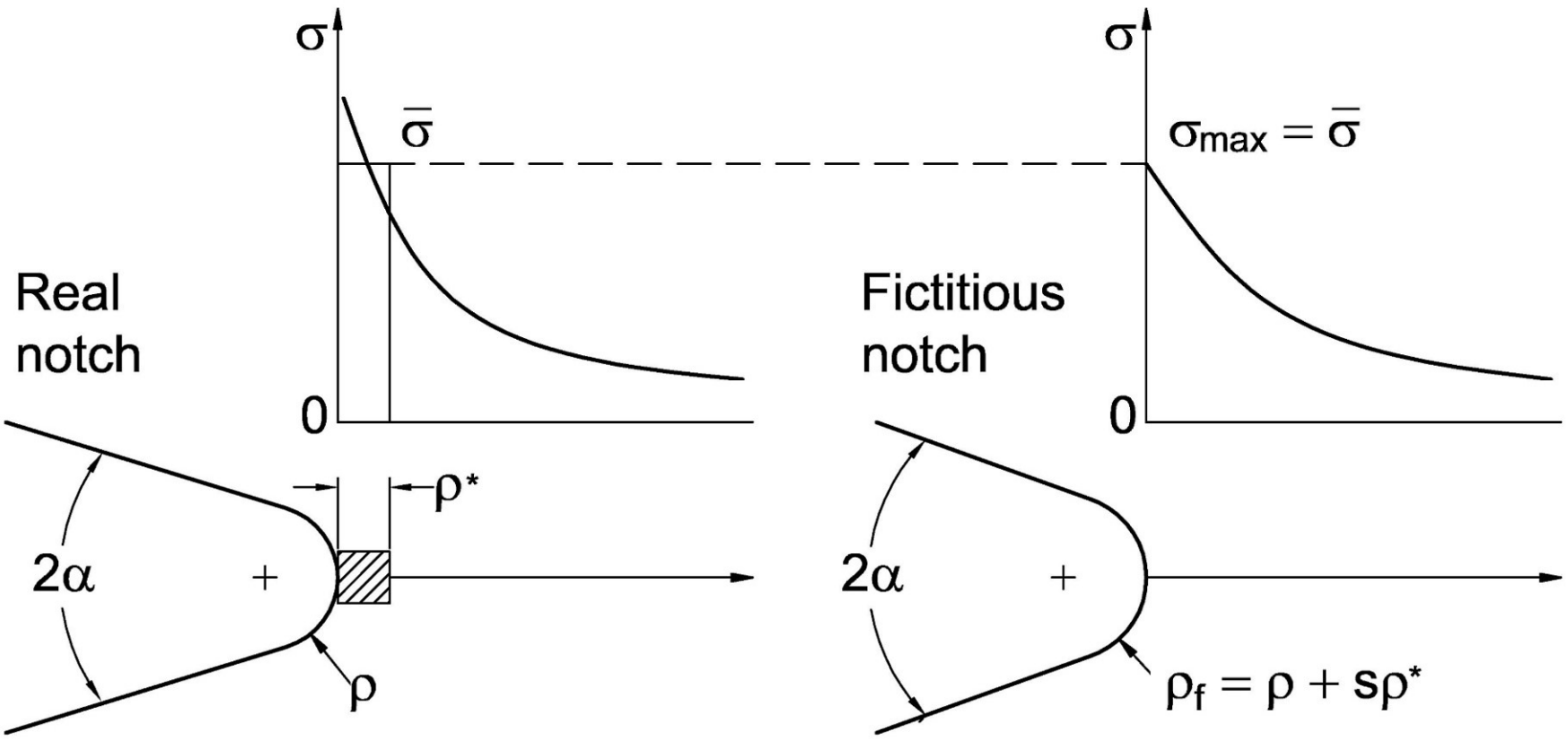

Neuber's notch stress theory, contents and results

Available notch stress field solutions:

- In-plane and bending loaded plates, prismatic and round bodies
- Elliptic, parabolic, hyperbolic and circular notch shapes
- Pointed, sharp and mild notches
- Tensile and transverse shear forces, bending and torsional moments

Stress concentration factors evaluated dependent on:

- Notch acuity $(t/\rho)^{1/2}$ or $(a/\rho)^{1/2}$
- Notch opening angle 2α
- Notch depth to cross-section width ratio t/a
- Microsupport length ρ^*
- Nonlinear stress-strain curve

Closed-form expressions and graphical aids for SCFs.

Neuber's concept of microsupport

The SCF under linear-elastic conditions rises with $1/\rho^{1/2}$ resulting in infinitely high notch stresses at pointed notch tips.

The considerable failure strength of such notches indicates (elastic) microsupport in cases of brittle fracture behaviour (inclusive of high-cycle fatigue) and (plastic) macrosupport in cases of ductile fracture behaviour.

Neuber's microsupport hypothesis considers stresses σ at the notch tip as failure-relevant which are averaged in the direction of crack propagation over a material-dependent particle size:

- Microsupport length $\rho^* \approx 0.1$ mm for steels and aluminium alloys

The particle size being small, the original notch stress field remains unchanged outside the averaging area at the notch tip.

The microsupport hypothesis also explains the geometrical size effect on the global strength of notched members.

Neuber's concept of microsupport

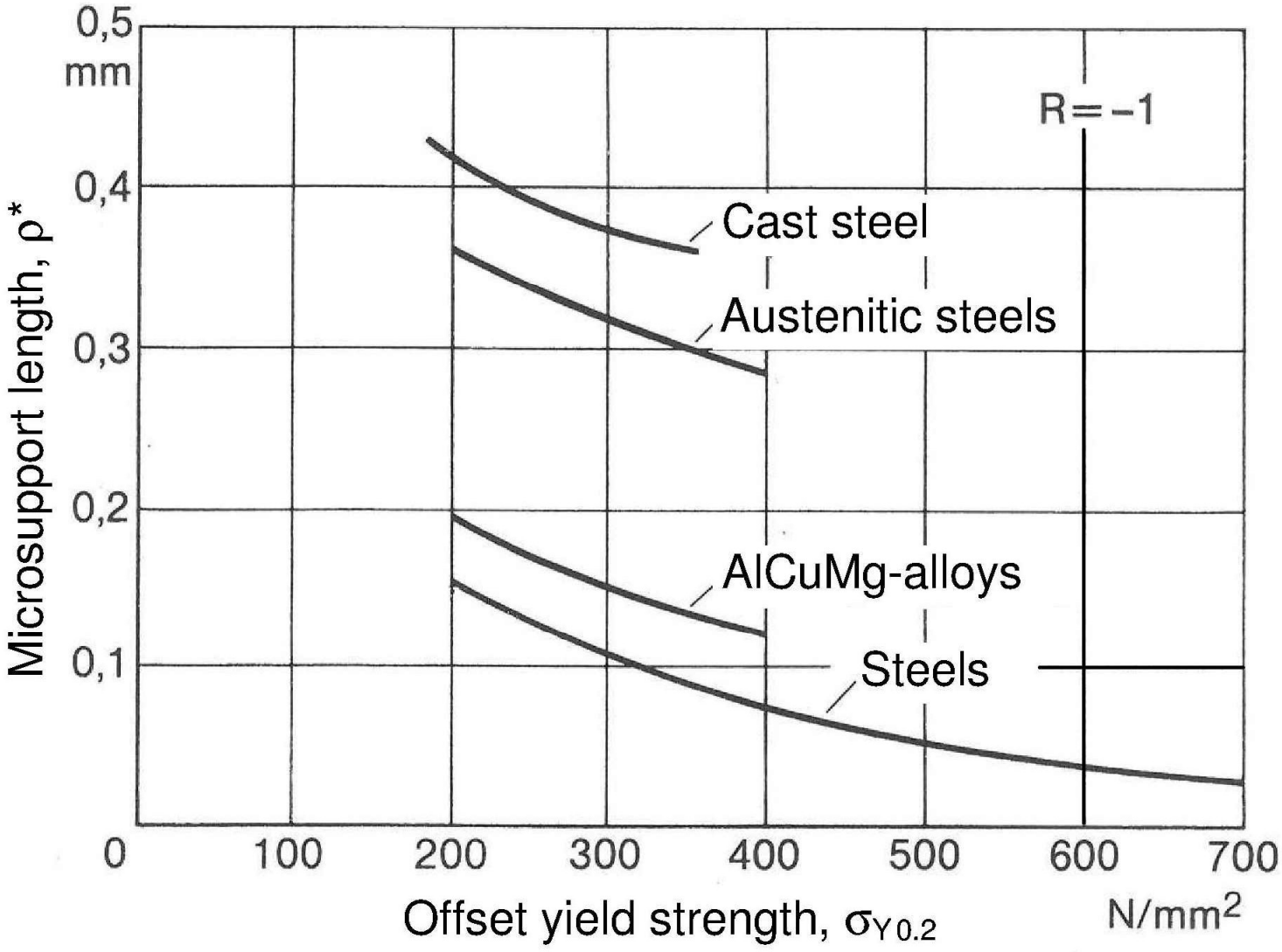

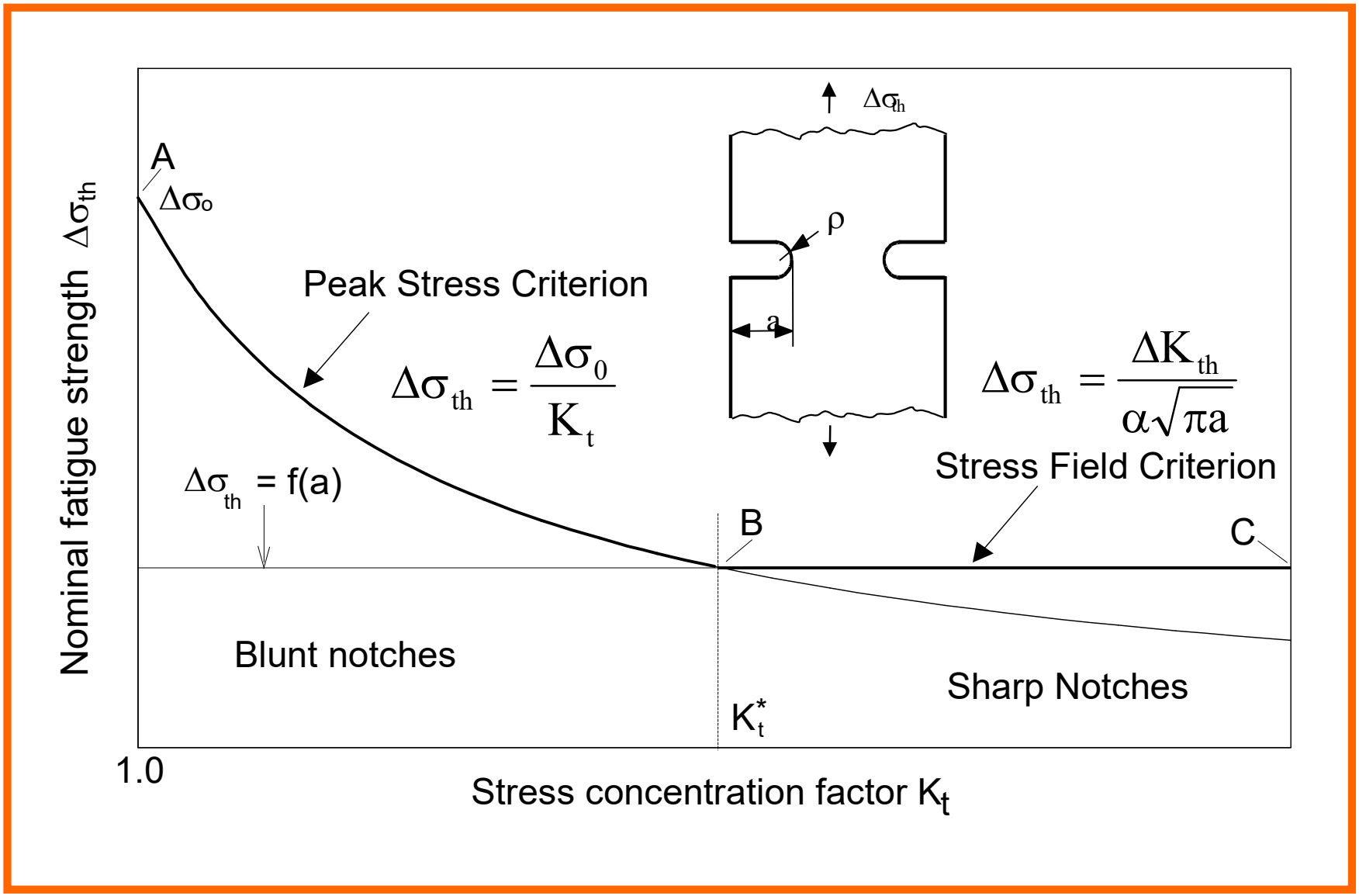

The Frost-Miller diagram

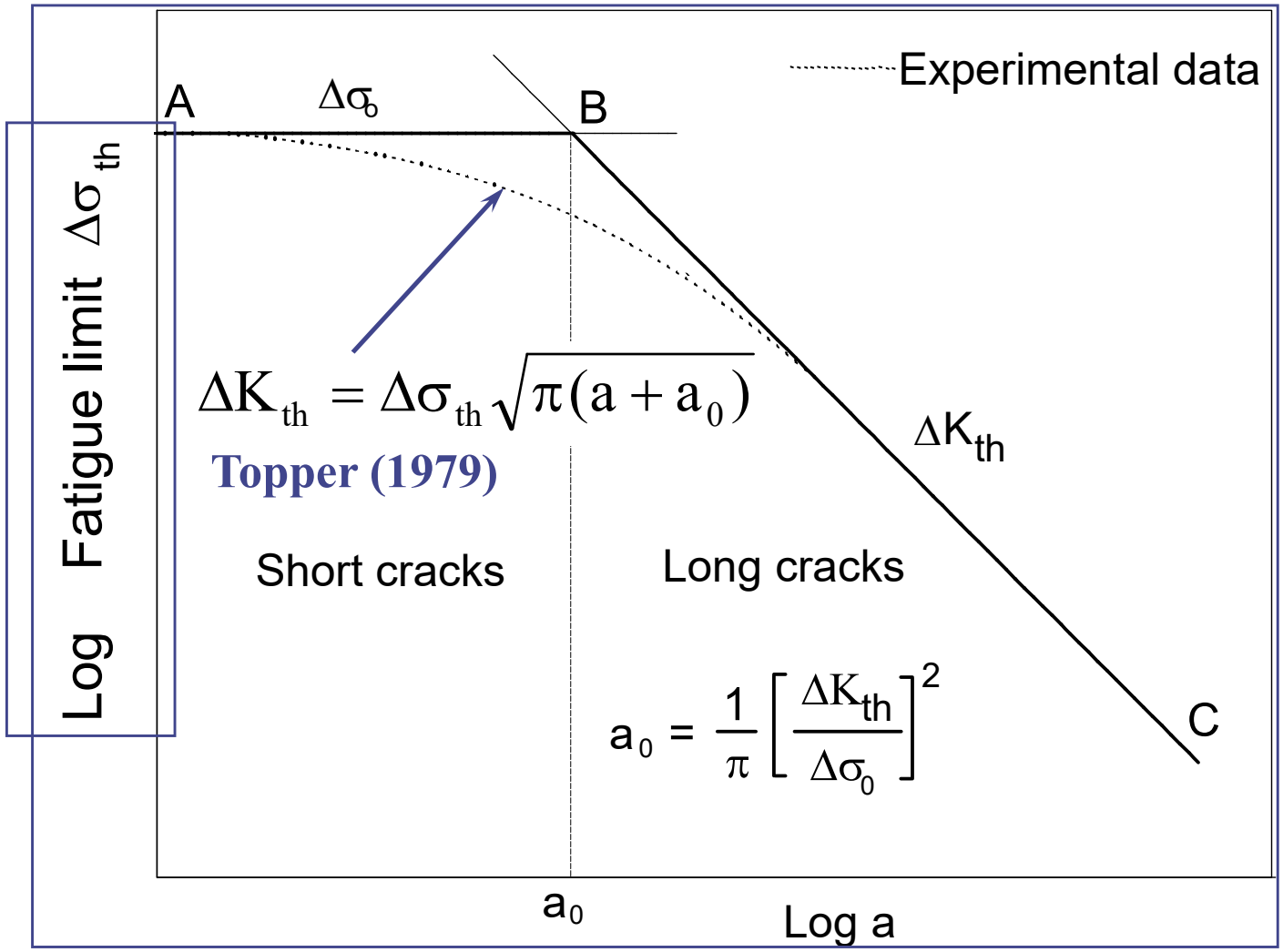

The Kitagawa diagram

Neuber's procedure of fictitious notch rounding

$$\rho_f = \rho + s\rho^*$$

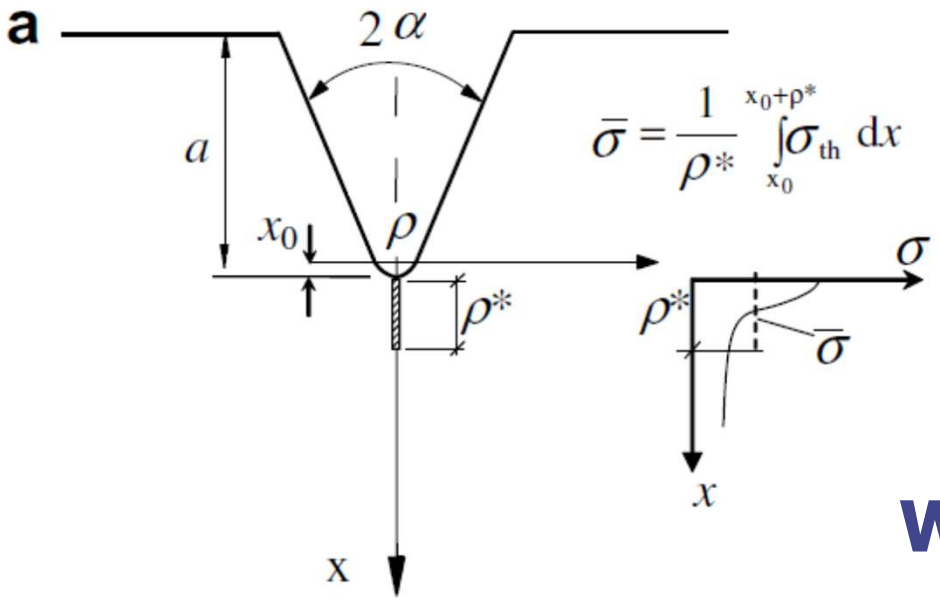

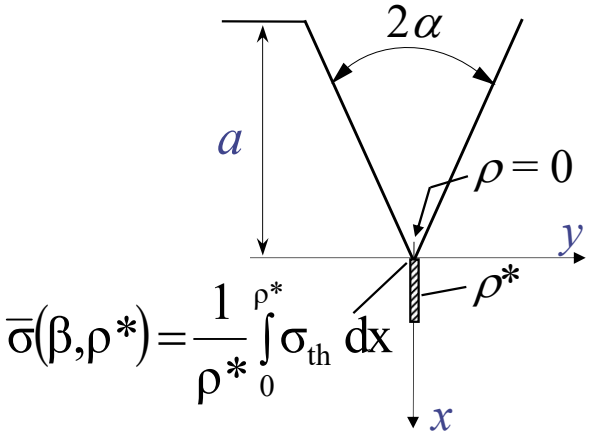

Worst case

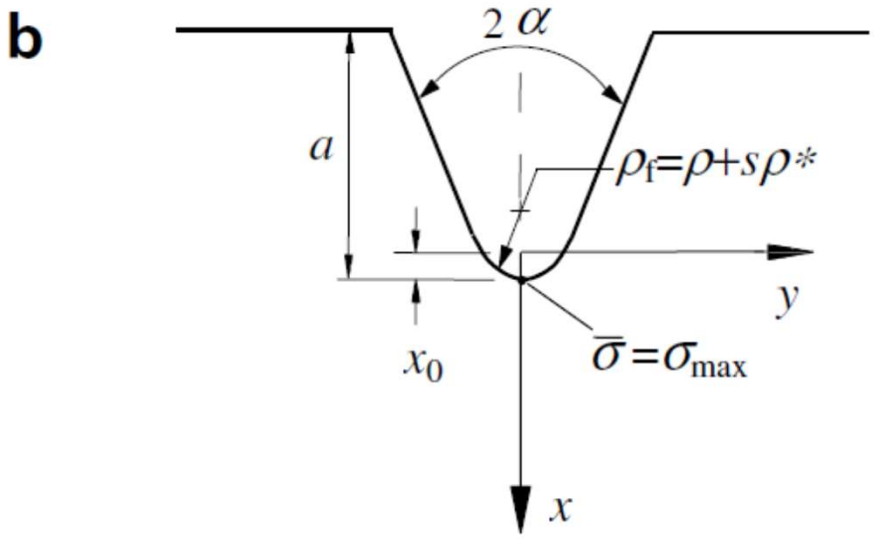

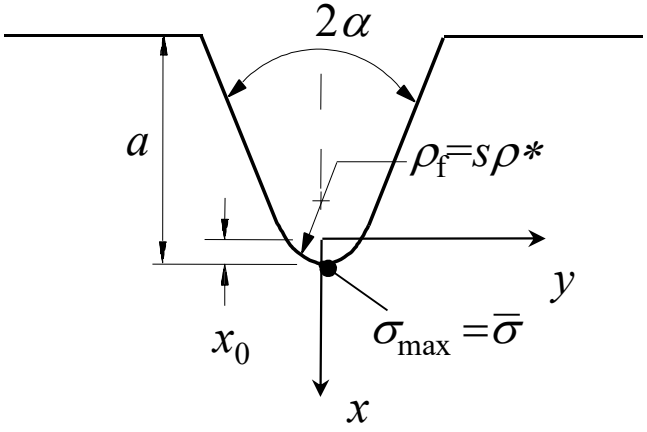

Criteria

Criteria: nominal stresses, hot-spot stresses, MFLE.

Among the local criteria:
Radaj (1969, 1990), *'Notch rounding approach*,
IIW (2007) e FKM (2003).

$$\rho_f = \rho + s\,\rho^* = 1.0 \text{ mm}$$

(real radius ρ =0, microstructural support length ρ^*=0.4 mm '*cast iron*', multiaxiality factor s = 2.5).

Lower values of ρ^* suggested for thin welded joints

Local criterion

Thin welded joints. Criterion based on a '*Substitute notch radius*, ρ_s**=0.05 mm**

Eibl, M., Sonsino, C.M., Kaufmann, H. and Zhang, G. (2003) Int J Fatigue **25**.

Karakas Ö., Morghenstern C., Sonsino C. M. (2008) Int J Fatigue **30**, 2210-2219.

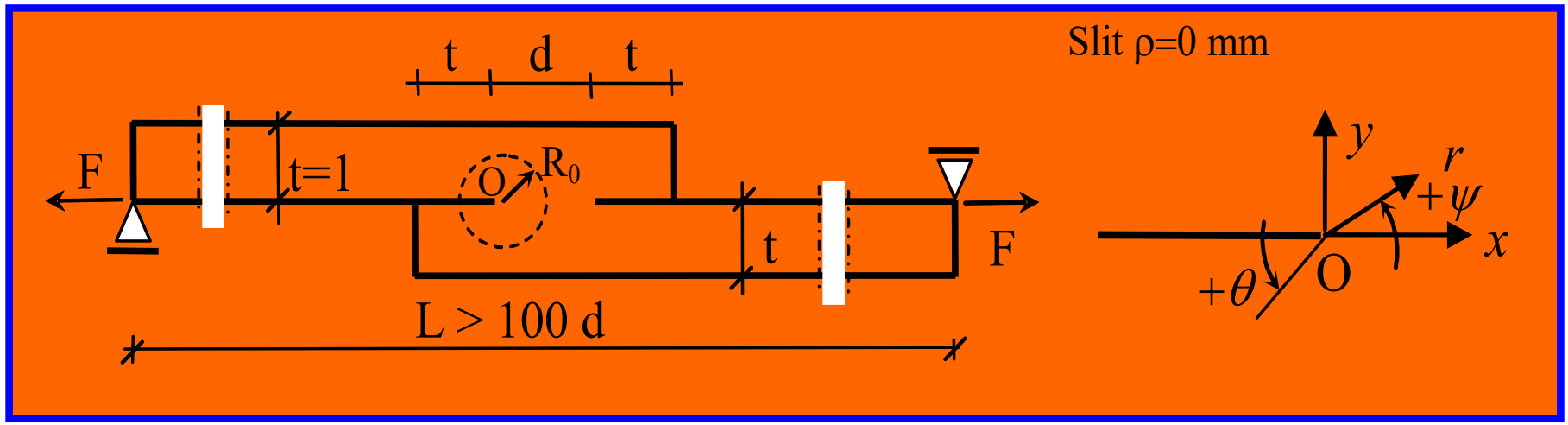

Notch rounding approach and SED approach

Comparison between the two criteria

Radaj D., Berto F., Lazzarin P. (2009). Engng Fract Mech.
Radaj D., Lazzarin P., Berto F. (2009). Int J Fatigue.

A local approach for the fatigue assessment of welded joints with potential to substitute the IIW notch rounding procedure is the strain energy density (SED) concept

IIW RECOMMENDATIONS FOR FATIGUE DESIGN OF WELDEDJOINTS AND COMPONENTS

2.2.4.3 Measurement of Effective Notch Stress

Because the effective notch radius is an idealization, the effective notch stress cannot be measured directly in the welded component. In contrast, the simple definition of the effective notch can be used for photo-elastic stress measurements in resin models.

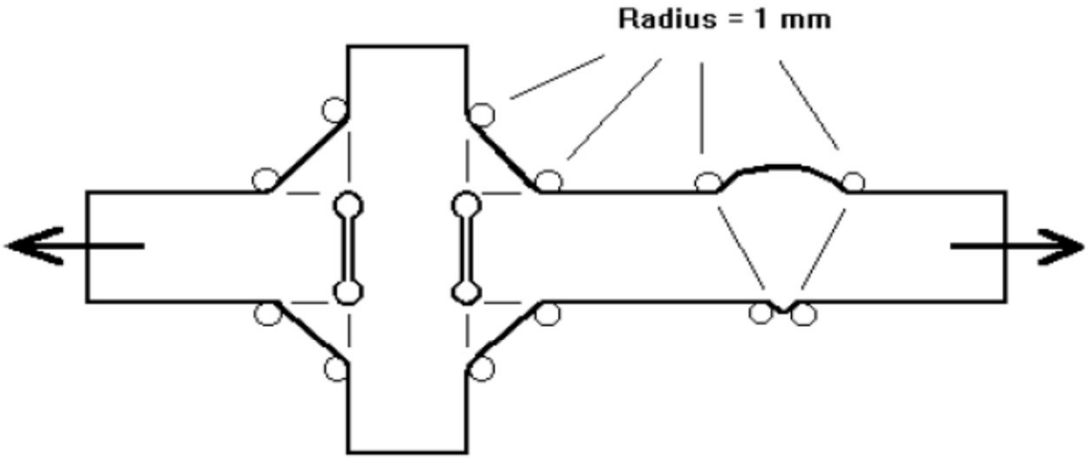

Fig. (2.2)-14 Fictitious rounding of weld toes and roots

ρ_f=1 mm indipendent of the notch opening angle

"s" is referred to the case of normal stress (under plane stress)

$\rho_f = \rho + s\,\rho^* = 1.0$ mm s=2.5, $\rho = 0$, $\rho^* = 0.4$ mm

Fictitious notch rounding concept for welded joints

Fictitious notch rounding simulating stress averaging over ρ^* in the direction of crack propagation has successfully been applied to the fatigue assessment of welded joints (Radaj 1969, 1975, 1990).

Within a worst case consideration, the parameter values:

- $\rho = 0$ (worst case), $\rho^* \approx 0.4$ mm (welded steel), $s \approx 2.5$

  result in the fictitious notch radius:
- $\rho_f = \rho + s\rho^* = 1$ mm

This very rough estimate is applied to the cross-sectional model of welded joints in the form of a blunt circular notch at the weld toe and a keyhole at the weld root.

The SCFs at these notches are considered as theoretical fatigue notch factors characterising the endurance limit of the joints.

Tabelle 4.4: Faktor s der Mikrostützwirkung an Kerben für unterschiedliche Mehrachsigkeitsgrade und Festigkeitshypothesen (mit Querkontraktionszahl ν); in Anlehnung an Neuber [587, 660], mit Korrektur nach Radaj u. Zhang [692]

Festigkeitshypothese	Mehrachsigkeitsgrad		
	ESZ Flachstab unter Zug-Druck oder Biegung Faktor s	EDZ Rundstab unter Zug-Druck oder Biegung Faktor s	NES Rundstab unter Torsion Faktor s*)
Normalspannungshypothese	2	2	0,5 bzw. 1,0
Schubspannungshypothese	2	$\frac{2-\nu}{1-\nu}$	0,5 bzw. 1,0
Oktaederschubspannungs- u. Gestaltänderungsenergie-hypothese	2,5	$\frac{5-2\nu+2\nu^2}{2-2\nu+2\nu^2}$	0,5 bzw. 1,0
Dehnungshypothese	$2+\nu$	$\frac{2-\nu}{1-\nu}$	0,5 bzw. 1,0
Formänderungsenergiehypothese	$2+\nu$	$\frac{2-\nu}{1-\nu}$	0,5 bzw. 1,0

ESZ: ebener Spannungszustand, EDZ: ebener Dehnungszustand, NES: nichtebene Schubbeanspruchung

*) $s = 0{,}5$ nach Neuber [587] und Radaj u. Zhang [692] für rißartige Kerben,
$s = 1{,}0$ nach Neuber [660] für allgemeine Kerben, Widerspruch ungeklärt

s valid for the case $2\alpha=0°$ (plane stress o plane strain)???

s under torsion s=0.5 o 1.0 ???

Neuber's procedure of fictitious notch rounding

The support factor *s* depends on:

- Loading modes 1, 2, 3 and mixed mode
- Multiaxiality condition (plane stress, plane strain, pure shear)
- Strength criterion (Rankine, Beltrami, von Mises)
- V-notch opening angle
- V-notch shape (blunt hyperbolic, root hole, blunt circular)

There should be no dependency on ρ and ρ^*, but this is not always true.

Expression for finding the relationship between real and fictitious notch radius by functional analysis (Neuber 1937):

$$\overline{\sigma}(\rho, \rho^*) = \overline{\sigma}(\rho_f, \rho^* \to 0)$$

$$s = (\rho_f - \rho) / \rho^*$$

Support factor dependent on notch opening angle

Support factor s is dependent on V-notch opening angle 2α for loading modes 1, 2, 3, different multiaxiality conditions and strength criteria:

- Plateau values s for $\rho > \rho^*$ (Berto et al. 2009)
- Base point values s_0 for $\rho = 0$ (Neuber 1937)

Neuber's values s = 2.0-3.0 for mode 1 and s = 1.0 for mode 3, recommended for application, are plateau values for $2\alpha = 0$ (parabolic notch).

NOTCH ROUNDING APPROACH

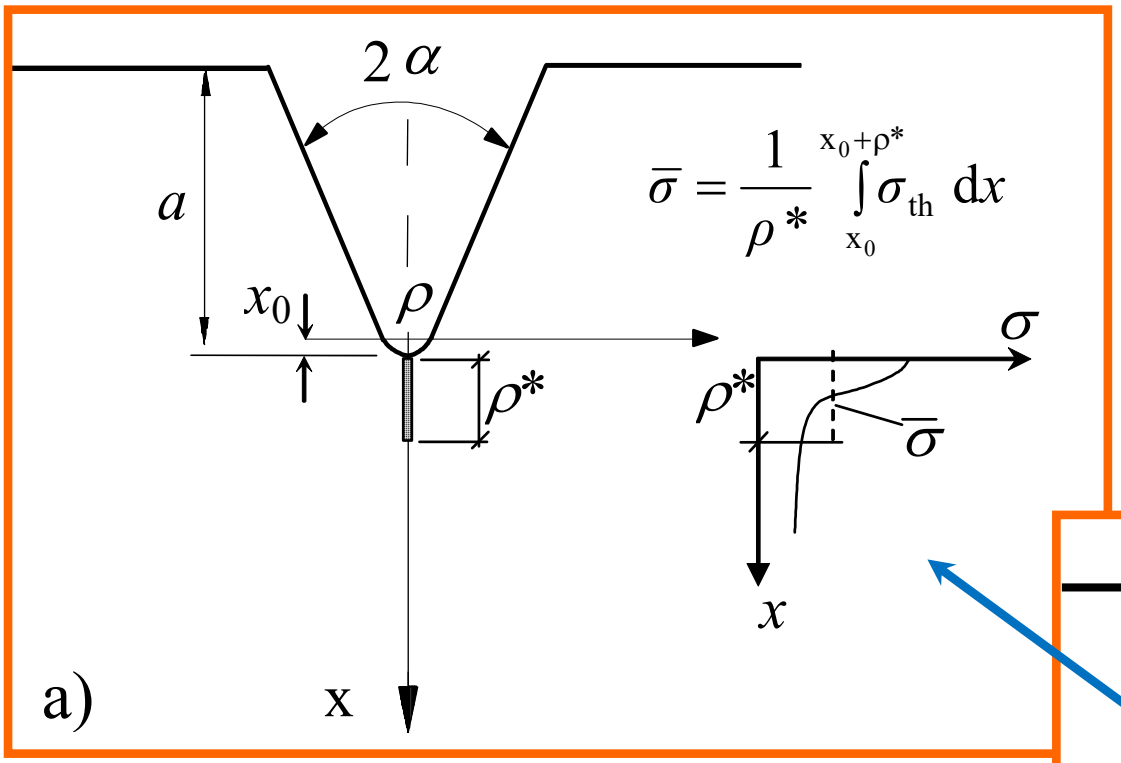

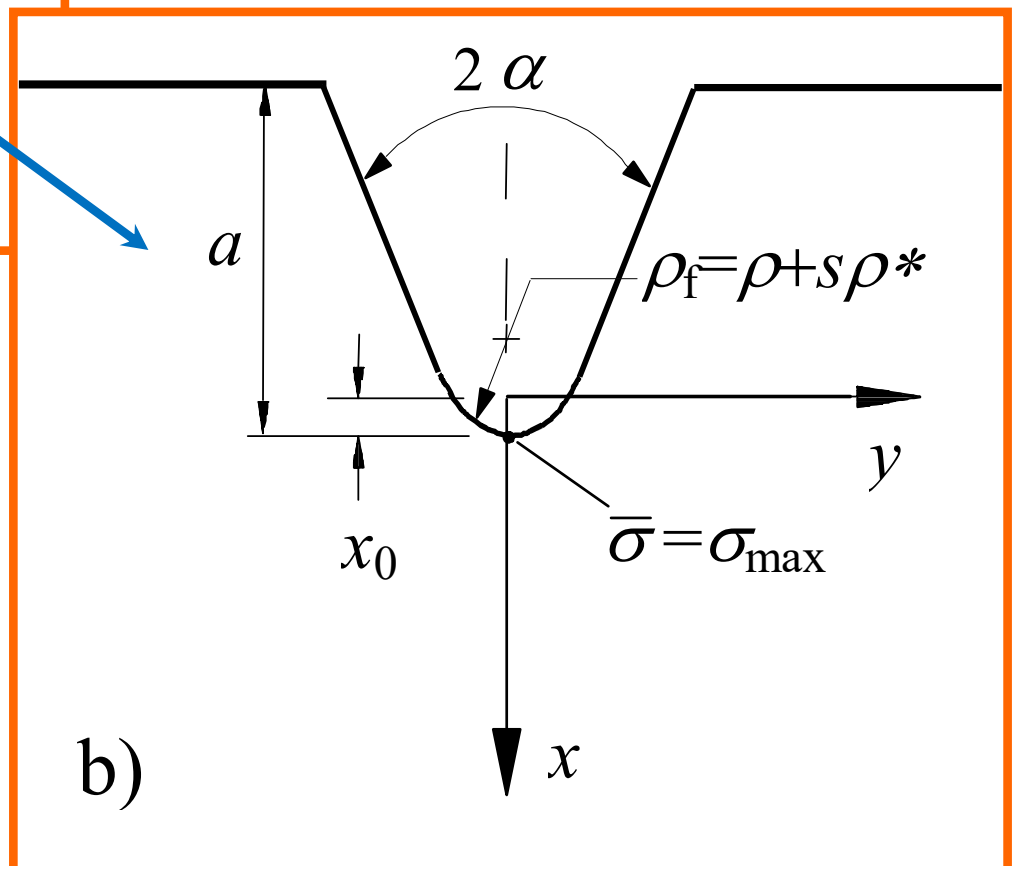

STEPS FOR THE APPLICATION OF THE FNR APPROACH

STEP 1

Choice of the fracture criterion (normal stress, von Mises, Beltrami) and Write the equivalent stress accordingly to the selected criterion σ (or τ) along the bisector line by means of the expressions valid for V-notches

STEP 2

Determine the effective stress as a function of ρ and ρ^*

$$\overline{\sigma}(\rho, \rho^*) = \frac{1}{\rho^*} \int_{x_0}^{x_0+\rho^*} \sigma_{th}\, dx$$

STEP 3

Solve the limit $\overline{\sigma}\max(\rho_f) = \lim_{\rho^* \to 0} \overline{\sigma}$

Solve the equation: **STEP 4**

$$\overline{\sigma}\,\max(\rho_f) = \overline{\sigma}(\rho^*, \rho)$$

STEP 5

Determine $\rho_f(\rho,\rho^*)$:

$$\rho_f = f(\rho^*, \rho)$$

STEP 6

Evaluation of s:

$$s=(\rho_f-\rho)/\rho^*$$

EXAMPLE

Beltrami criterion, plane strain (with Poisson's ratio)

Caso 2α=135°:

$$\bar{\sigma}^2 = \frac{1}{\rho^*}\int_{x_0}^{x_0+\rho^*}\sigma_B^2 \mathrm{d}r = -\frac{K_1^2\rho^{-2\mu}(1+\nu)}{\rho^*}\left[\frac{r^{2\mu-1}\rho^{2\lambda}\left(B^2(\nu-1)+G^2(\nu-1)+2BG\nu\right)}{-1+2\mu}+\right.$$
$$+\frac{r^{2\lambda-1}\rho^{2\mu}\left(A^2(\nu-1)+F^2(\nu-1)+2AF\nu\right)}{-1+2\lambda}+\frac{2Gr^{\lambda+\mu-1}\rho^{\lambda+\mu}\left(F(\nu-1)+\nu A\right)}{-1+\lambda+\mu}+$$
$$\left.+\frac{2Br^{\lambda+\mu-1}\rho^{\lambda+\mu}\left(A(\nu-1)+F\nu\right)}{-1+\lambda+\mu}\right]_{x_0}^{x_0+\rho^*}$$

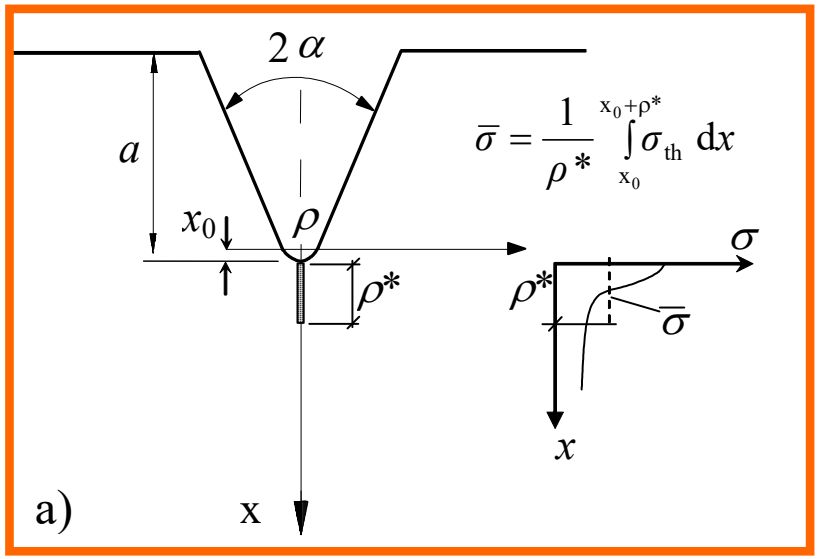

$$\lim_{\substack{\rho^*\to 0\\ \nu=0.3}}\overline{\sigma}^2 = -1.3K_1^2\rho^{-2\mu}\left(-\frac{1}{\left(\rho-\frac{\rho}{q}\right)^2}\left(\frac{\left(-0.7A^2+0.6AF-0.7F^2\right)\rho^{2\mu}\left(\rho-\frac{\rho}{q}\right)^{2\lambda}}{2\lambda-1}+\right.\right.$$

$$+\frac{\left(-0.7B^2+0.6BG-0.7G^2\right)\rho^{2\lambda}\left(\rho-\frac{\rho}{q}\right)^{2\mu}}{-1+2\mu}+$$

$$\left.+\frac{2B\left(-0.7A+0.3F\right)\rho^{\lambda+\mu}\left(\rho-\frac{\rho}{q}\right)^{\lambda+\mu}}{\lambda+\mu-1}+\frac{2G\left(0.3A-0.7F\right)\rho^{\lambda+\mu}\left(\rho-\frac{\rho}{q}\right)^{\lambda+\mu}}{\lambda+\mu-1}\right)+$$

$$\frac{1}{\left(\rho-\frac{\rho}{q}\right)}\left(\frac{2\left(-0.7A^2+0.6AF-0.7F^2\right)\lambda\rho^{2\mu}\left(\rho-\frac{\rho}{q}\right)^{2\lambda-1}}{2\lambda-1}+\right.$$

$$+\frac{2B\left(-0.7A+0.3F\right)(\lambda+\mu)\rho^{\lambda+\mu}\left(\rho-\frac{\rho}{q}\right)^{\lambda+\mu-1}}{\lambda+\mu-1}+\frac{2G\left(0.3A-0.7F\right)(\lambda+\mu)\rho^{\lambda+\mu}\left(\rho-\frac{\rho}{q}\right)^{\lambda+\mu-1}}{\lambda+\mu-1}$$

$$\left.\left.+\frac{2\left(-0.7B^2+0.6BG-0.7G^2\right)\mu\rho^{2\lambda}\left(\rho-\frac{\rho}{q}\right)^{2\mu-1}}{2\mu-1}\right)\right)$$

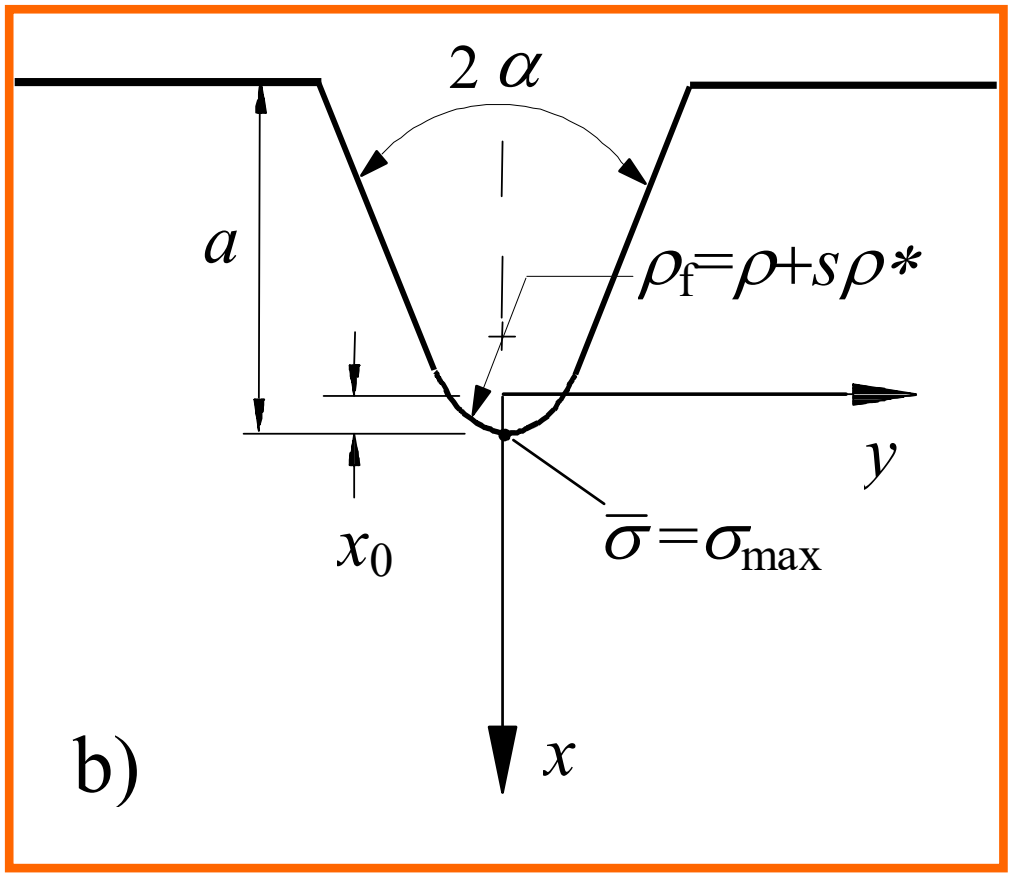

$$\rho_f(\rho,\rho^*) = \left(\frac{(\rho^* + 0.2\rho)^{0.3472}}{2.45723\rho^*} - \frac{\rho^{0.3472}}{16.74934\rho^*} - \frac{\rho^{0.8934}}{16.5645\rho^*(\rho^* + 0.2\rho)^{0.5462}} - \frac{\rho^{1.7868}}{367.22974\rho^*(\rho^* + 0.2\rho)^{1.4396}} \right)^{-1.5319}$$

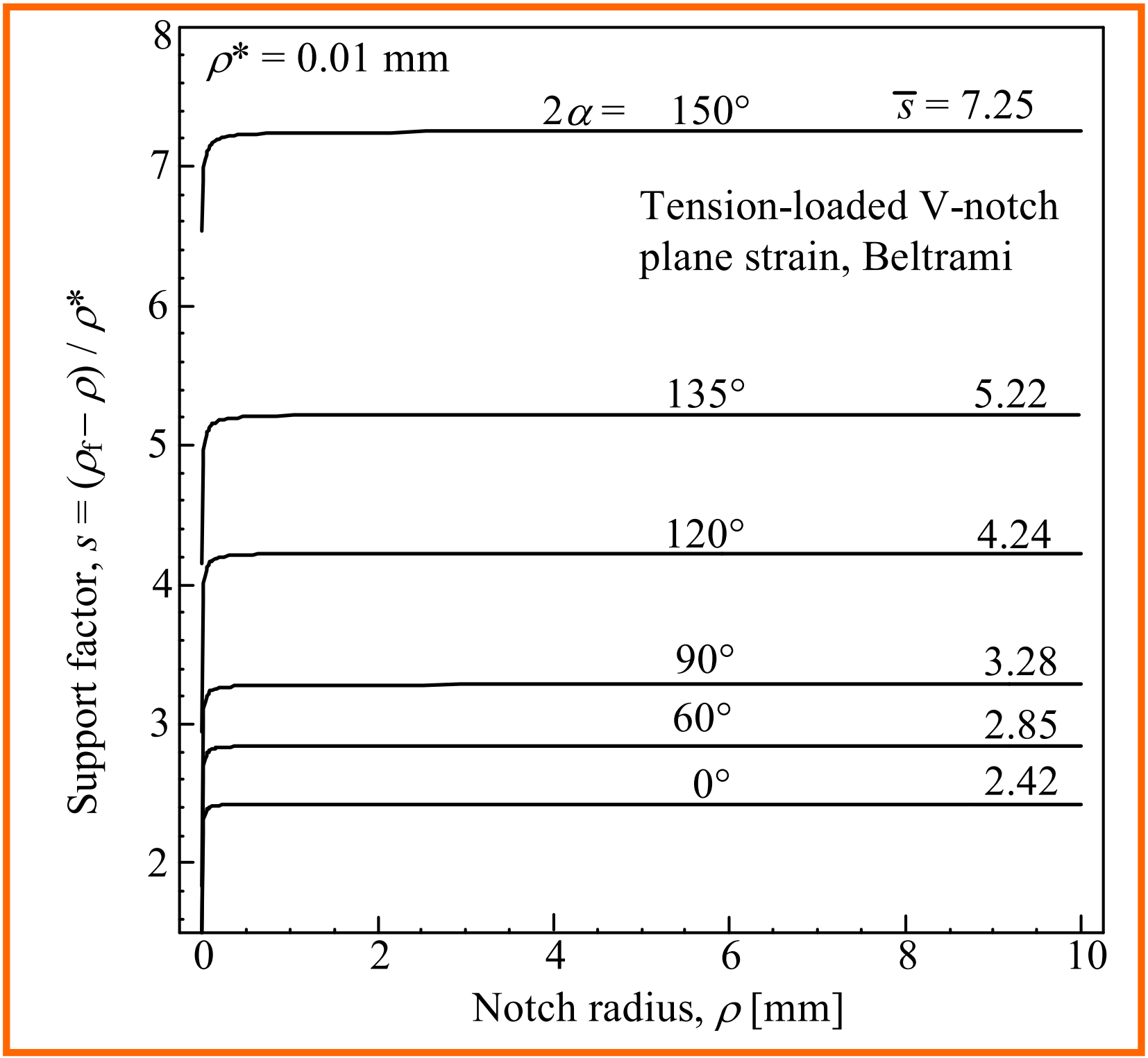
ρ* = 0.01 mm
2α = 150°
s̄ = 7.25
Tension-loaded V-notch
plane strain, Beltrami
135°
5.22
120°
4.24
90°
3.28
60°
2.85
0°
2.42
Support factor, s = (ρf – ρ) / ρ*
Notch radius, ρ [mm]
8
7
6
5
4
3
2
0
2
4
6
8
10

VALUES OF "s" FOR DIFFERENT NOTCH ANGLES

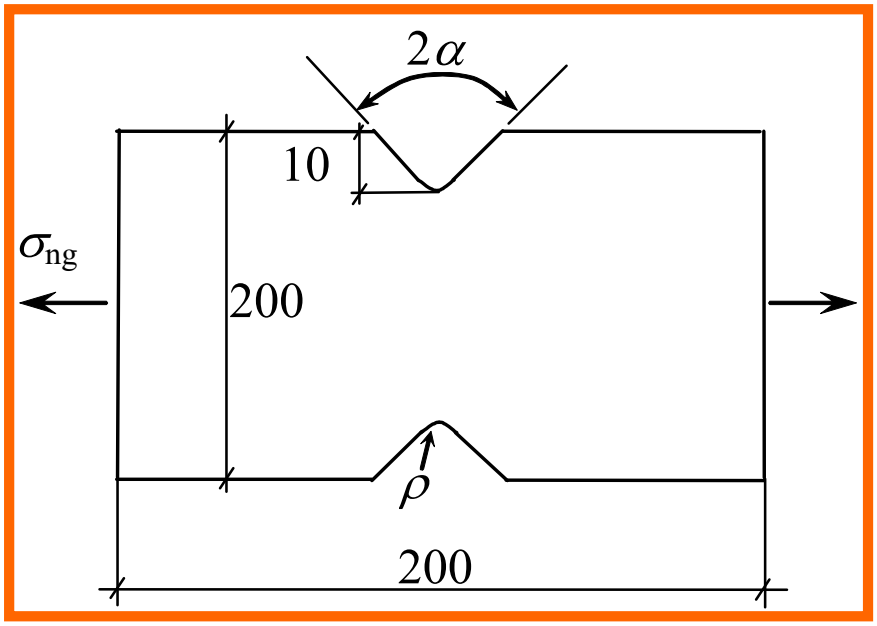

2α	Neuber	Filippi, Lazzarin and Tovo				
	Normal stress	Normal stress	von Mises plane stress	von Mises plane strain	Beltrami plane stress	Beltrami plane strain
0°	2.00	2.00	2.50	2.90	2.30	2.42
60°	2.36	2.41	2.90	3.33	2.72	2.85
90°	2.72	2.81	3.37	3.80	3.14	3.28
120°	3.47	3.67	4.32	4.84	4.06	4.24
135°	4.21	4.56	5.33	5.94	5.02	5.22
150°	5.73	6.38	7.41	8.20	6.99	7.25

$$\rho_f = 2.50 \times 0.4 = 1 \text{ mm}$$

VALUES OF "s" FOR DIFFERENT NOTCH ANGLES

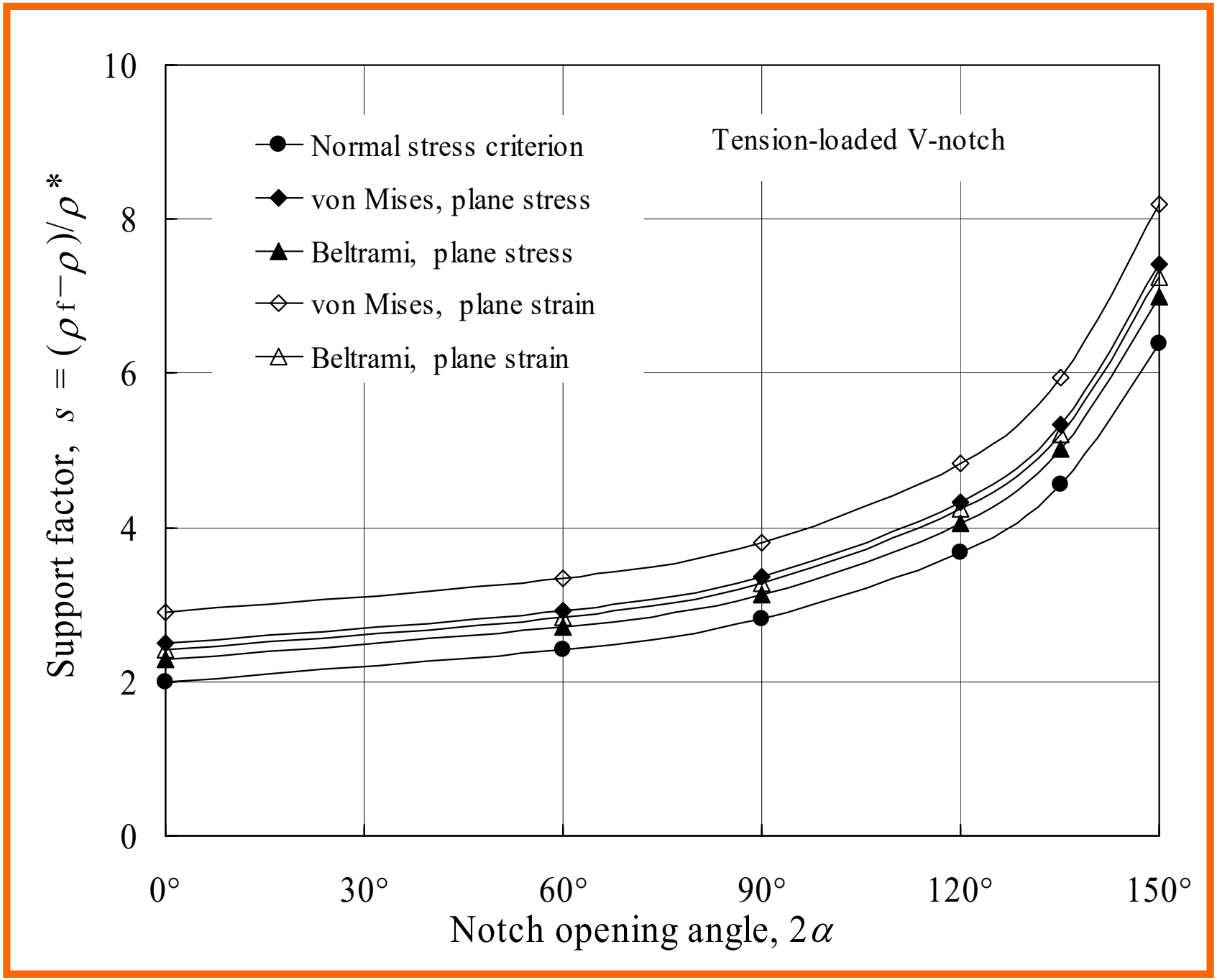

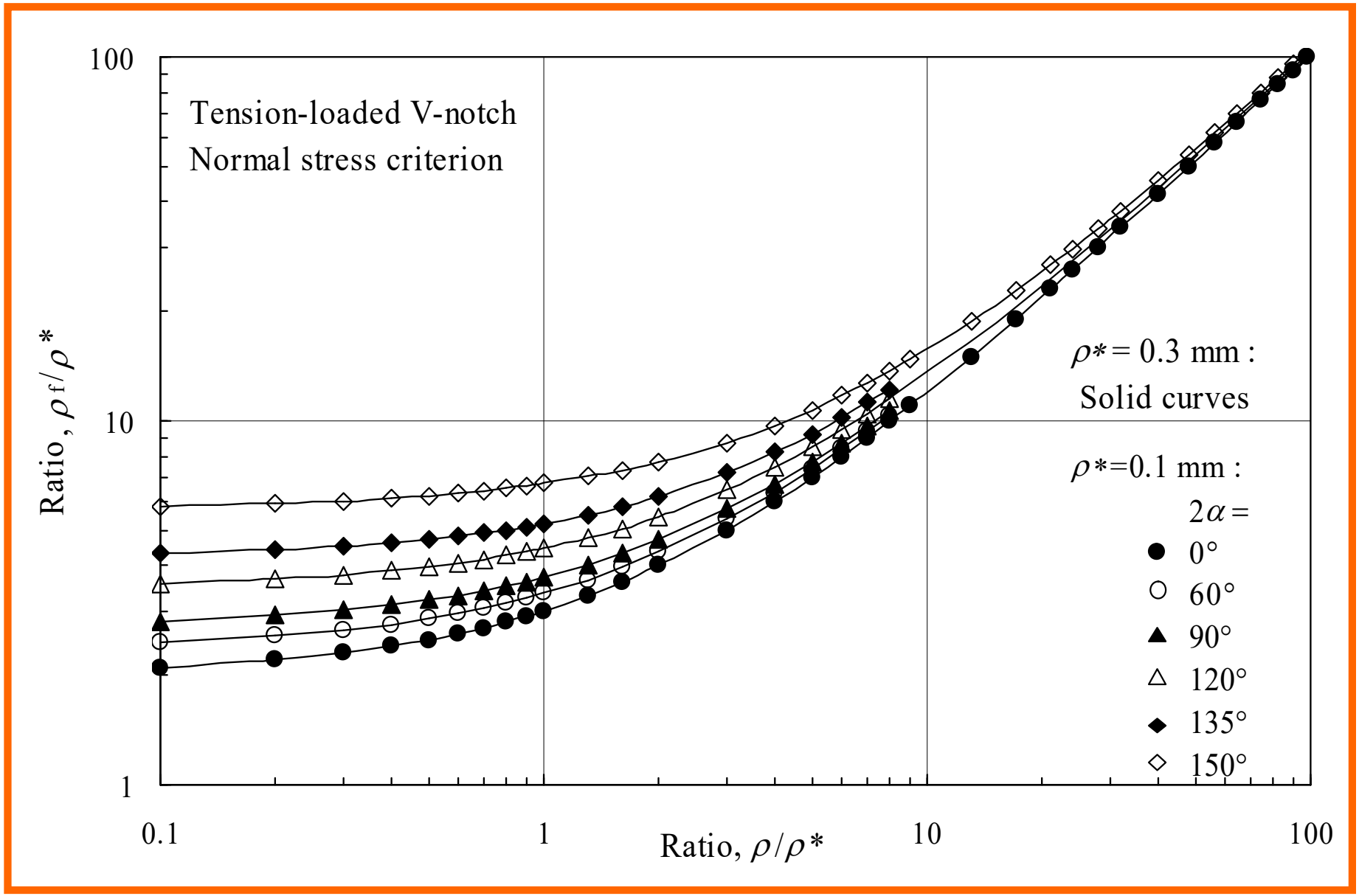
Tension-loaded V-notch
Normal stress criterion
ρ* = 0.3 mm :
Solid curves
ρ*=0.1 mm :
2α =
0°
60°
90°
120°
135°
150°
100
10
1
0.1
1
10
100
Ratio, ρf/ρ*
Ratio, ρ/ρ*

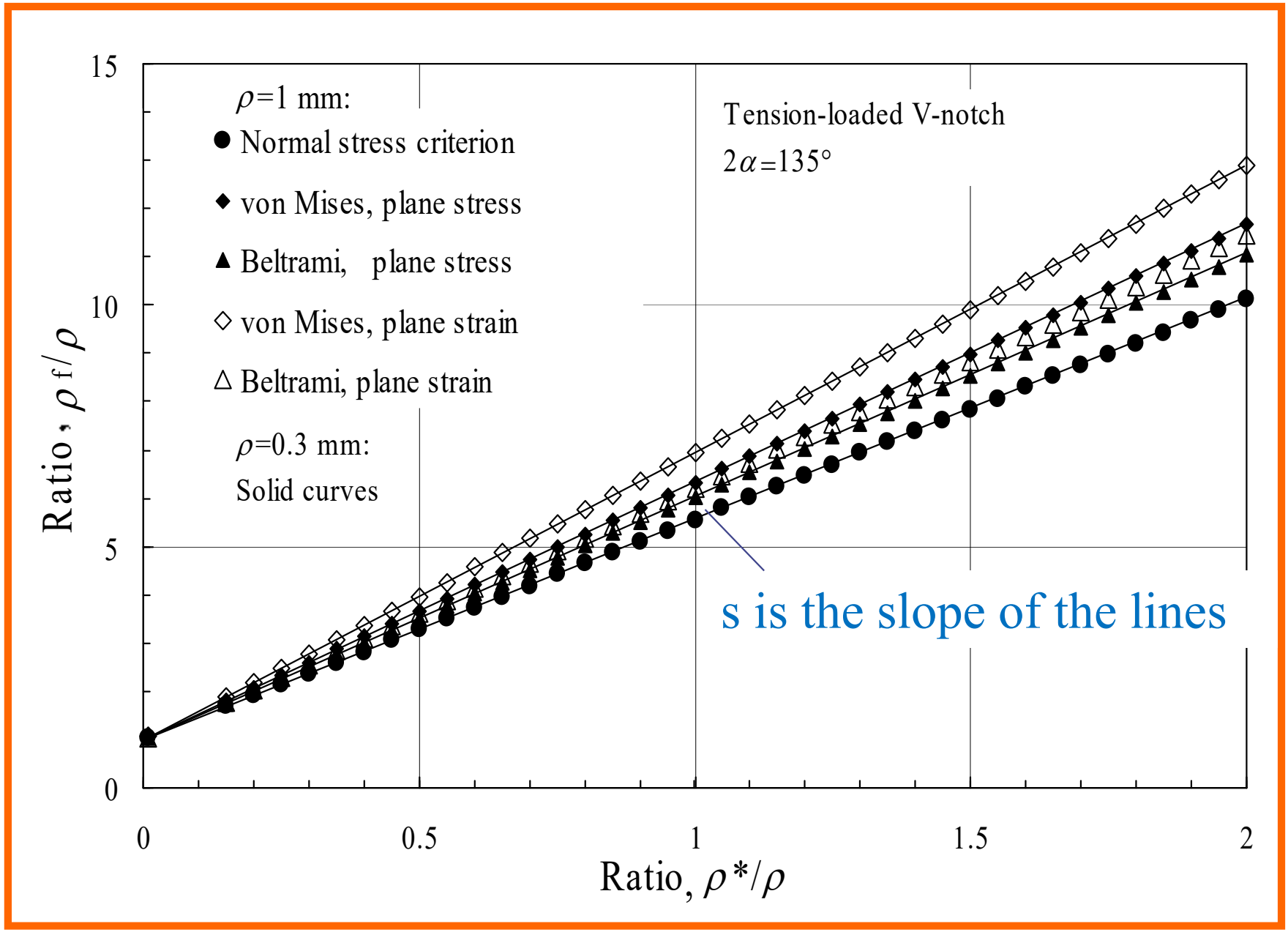
15
10
5
0
0
0.5
1
1.5
2
Ratio, ρ^*/ρ
Ratio, ρ_f/ρ
ρ=1 mm:
Normal stress criterion
von Mises, plane stress
Beltrami, plane stress
von Mises, plane strain
Beltrami, plane strain
ρ=0.3 mm:
Solid curves
Tension-loaded V-notch
2α=135°
s is the slope of the lines

TORSION

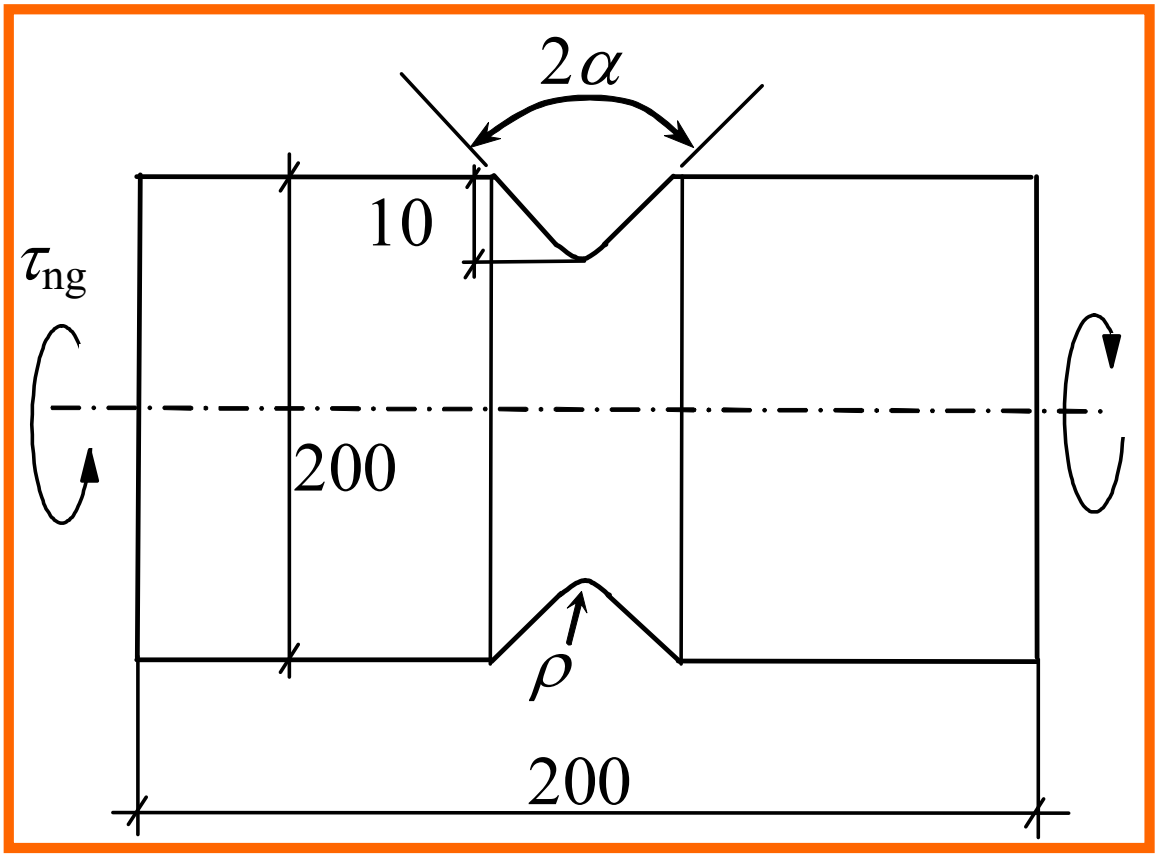

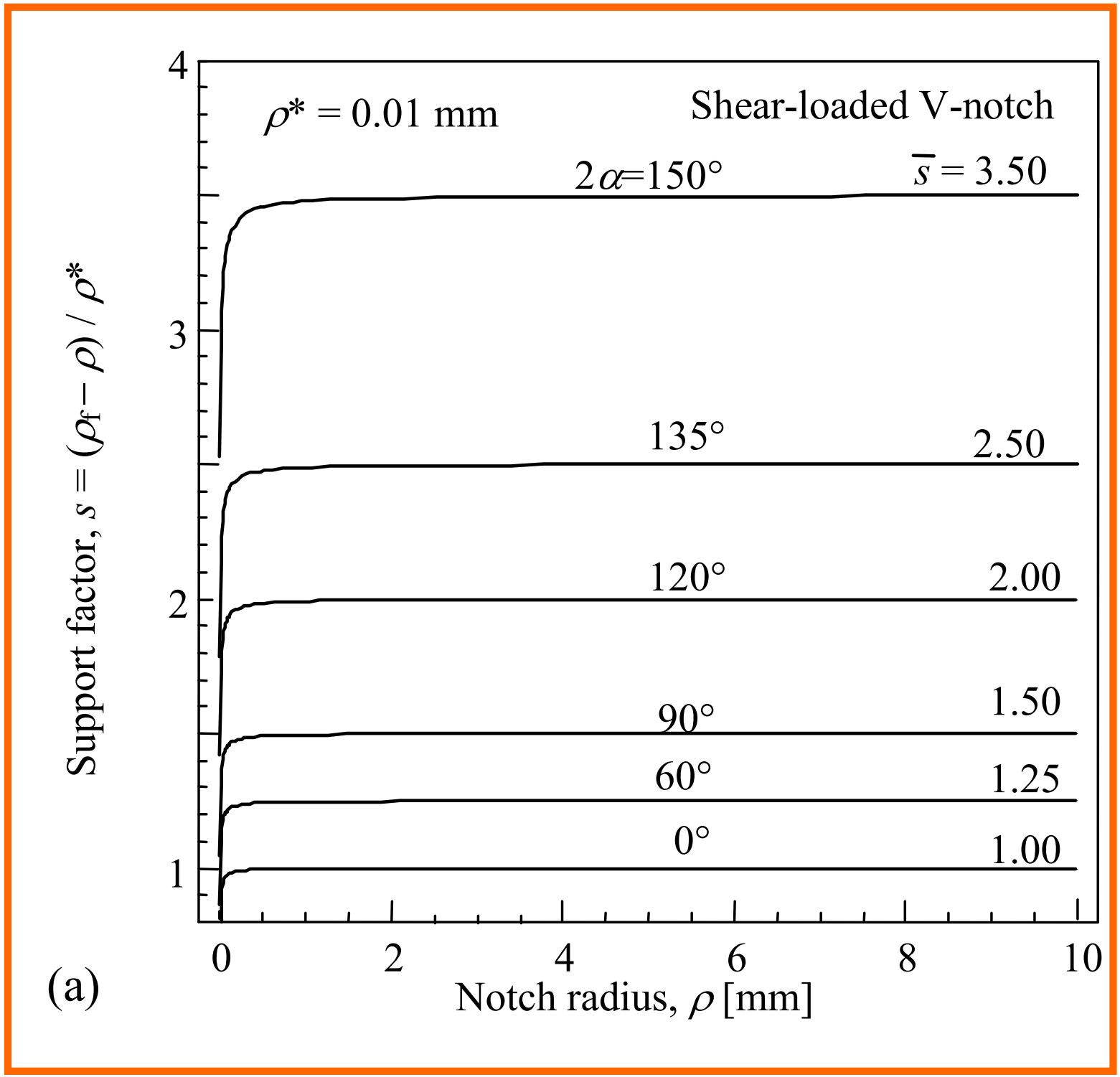
ρ* = 0.01 mm
Shear-loaded V-notch
2α=150°
s̄ = 3.50
135°
2.50
120°
2.00
90°
1.50
60°
1.25
0°
1.00
Support factor, s = (ρf − ρ) / ρ*
Notch radius, ρ [mm]
0
2
4
6
8
10
1
2
3
4
(a)

ASSESSMENT UNDER TORSION

Fictitious notch rounding for pointed V-notch specimens ($\rho = 0$) under torsion loading using the plateau values of s; comparison of $K_t(\rho_f)$ with $\overline{K}_t$ obtained from FE analysis (relative deviation Δ); variation of notch opening angle 2α and support length ρ^* (data for further variations are available)

2α	$\bar{s}$	$\rho^* = 0.05$ mm				$\rho^* = 0.1$ mm				$\rho^* = 0.3$ mm				$\rho^* = 0.5$ mm			
		ρ_f [mm]	$K_t(\rho_f)$	$\overline{K}_t$	Δ %	ρ_f [mm]	$K_t(\rho_f)$	$\overline{K}_t$	Δ %	ρ_f [mm]	$K_t(\rho_f)$	$\overline{K}_t$	Δ %	ρ_f [mm]	$K_t(\rho_f)$	$\overline{K}_t$	Δ %
0	1.00	0.050	21.08	22.00	−4.18	0.100	15.00	15.59	−3.78	0.300	8.84	9.03	−2.10	0.500	6.96	7.01	−0.71
90°	1.50	0.075	10.27	10.14	1.28	0.150	8.18	8.04	1.74	0.450	5.72	5.56	2.88	0.750	4.83	4.69	2.99
135°	2.50	0.125	5.01	4.85	3.30	0.250	4.36	4.22	3.32	0.750	3.51	3.39	3.54	1.250	3.17	3.06	3.59

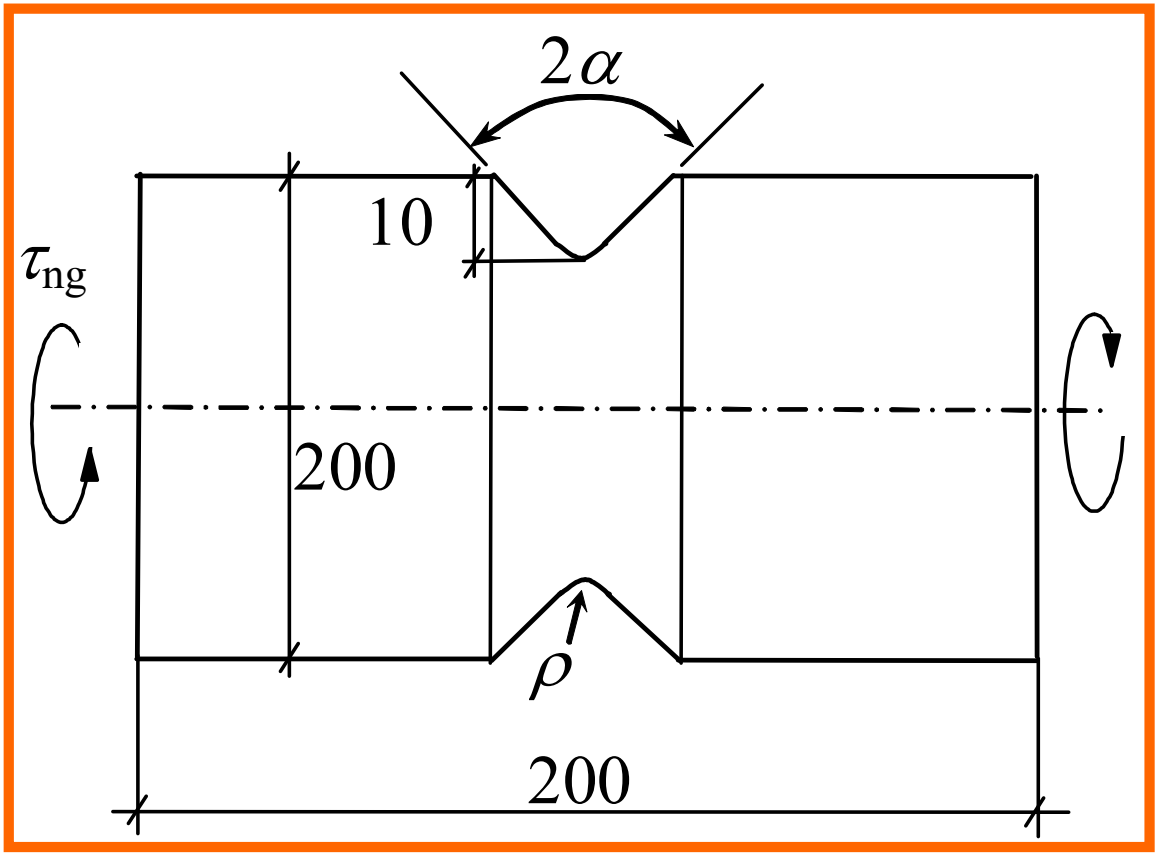

V-notch with end holes

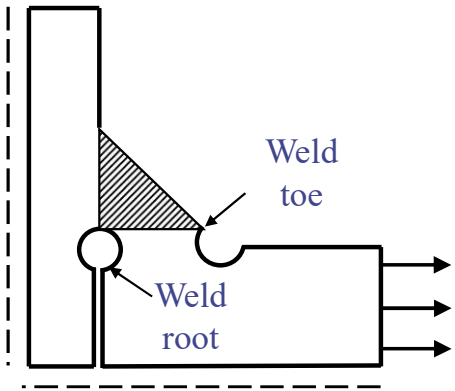

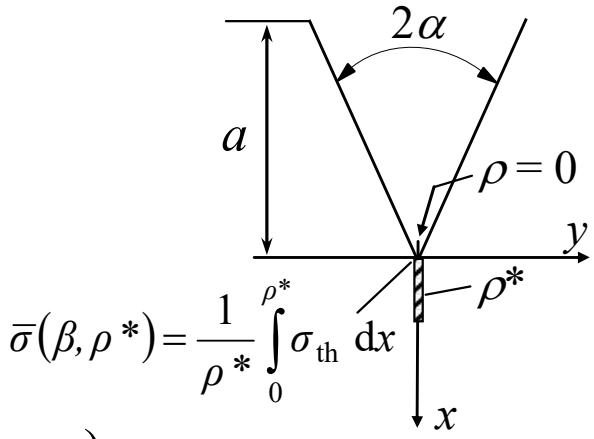

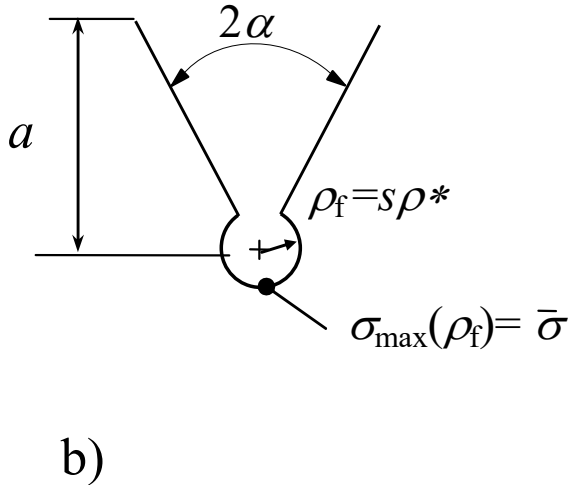

V-notch with end holes

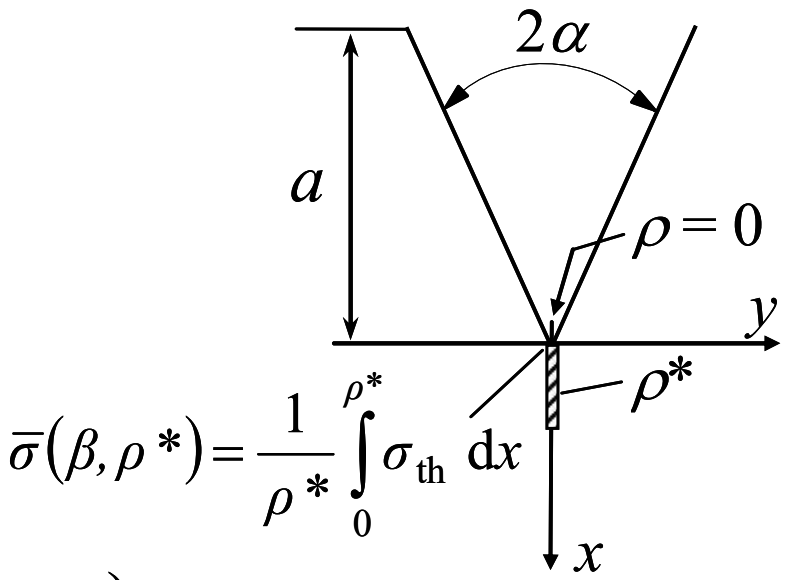

$$\bar{\sigma}(\beta, \rho^*) = \frac{1}{\rho^*} \int_0^{\rho^*} \sigma_{th}\, dx$$

a)

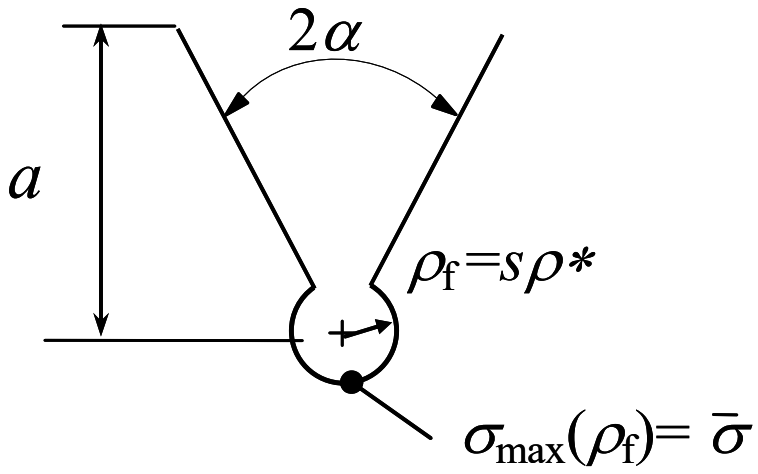

b)

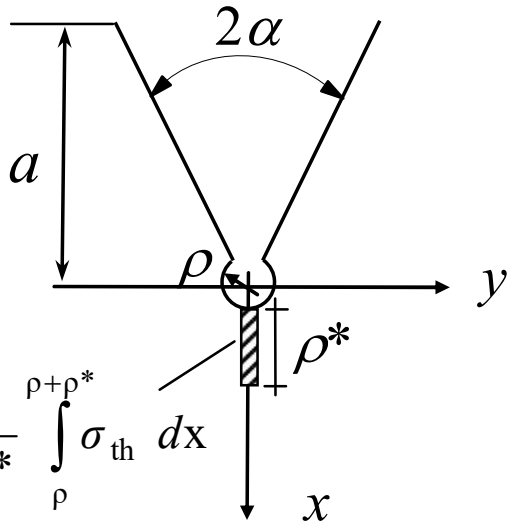

$$\bar{\sigma}(\bar{\theta}, \rho^*) = \frac{1}{\rho^*} \int_{\rho}^{\rho+\rho^*} \sigma_{th}\, dx$$

a)

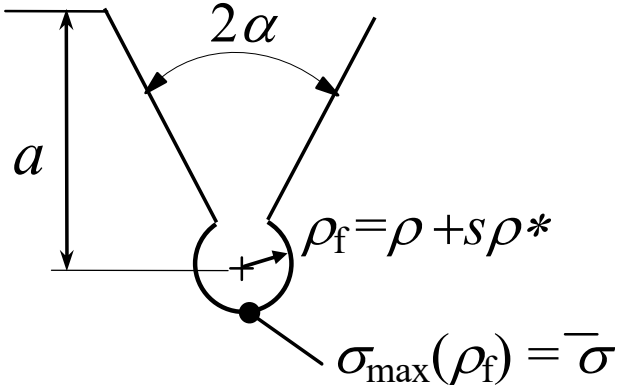

b)

Comparison between V-notch with end holes and blunt notches: s values

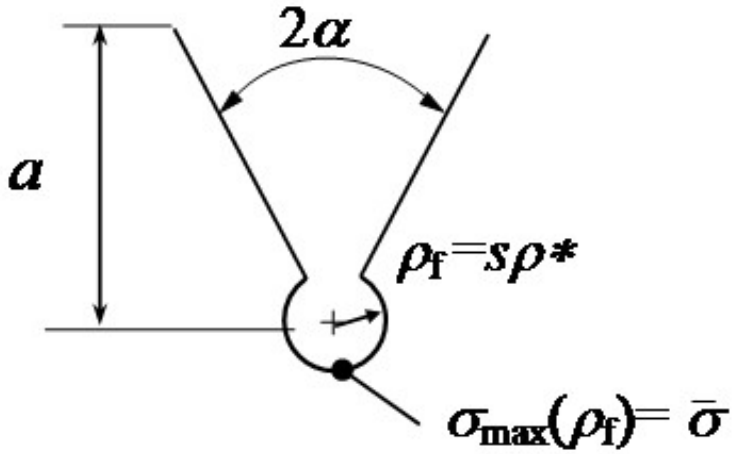

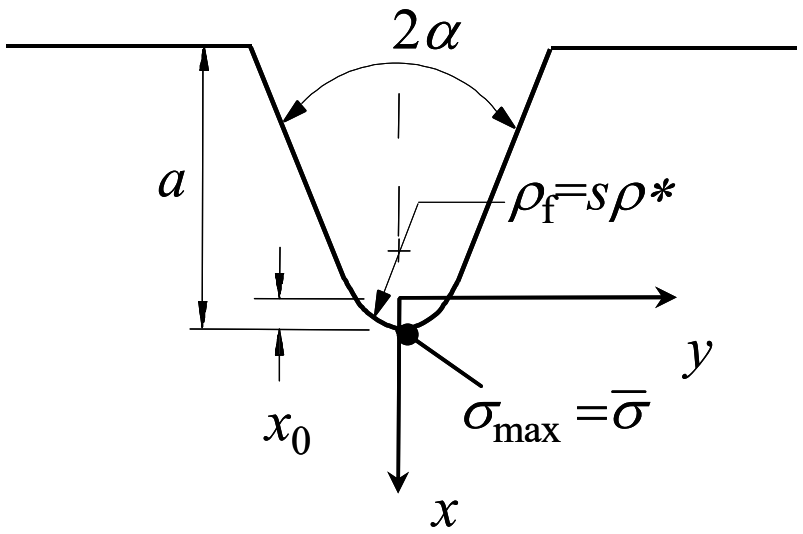

2α	V-notch with end hole	Blunt V-notch
0°	2.25	2.00
60°	2.49	2.41
90°	3.13	2.81
120°	5.42	3.67
135°	9.64	4.56

Pure mode II loading

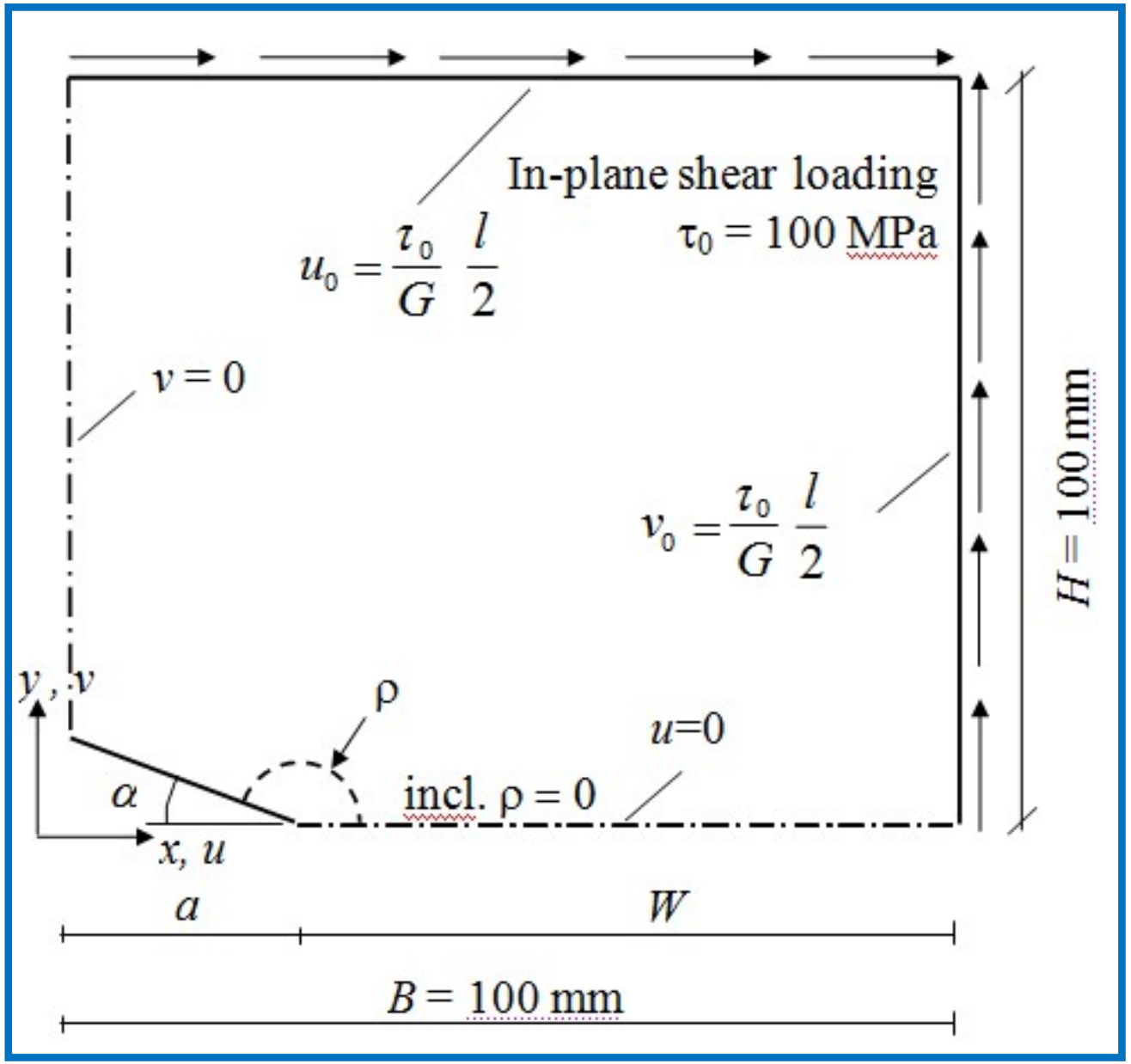

- a = 5 mm
- a = 10 mm
- a = 25 mm
- a = 50 mm

- $2\alpha = 0°$
- $2\alpha = 30°$
- $2\alpha = 45°$
- $2\alpha = 60°$

$\rho_f = \rho + s\rho^*$

- ρ^* = 0.05 mm
- ρ^* = 0.1 mm
- ρ^* = 0.2 mm
- ρ^* = 0.3 mm
- ρ^* = 0.4 mm
- ρ^* = 0.5 mm

Different Methods for the evaluation of s under pure mode 2 loading

$$\rho_f = \rho + s\,\rho^*$$

$$\rho = 0$$

-**Method 1:** direct comparison between the mean stress obtained by a sharp V-notch along the direction of provisional crack propagation (Sih, Erdogan-Sih) and the maximum stress along the edge of the notch with radius r_f (normal stress, von Mises, Beltrami, plane stress e plane strain)

-**Method 2:** Neuber's approach, by using the analytical frame for notches with "end holes at the tip" and evaluation of the fictitious notch radius (normal stress only)

- **Method 3:** Numerical method (trial and error) considering a sharp V-notch and a round notch with an end hole.

Method 1

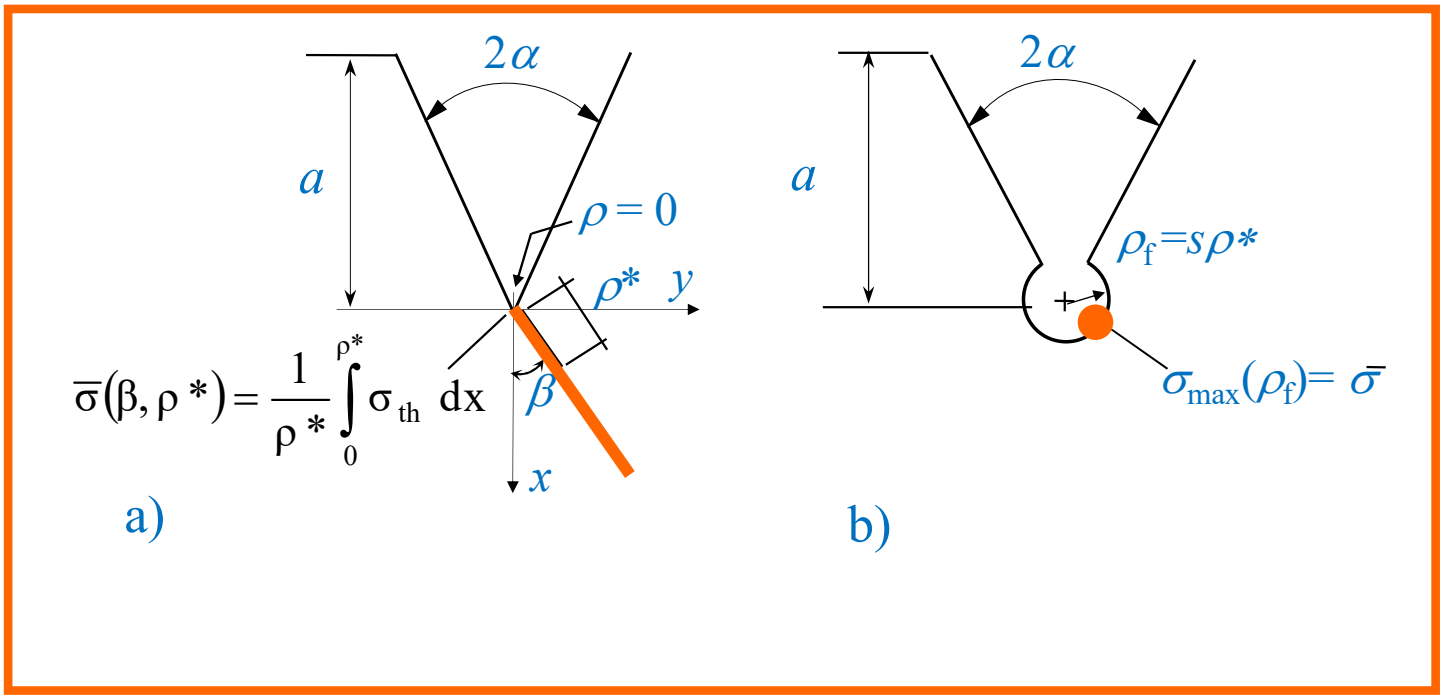

$$\bar{\sigma}(\beta, \rho^*) = \frac{1}{\rho^*} \int_0^{\rho^*} \sigma_{th}\, dx$$

Method 1: direct comparison between the mean stress obtained by a sharp V-notch along the direction of provisional crack propagation (Sih, Erdogan-Sih) and the maximum stress along the edge of the notch with radius rf (normal stress, von Mises, Beltrami, plane stress e plane strain)

Method 1

Notch (end-hole at the tip)

$$\sigma_{max} = \frac{\xi_\theta}{\sqrt{2\pi}\,\rho_f^{\,1-\lambda_2}}$$

Comparison between the averaged stress (sharp notch) and the maximum stress along the notch edge (blunt notch with end-hole)

$$-\frac{(1+\lambda_2)(\rho^*)^{\lambda_2}\left(\chi_2 \sin[\beta(1+\lambda_2)] + \sin[(1-\lambda_2)\beta]\right)}{\lambda_2\sqrt{2\pi}\rho^*\left(1+\lambda_2(-1+\chi_2)+\chi_2\right)} = \frac{1}{\sqrt{2\pi}(\rho_f)^{1-\lambda_2}}\xi_\theta$$

$$\rho_f = \left(-\frac{(1+\lambda_2)\left(\chi_2 \sin[\beta(1+\lambda_2)] + \sin[(1-\lambda_2)\beta]\right)}{\xi_\theta\,\lambda_2\left(1+\lambda_2(-1+\chi_2)+\chi_2\right)}\right)^{\frac{1}{-1+\lambda_2}}\rho^*$$

Method 2

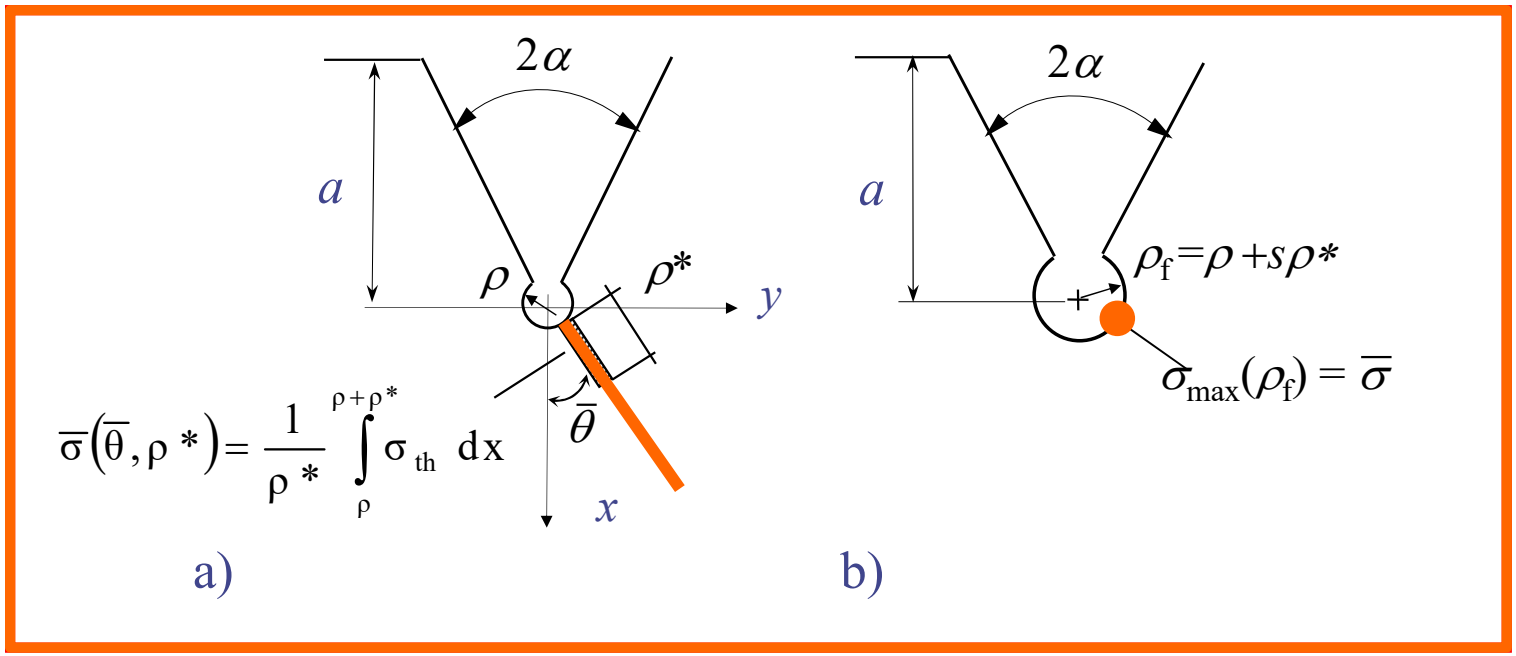

Method 2: Neuber's approach, by using the analytical frame for notches with "end holes at the tip" and evaluation of the fictitious notch radius (normal stress only)

Method 3

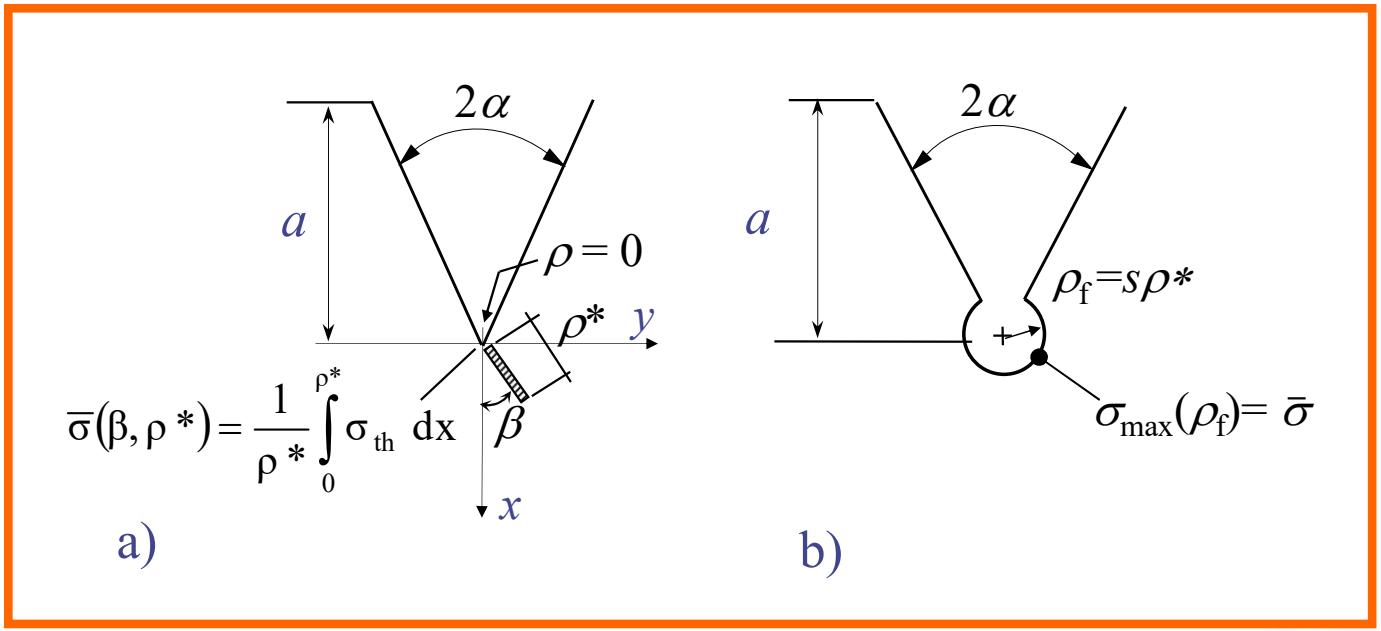

Method 3: Numerical approach

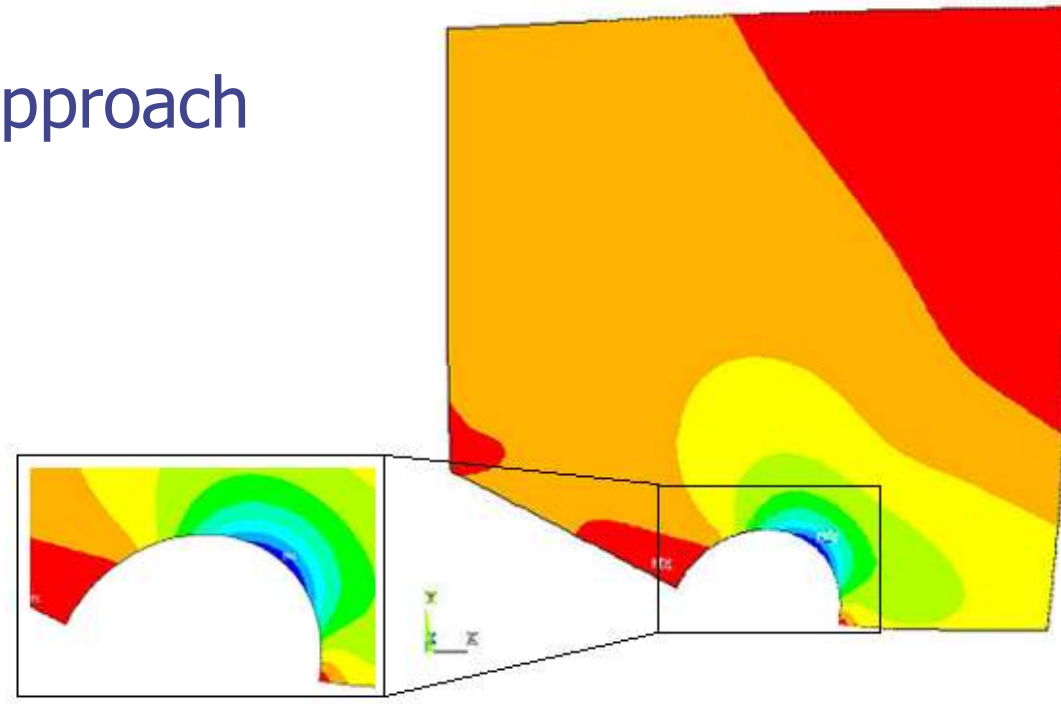

Multiaxiality factor s

Normal stress (Rankine) MTS and MSED

	MTS (plane stress and plane strain)		
2α	Method 1	Method 2	Method 3
0°	3.06	3.06	3.13
30°	6.34	6.40	6.35
45°	11.87	11.97	11.90
60°	33.03	33.45	33.00

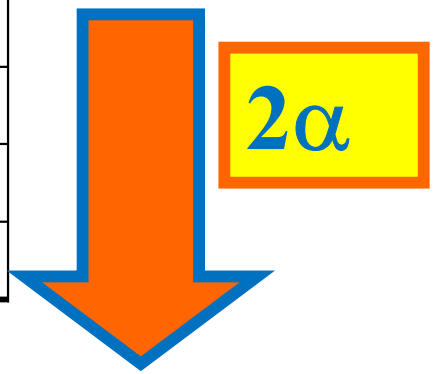

	MSED (plane stress)	MSED (plane strain)
2α	Method 1	Method 1
0°	3.03	2.99
30°	6.15	6.12
45°	11.32	11.31
60°	31.00	31.29

Comparison between s for notches with end-hole and blunt notches

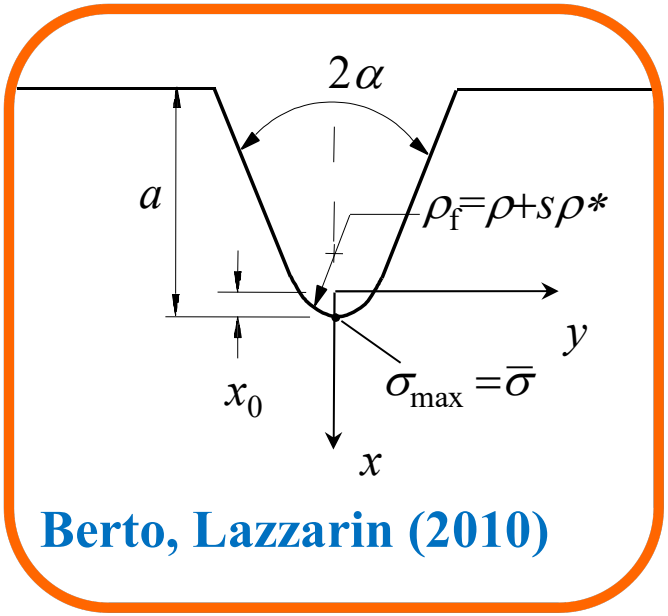

Berto, Lazzarin (2010)

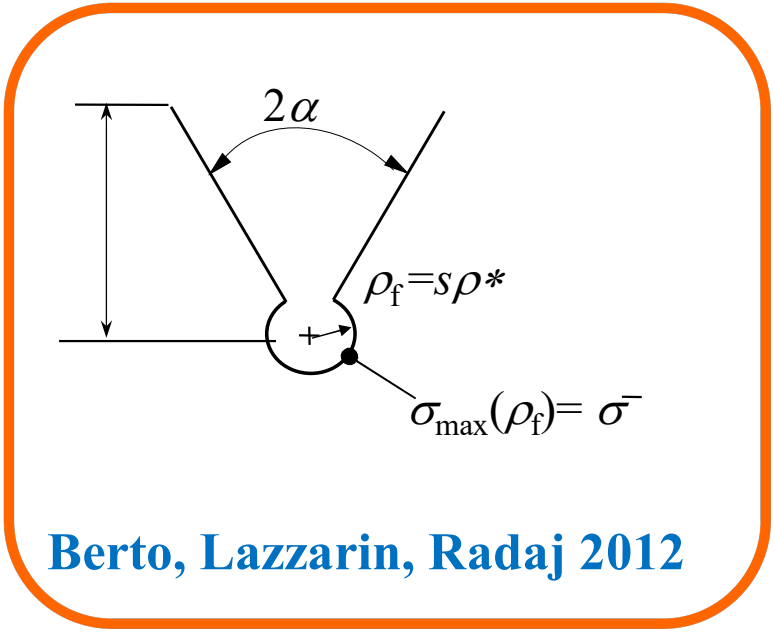

Berto, Lazzarin, Radaj 2012

	MTS	MSED (plane strain)	MSED (plane strain)
2α	Method 3	Method 3	Method 3
0°	2.47	2.46	2.45
30°	4.00	3.90	3.85
45°	5.90	5.59	5.40
60°	10.90	10.00	9.46

	MTS (plane stress and plane strain)		
2α	Method 1	Method 2	Method 3
0°	3.06	3.06	3.13
30°	6.34	6.40	6.35
45°	11.87	11.97	11.90
60°	33.03	33.45	33.00

Multiaxiality factor under PURE MODE 2

MTS

	Factor *s*				
2α	Normal stress	von Mises plane stress	von Mises plane strain	Beltrami plane stress	Beltrami plane strain
0°	3.06	3.06	3.88	3.06	3.37
30°	6.34	5.05	5.93	5.44	5.83
45°	11.87	7.60	9.27	9.02	9.62
60°	33.03	17.75	20.44	21.03	22.43

MSED

	Factor *s*					
2α	Normal Stress Plane stress	Normal stress Plane strain	von Mises plane stress	von Mises plane strain	Beltrami plane stress	Beltrami plane strain
0°	3.03	2.99	3.31	4.75	3.17	3.60
30°	6.15	6.12	5.97	8.10	6.01	6.75
45°	11.32	11.31	10.19	13.87	10.54	11.89
60°	31.00	31.29	25.17	35.61	26.82	30.79

Application of the FNR approach under pure mode 2 loading

$$\bar{\sigma} = \frac{1}{\rho^*}\int_0^{\rho^*} \sigma_{th}(\beta, r)\, dr$$

$$\bar{K}_t = \frac{\bar{\sigma}}{\tau_0} = \frac{1}{\rho^* \tau_0}\int_0^{\rho^*} \sigma_{th}\, dr$$

$$K_t(\rho_f) = \frac{\sigma_{max}(\rho^*, s)}{\tau_0}$$

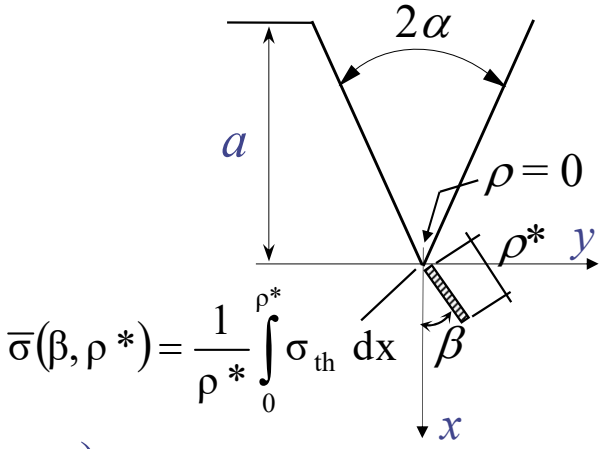

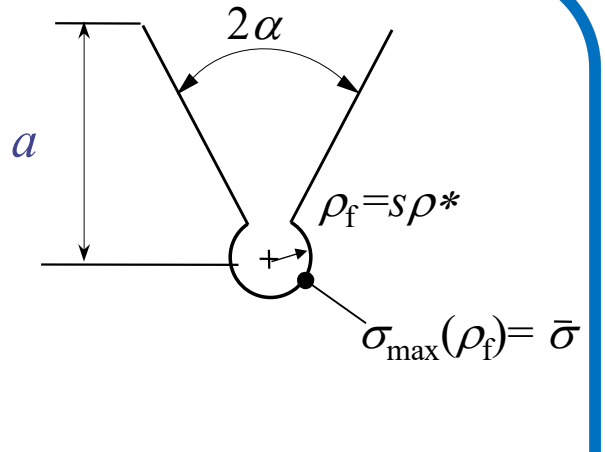

$$\Delta = \frac{K_t(\rho_f) - \bar{K}_t}{K_t(\rho_f)}$$

Application of the FNR approach under pure mode 2 loading

FNR results according to the normal stress failure criterion combined with the MTS criterion for β; different values of ρ^* and notch depth a; in-plane-shear loading.

Notch depth			a=10 mm			a=50 mm		
	ρ^*	ρ_f[mm]	$K_t(\rho_f)$	$\overline{K}_t$	Δ %	$K_t(\rho_f)$	$\overline{K}_t$	Δ %
2α=0°	0.05	0.153	22.97	23.07	-0.45	50.50	50.27	0.46
s=3.06	0.10	0.306	16.40	16.31	0.52	35.77	35.54	0.63
	0.20	0.612	11.80	11.54	2.23	25.34	25.13	0.82
	0.30	0.918	9.82	9.42	4.12	20.74	20.52	1.05
	0.40	1.224	8.68	8.16	6.07	18.00	17.77	1.27
2α=30°	0.05	0.32	14.67	14.63	0.25	27.05	27.09	-0.15
s=6.40	0.10	0.64	11.14	11.07	0.58	20.48	20.50	-0.11
	0.20	1.28	8.50	8.38	1.43	15.49	15.52	-0.17
	0.30	1.92	7.32	7.12	2.77	13.15	13.18	-0.25
	0.40	2.56	6.64	6.34	4.40	11.70	11.74	-0.36
2α=45°	0.05	0.60	10.76	10.80	-0.36	17.96	18.02	-0.32
s=11.97	0.10	1.20	8.50	8.53	-0.37	14.17	14.23	-0.45
	0.20	2.39	6.75	6.74	0.15	11.15	11.25	-0.85
	0.30	3.59	5.97	5.87	1.62	9.68	9.80	-1.25
	0.40	4.79	5.53	5.32	3.64	8.74	8.88	-1.69
2α=60°	0.05	1.67	7.39	7.45	-0.79	11.02	11.02	0.03
s=33.45	0.10	3.35	6.08	6.18	-1.69	9.09	9.14	-0.55
	0.20	6.69	5.13	5.13	-0.06	7.43	7.59	-2.11
	0.30	10.04	/	/	/	6.53	6.80	-4.15
	0.40	13.38	/	/	/	5.91	6.30	-6.46

Application of the FNR approach under pure mode 2 loading

FNR concept combined with the MTS criterion applied with different failure criteria; ρ^*=0.2 mm, a=50 mm and w=50 mm; in-plane shear loading. Abbreviations: vM von Mises criterion, B Beltrami criterion, ps plane stress, pn plane strain.

	2α=0°					2α=30°				
ρ^* = 0.2 mm	s	$\rho_f=s\rho^*$	$K_t(\rho_f)$	$\overline{K}_t$	Δ %	s	$\rho_f=s\rho^*$	$K_t(\rho_f)$	$\overline{K}_t$	Δ %
vM, ps	3.06	0.612	25.60	25.14	1.80	5.05	1.010	16.97	17.00	-0.21
vM, pn	3.88	0.776	22.75	22.35	1.76	5.93	1.186	15.92	15.95	-0.19
B, ps	3.06	0.612	25.60	25.14	1.80	5.44	1.088	16.46	16.51	-0.30
B, pn	3.37	0.674	24.39	23.98	1.68	5.83	1.166	16.03	16.05	-0.13
	2α=45°					2α=60°				
ρ^* = 0.2 mm	s	$\rho_f=s\rho^*$	$K_t(\rho_f)$	$\overline{K}_t$	Δ %	s	$\rho_f=s\rho^*$	$K_t(\rho_f)$	$\overline{K}_t$	Δ %
vM, ps	7.60	1.520	13.02	12.84	1.38	17.75	3.550	8.90	8.97	-0.81
vM, pn	9.27	1.854	12.16	12.23	-0.58	20.44	4.088	8.55	8.64	-1.07
B, ps	9.02	1.804	12.26	12.35	-0.73	21.03	4.206	8.48	8.57	-1.07
B, pn	9.62	1.924	12.00	12.08	-0.67	22.43	4.486	8.32	8.42	-1.15

Application of the FNR approach under pure mode 2 loading

FNR concept combined with the MSED criterion applied to different failure criteria; ρ^*=0.2 mm, a=50 mm and W=50 mm;

In-plane shear loading. Abbreviations: NS normal stress criterion, vM von Mises criterion, B Beltrami criterion, ps plane stress, pn plane strain

	2α=0°					2α=30°				
ρ^* = 0.2 mm	s	ρ_f=sρ^*	$K_t(\rho_f)$	$\overline{K}_t$	Δ %	s	ρ_f=sρ^*	$K_t(\rho_f)$	$\overline{K}_t$	Δ %
NS, ps	3.03	0.606	25.71	25.25	1.79	6.15	1.230	15.68	15.72	-0.26
NS, pn	2.99	0.598	25.88	25.31	2.20	6.12	1.224	15.70	15.74	-0.26
vM, ps	3.31	0.662	24.61	24.17	1.79	5.97	1.194	15.86	15.89	-0.19
vM, pn	4.75	0.950	20.59	20.17	2.04	8.10	1.620	14.04	14.07	-0.21
B, ps	3.17	0.634	25.14	24.70	1.75	6.01	1.202	15.81	15.85	-0.25
B, pn	3.60	0.720	23.61	23.19	1.78	6.75	1.350	15.10	15.13	-0.20
	2α=45°					2α=60°				
ρ^* = 0.2 mm	s	ρ_f=sρ^*	$K_t(\rho_f)$	$\overline{K}_t$	Δ %	s	ρ_f=sρ^*	$K_t(\rho_f)$	$\overline{K}_t$	Δ %
NS, ps	11.32	2.264	11.35	11.43	-0.71	31.00	6.200	7.56	7.71	-1.92
NS, pn	11.31	2.262	11.35	11.43	-0.71	31.29	6.258	7.54	7.70	-2.07
vM, ps	10.19	2.038	11.77	11.84	-0.60	25.17	5.034	8.04	8.16	-1.51
vM, pn	13.87	2.774	10.57	10.66	-0.85	35.61	7.122	7.25	7.44	-2.56
B, ps	10.54	2.108	11.63	11.71	-0.69	26.82	5.364	7.89	8.02	-1.59
B, pn	11.89	2.378	11.16	11.24	-0.72	30.79	6.158	7.58	7.73	-1.98

Theory of Critical Distance

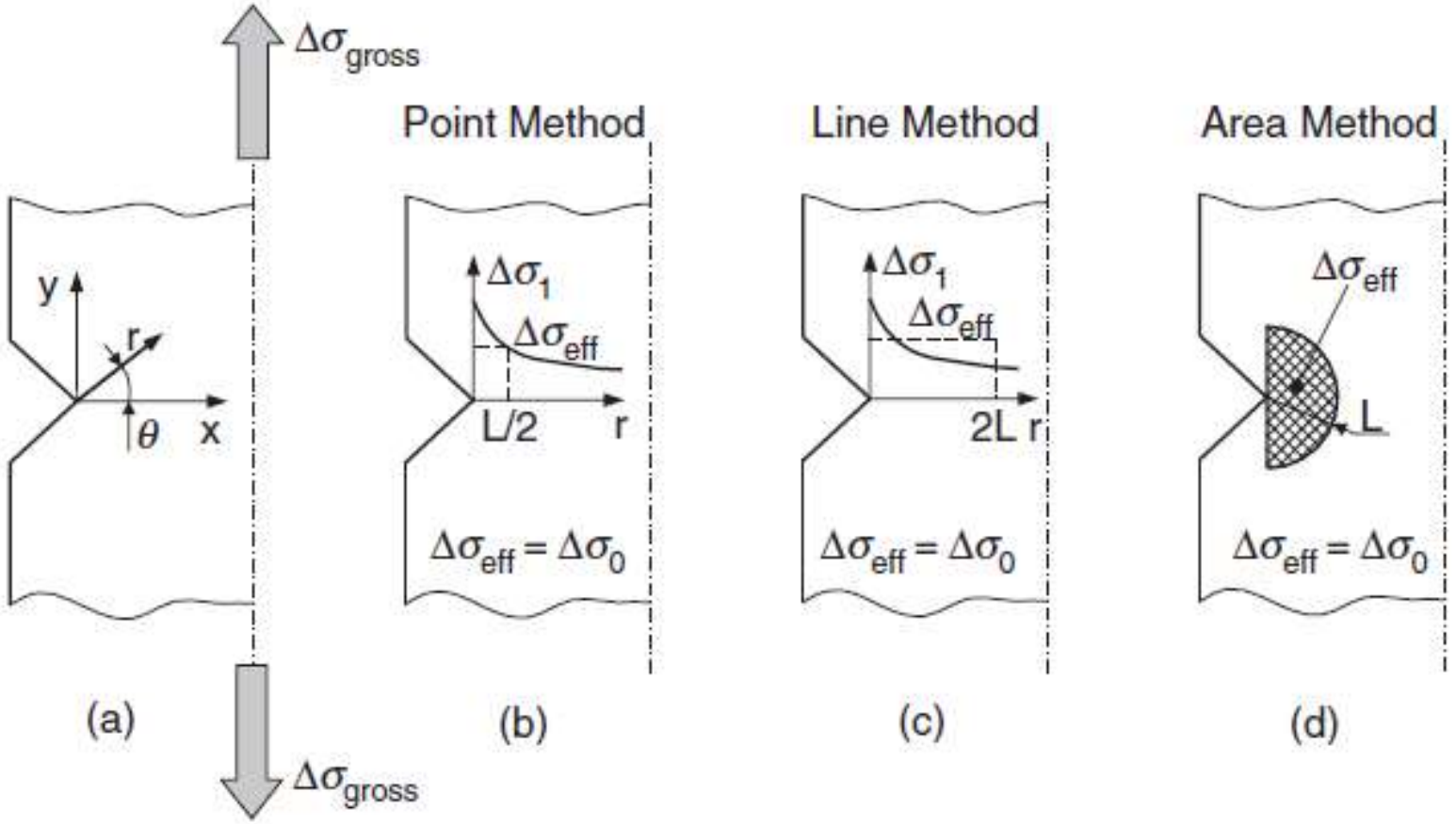

D. Taylor, The Theory of Critical Distances 2007

L. Susmel, Multiaxial Notch Fatigue 2009

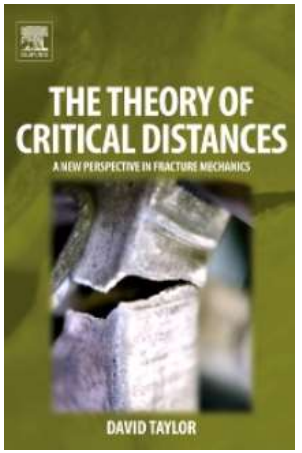

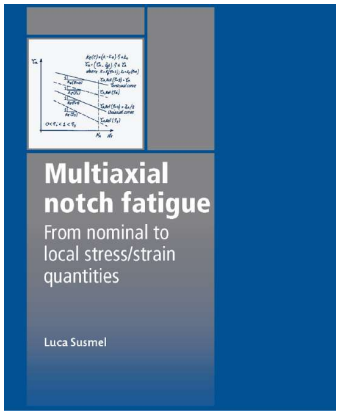

Peterson RE. Notch sensitivity. In: Sines G, Waisman JL, editors. Metal fatigue. New York, USA: McGraw Hill; 1959. p. 293–306.

Tanaka K. Engineering formulae for fatigue strength reduction due to cracklike notches. Int J Fract 1983;22:R39–46.

Taylor D. Geometrical effects in fatigue: a unifying theoretical model. Int J Fatigue 1999;21:413–20.

Seweryn A. Brittle fracture criterion for structures with sharp notches. Eng Fract Mech 1994;47:673–81.

A. Seweryn

K. Tanaka

ENGINEERING FORMULAE FOR FATIGUE STRENGTH REDUCTION DUE TO CRACK-LIKE NOTCHES

K. Tanaka
Department of Mechanical Engineering and Mechanics, Lehigh University
Bethlehem, Pennsylvania 18015 USA
tel: (215) 861-4547

Among fatigue engineers, it is well known that the fatigue strength reduction factor K_f is lower than the elastic stress concentration factor K_t. This discrepancy means that the highest stress alone is no longer appropriate for characterizing the microprocess of fatigue occurring in the microstructure at the notch tip. To rectify this microstructural size effect, Neuber [1-3] has hypothesized that the controlling fracture parameter is the mean stress over the structural size ahead of the notch tip. On the other hand, Ishibashi [4] and Peterson [5] postulated that the controlling factor is the stress at the distance of the structural size ahead of the notch tip. Both Neuber [1] and Peterson [5] started with the stress distribution for deep notches and derived the following approximate formulae of the K_f-K_t relationship which were claimed to be applicable to various notches:

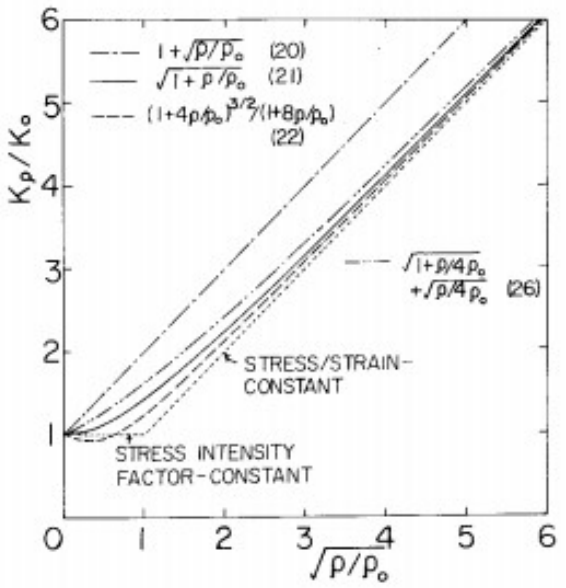

Figure 4. Effect of notch-tip radius on critical stress intensity.

$$\overline{\sigma}_o = \frac{1}{\ell_o}\int_a^{a+\ell_o} \sigma_y\, dx = \frac{1}{\ell_o}\int_o^{\ell_o} \sigma_y\, dx'$$

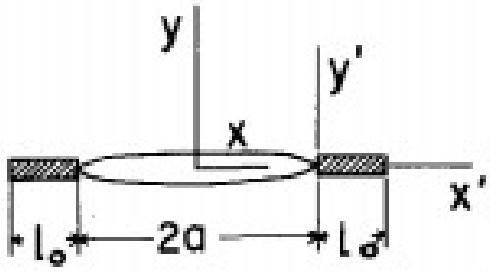

Volume method

S. Sheppard

Sheppard, S. D. (1991) Field effects in fatigue crack initiation:long life fatigue strength.Trans. ASME. J. Mech. Des.113,188–194

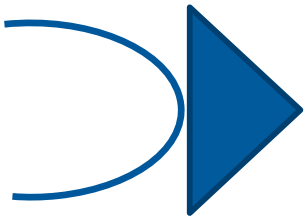

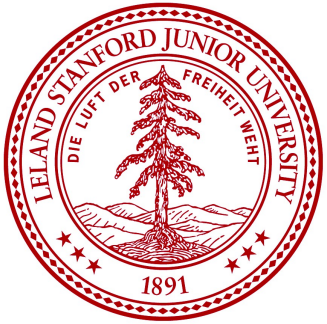

A semi-circular sector of radius M (then restricted to the inscribed triangle) was used, for example, by Sheppard who quantified the stress state near a notch by means of a single parameter, the average value of the principal stress

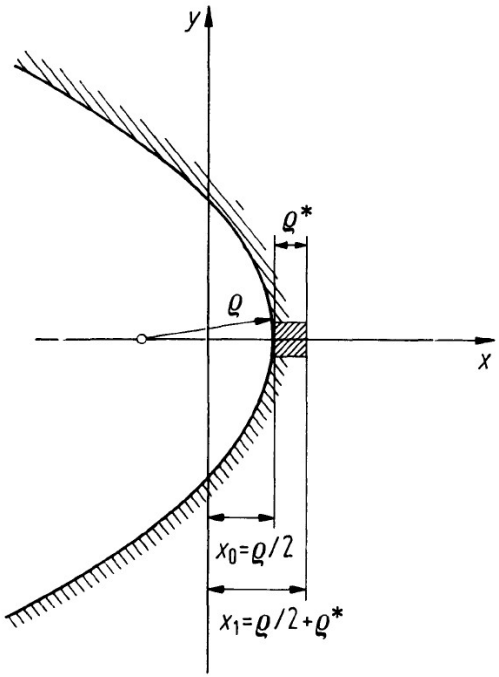

Bild 4.8. Zur Definition der Mikrostützwirkung

Die gemäß dem Konzept der Mikrostützwirkung gewonnenen Spannungen seien „fiktive Spannungen" genannt und mit σ_F bezeichnet. Es gilt

$$\sigma_F = \frac{1}{\varrho^*} \int_{x_0}^{x_1} \sigma_e dx = 4C_1 / \sqrt{\varrho_F / 2}. \tag{16}$$

Die fiktiven Spannungen können direkt auf (9) bezogen werden, wenn der Krümmungsradius ϱ formal durch den „fiktiven" Krümmungsradius ϱ_F ersetzt wird, wie die rechte Seite von (16) zeigt. Damit ist das Verfahren der Mikrostützwirkung auf die Ermittlung von ϱ_F zurückgeführt.

Bei Anwendung auf *die 0°-Spitzkerbe bzw. den Riß* ($\varrho = 0$) ergibt sich für die erste, zweite und dritte Hypothese der gemeinsame Wert

$$\varrho_F = 2\varrho^*. \tag{17}$$

BRITTLE FRACTURE CRITERION FOR STRUCTURES WITH SHARP NOTCHES

ANDRZEJ SEWERYN

Białystok Technical University, Faculty of Mechanics, ul. Wiejska 45C, 15-351 Białystok, Poland

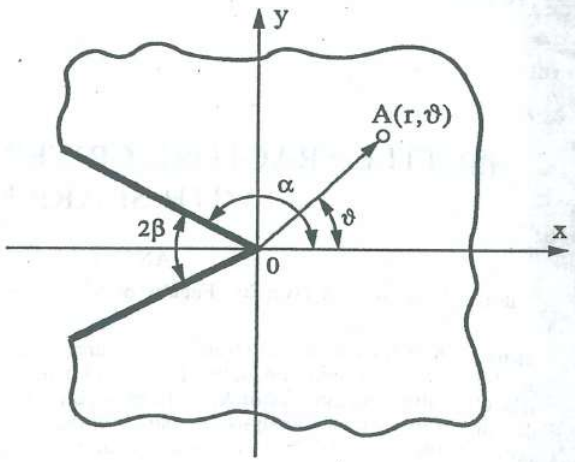

Fig. 1. Notch geometry in polar coordinate system.

The Mode I stress intensity factor K_I, the Mode II stress intensity factor K_{II} and III stress intensity factor K_{III} for V-shaped notches may be defined in a manner similar to for cracks [5, 6]

$$K_I = \lim_{\vartheta=0\, r\to 0+} [(2\pi r)^{\lambda_I}\sigma_\vartheta],$$

$$K_{II} = \lim_{\vartheta=0\, r\to 0+} [(2\pi r)^{\lambda_{II}}\tau_{r\vartheta}],$$

$$K_{III} = \lim_{\vartheta=0\, r\to 0+} [(2\pi r)^{\lambda_{III}}\tau_{z\vartheta}],$$

$$\max\left(\int_0^{d_o} \sigma_\vartheta \, dr\right) \geqslant d_o \sigma_c,$$

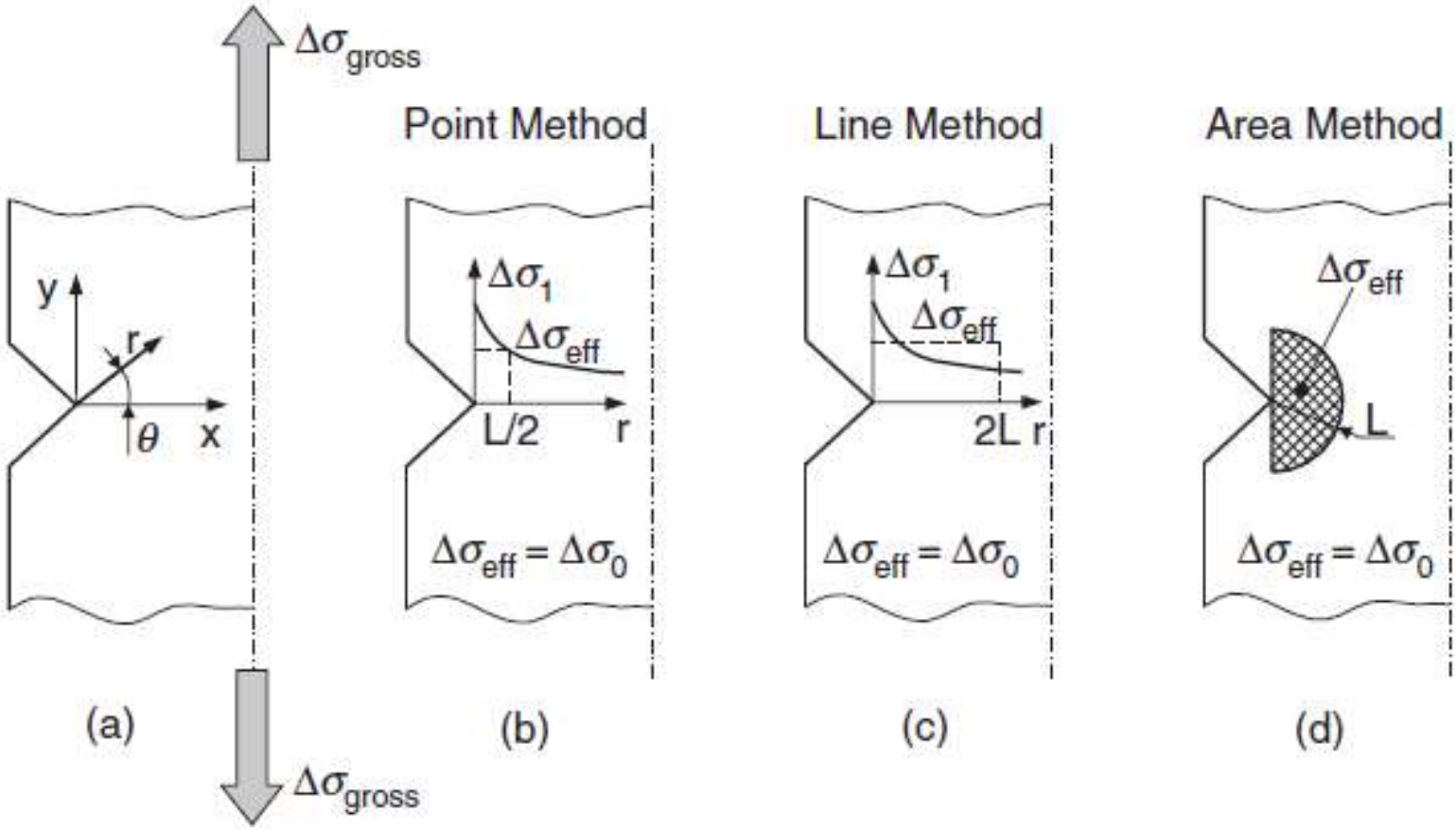

$$\Delta\sigma_{\text{eff}} = \Delta\sigma_1\left(\theta = 0, r = \frac{L}{2}\right) = \Delta\sigma_0$$ Point Method

$$\Delta\sigma_{\text{eff}} = \frac{1}{2L}\int_0^{2L} \Delta\sigma_1(\theta = 0, r)\,\mathrm{d}r = \Delta\sigma_0$$ Line Method

$$\Delta\sigma_{\text{eff}} = \frac{4}{\pi L^2}\int_0^{\pi/2}\int_0^{L} \Delta\sigma_1(\theta, r)\cdot r\cdot \mathrm{d}r\cdot \mathrm{d}\theta \cong \Delta\sigma_0$$ Area Method

Brittle Failure by TCD

Cylindrical Plain Specimen

Tubular Plain Torsional Specimen

V-Notched Cylindrical Specimen
(r_n=0.2 mm)

V-Notched Cylindrical Specimen
(r_n=0.4 mm)

V-Notched Cylindrical Specimen
(r_n=1.2 mm)

V-Notched Cylindrical Specimen
(r_n=4.0 mm)

V-Notched Flat Specimen
(r_n=0.2 mm)

V-Notched Flat Specimen
(r_n=0.4 mm)

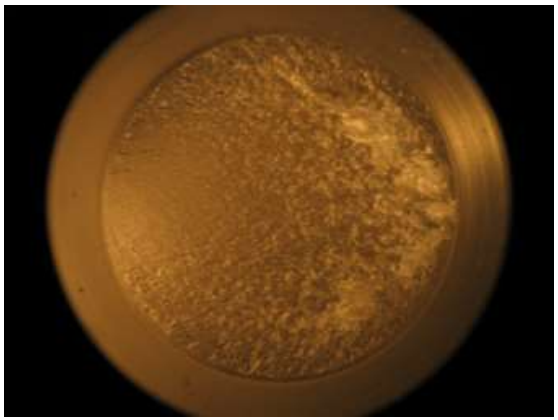

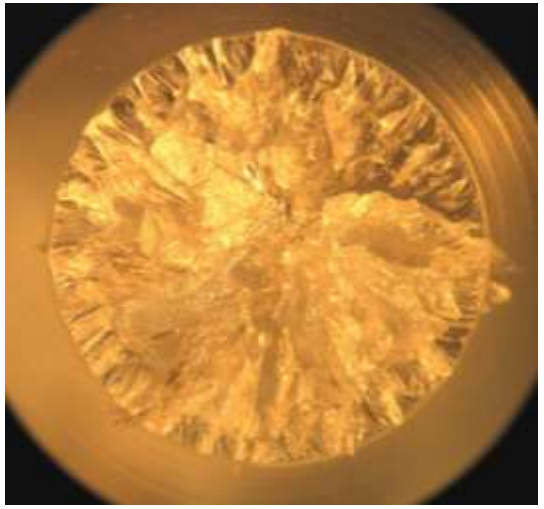

L. Susmel, D. Taylor, Engineering Fracture Mechanics 75 (2008) 534–550

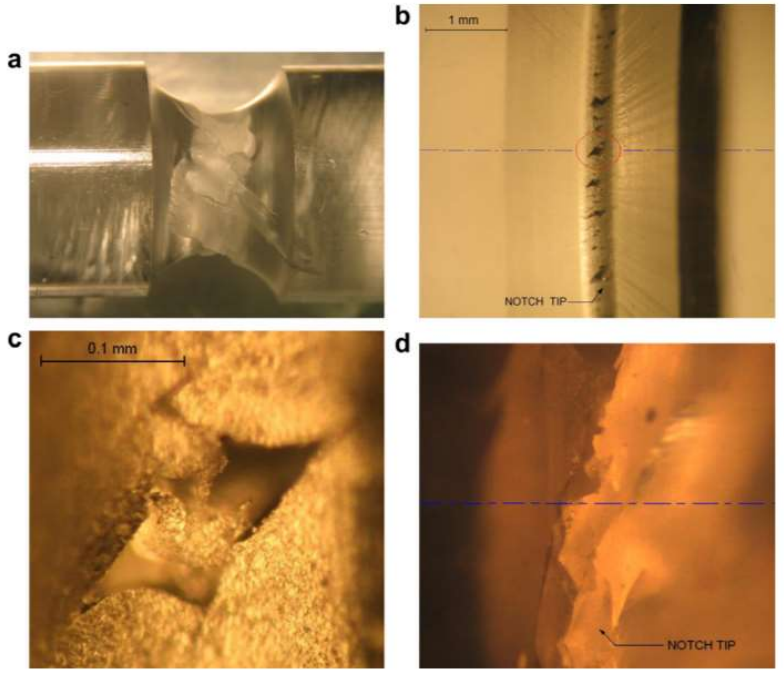

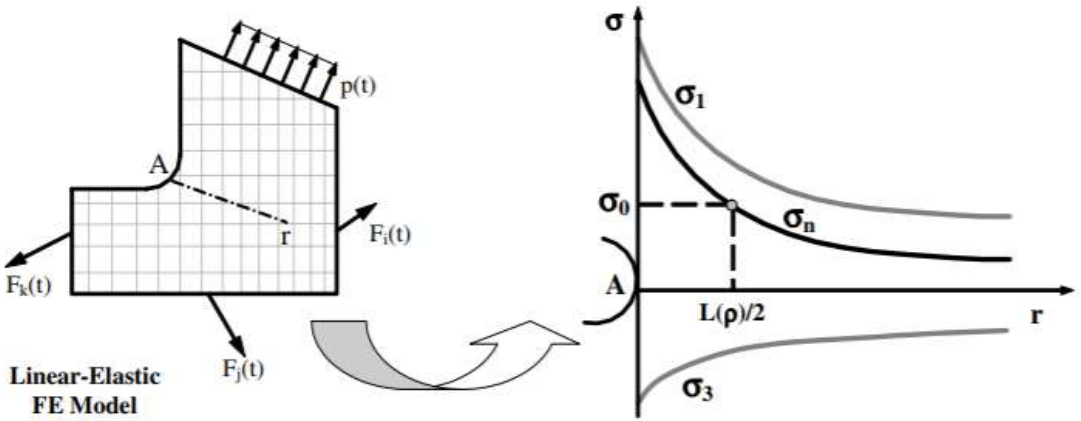

Multiaxial PM accuracy in predicting failures in the tested notched specimens

σ_{nom}/τ_{nom}	σ_{eff} [MPa]				Error [%]		
	$r_n = 0.2$ mm	$r_n = 0.4$ mm	$r_n = 1.2$ mm	$r_n = 4.0$ mm	$r_n = 0.2$ mm	$r_n = 0.4$ mm	$r_n = 1.2$ mm
∞	119.4	120.6	100.1	71.3	4.9	5.9	−12.1
1	127.8	128.2	125.3	109.9	12.2	12.6	10.0
0.55	134.5	126.1	105.7	91.3	18.1	10.7	−7.2
0.23	110.4	103.1	99.1	81.9	−3.1	−9.5	−13.0
0	113.7	117.5	115.1	65.2	−0.2	3.2	1.1

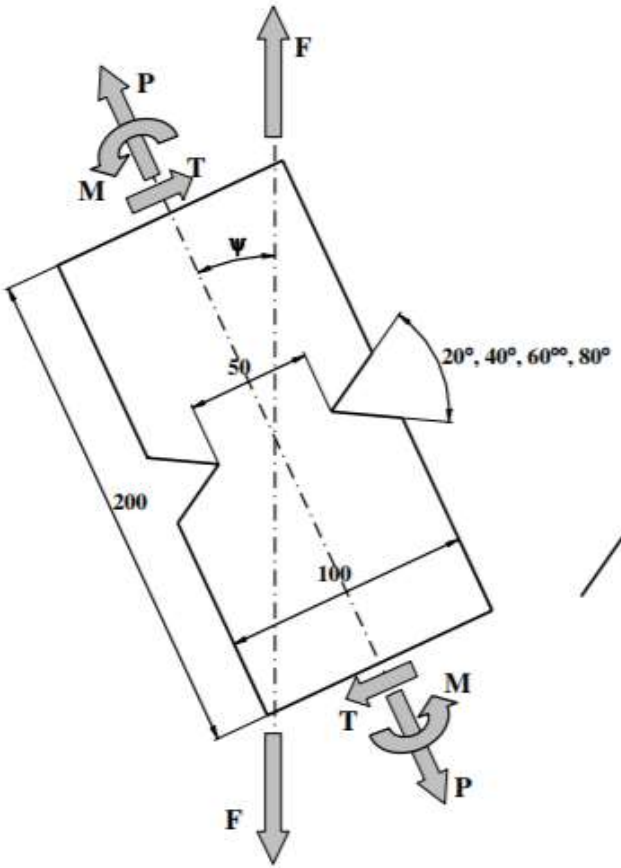
F
P
M
T
ψ
50
20°, 40°, 60°, 80°
200
100
M
T
P
F

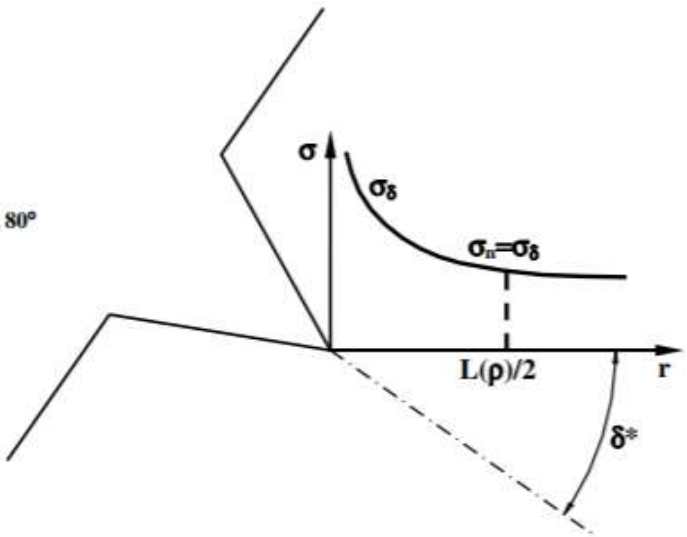
σ
σδ
σn=σδ
L(ρ)/2
r
δ*

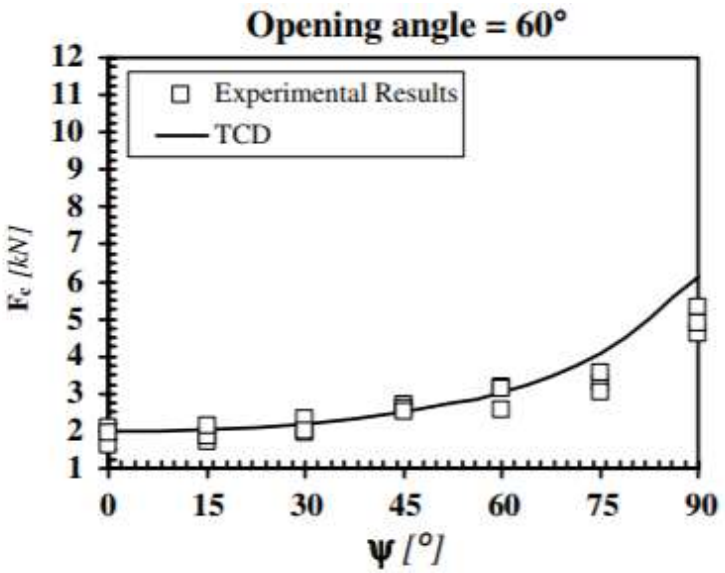
Opening angle = 60°
Experimental Results
TCD
Fc [kN]
ψ [°]
0
15
30
45
60
75
90
1
2
3
4
5
6
7
8
9
10
11
12

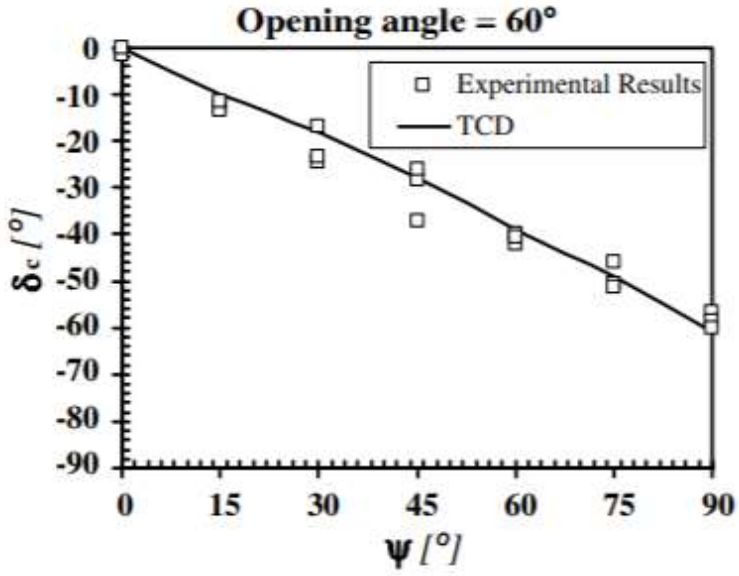
Opening angle = 60°
Experimental Results
TCD
δc [°]
ψ [°]
0
-10
-20
-30
-40
-50
-60
-70
-80
-90
0
15
30
45
60
75
90

Section 2:

Notch Stress Intensity Factors

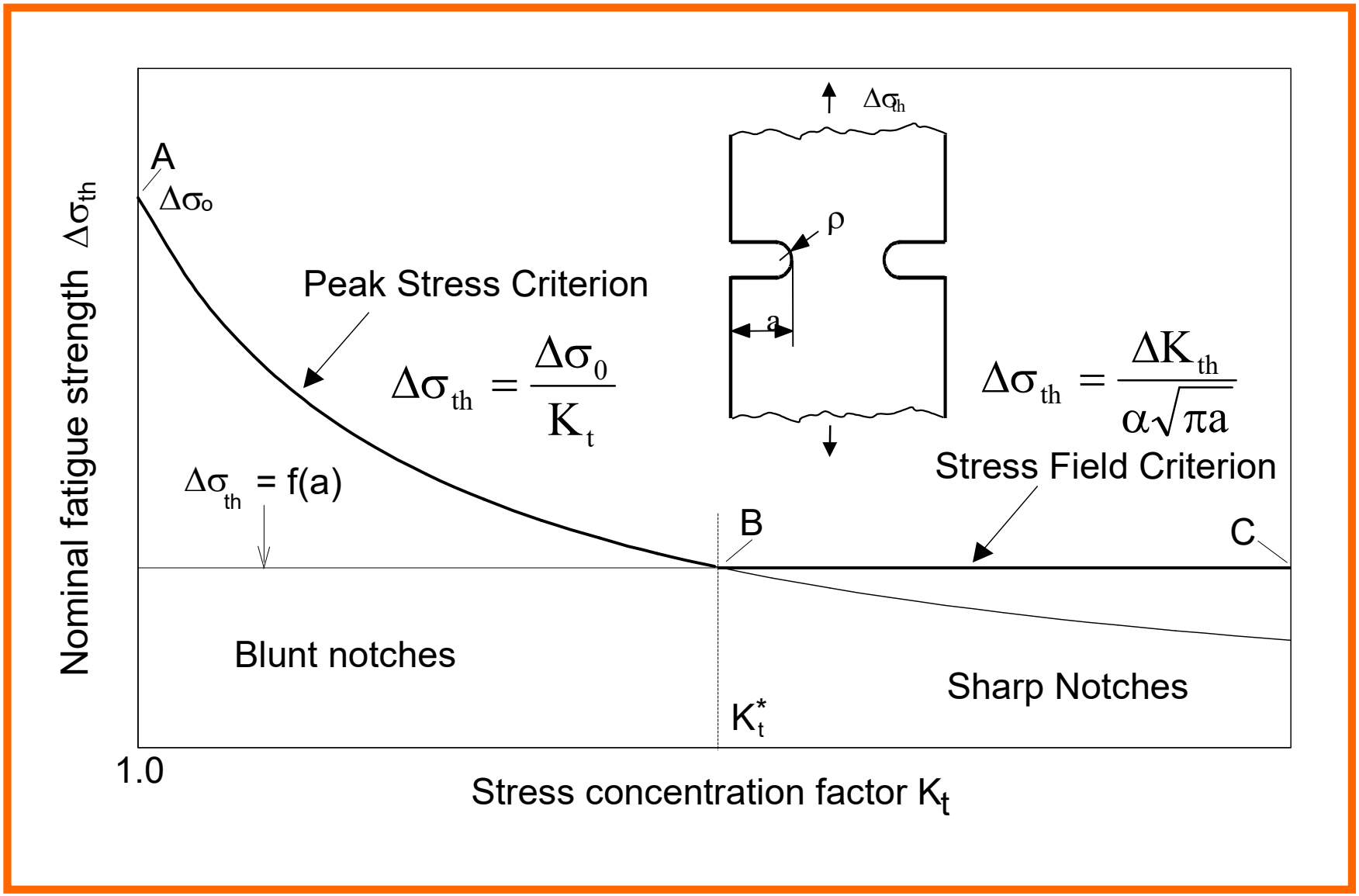

The Frost-Miller diagram

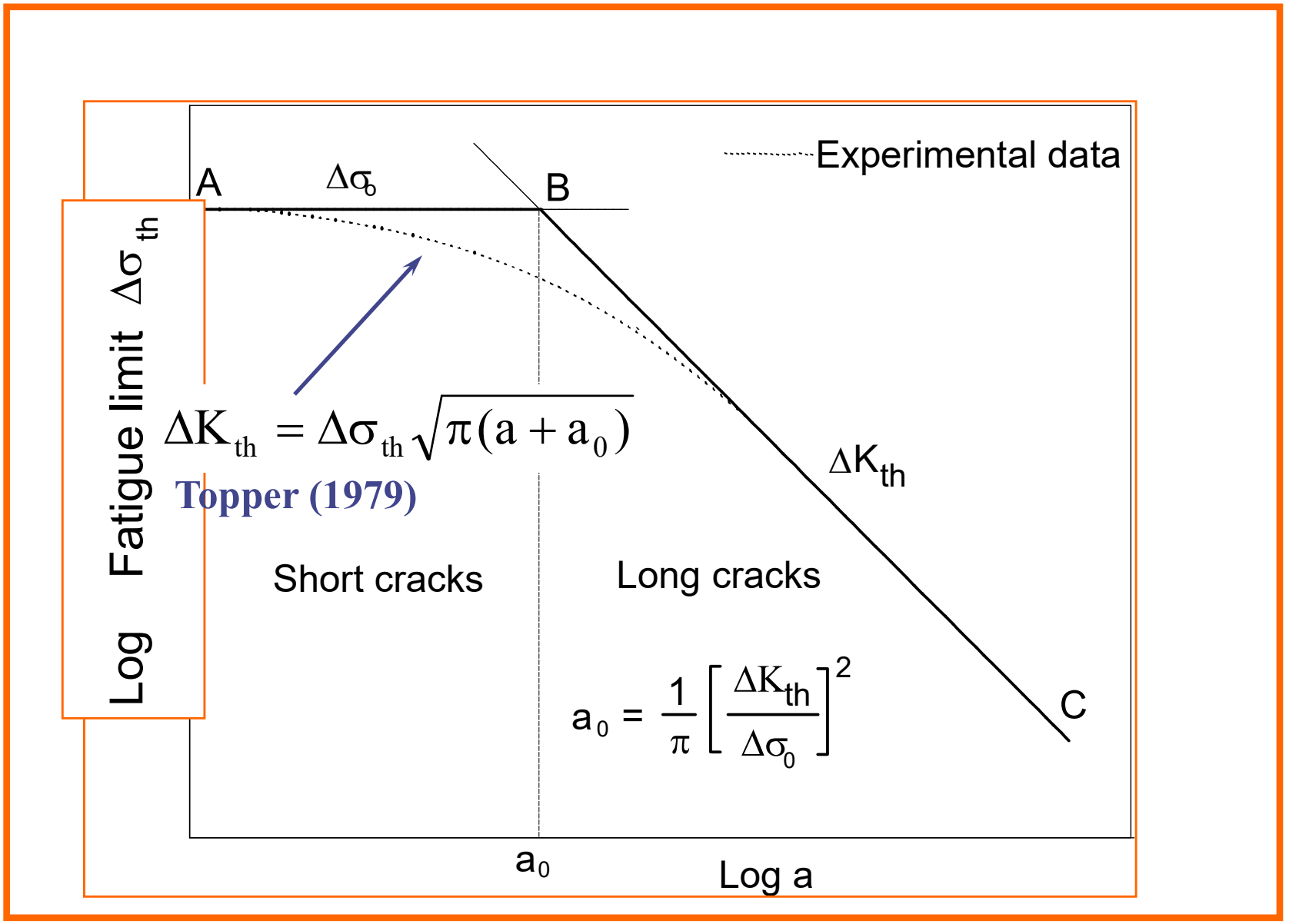

The Kitagawa diagram

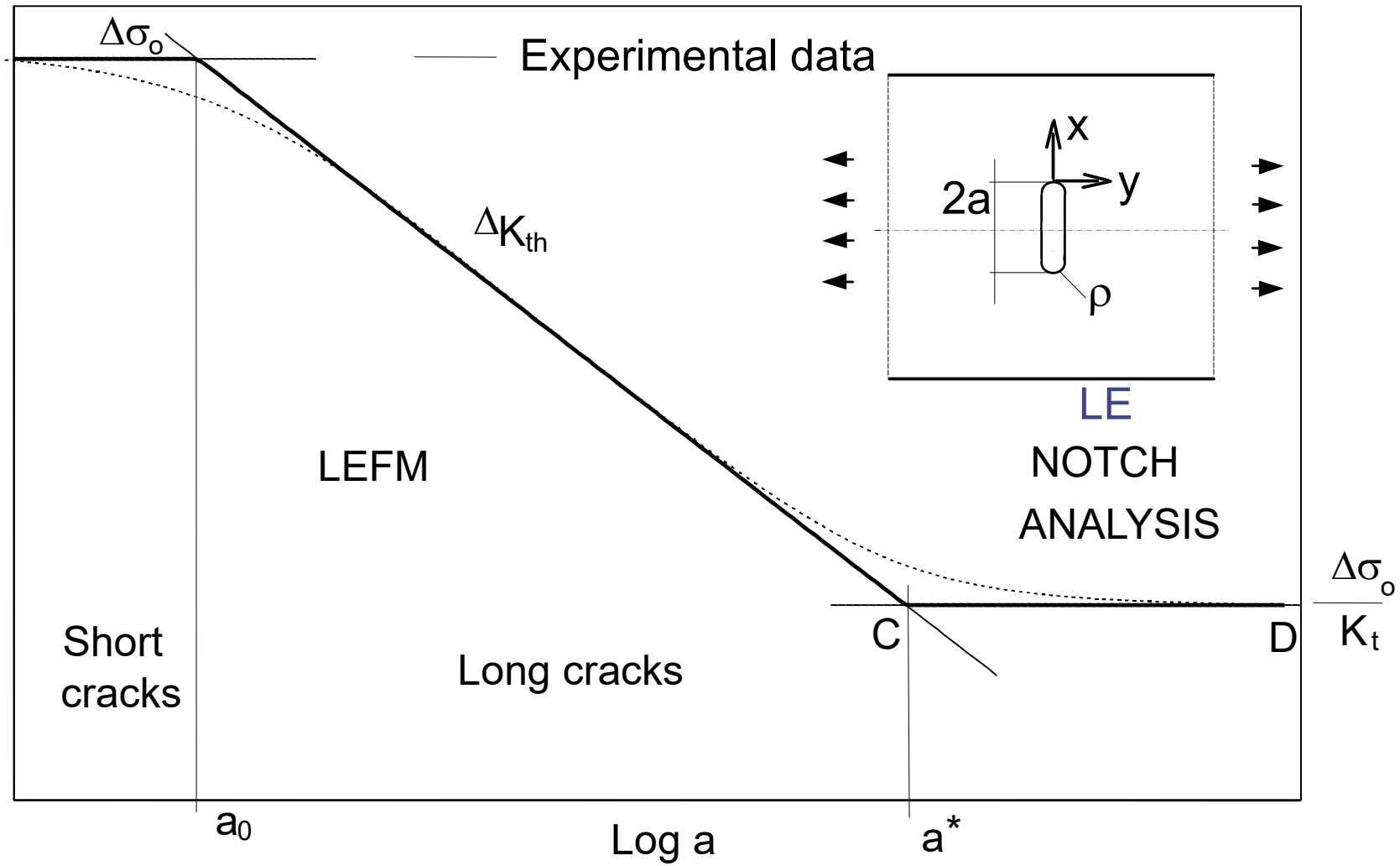

Fatigue behavior of a material weakened by notches or cracks

$$\frac{a^*}{a_0} = K_t^2$$

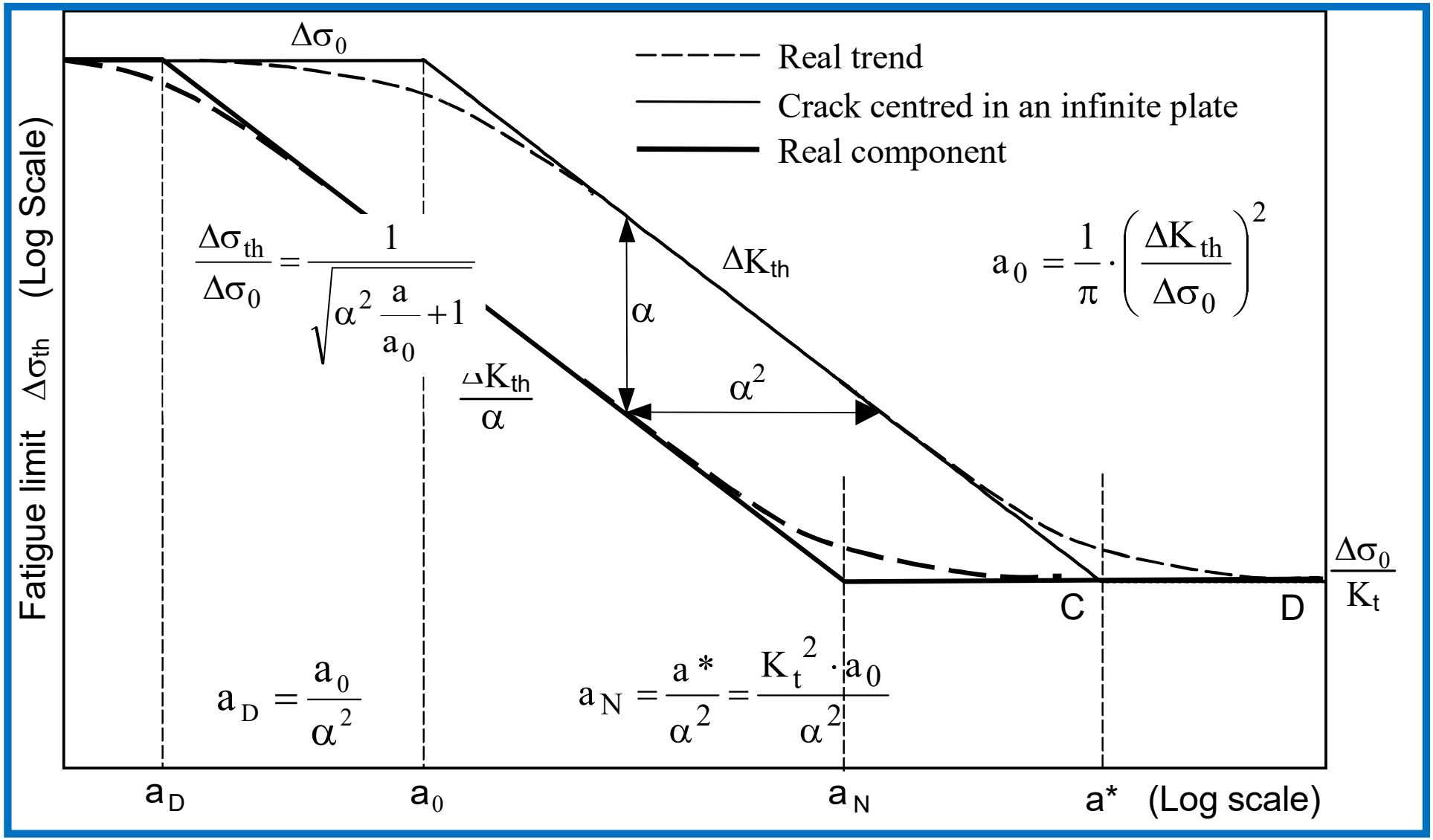

Fatigue behaviour for a real component

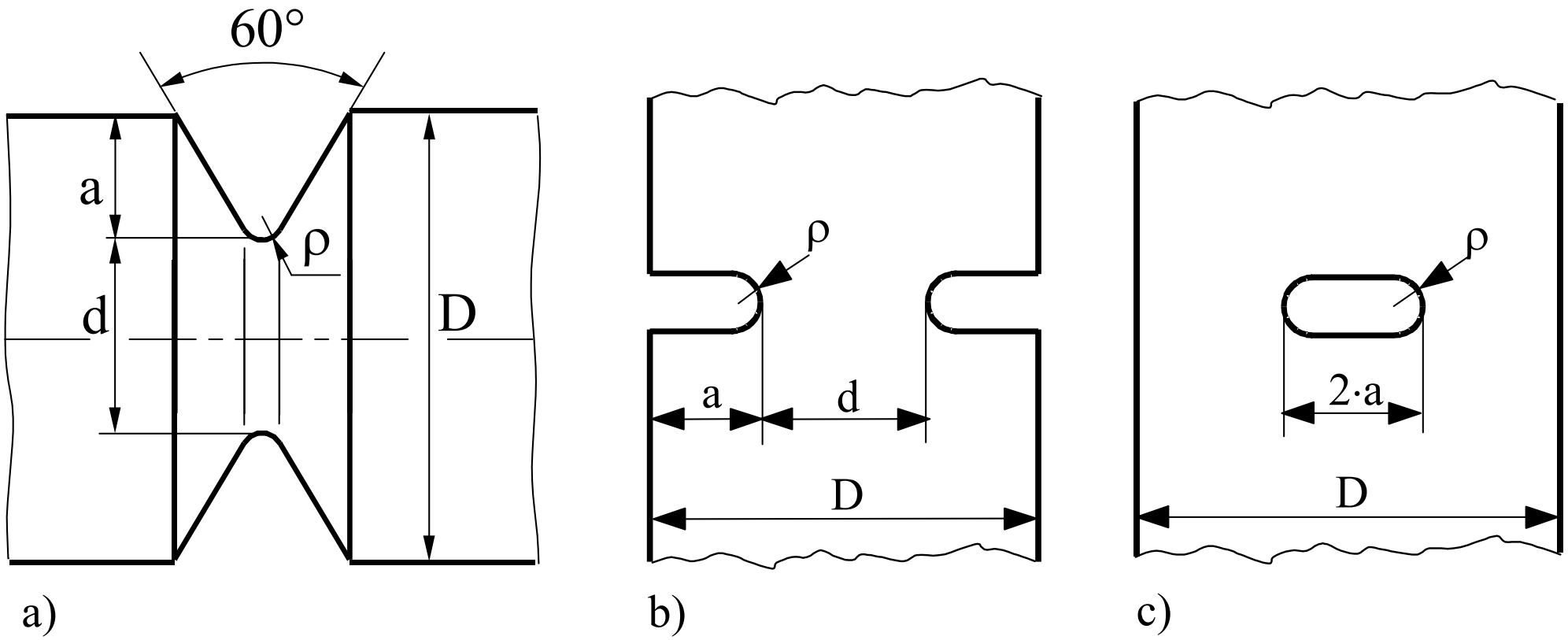

Geometry of the notched specimens:

a) V-shaped notch in a cylindrical bar (CNB),

b) double lateral notch in a flat plate (DENP),

c) hole in a flat plate (CNP).

Materials parameters

Materials	Refs	σ_y (MPa)	$\Delta\sigma_0$ (MPa)	a_0 (μm)	ΔK_{th} (MPa·m$^{0.5}$)	R
Annealed 0.45 carbon steel	[20]	364	582	61 [a]	8.1 [a]	-1
Annealed 0.36 carbon steel	[20]	/	446 [a]	92 [a]	7.6 [a]	-1
SAE 1045 steel	[6]	466	448	76	6.9	0
SAE 1045 steel	[6]	466	606	70	9.0	-1
2024-T351 Al alloy	[6]	360	172	172 [b]	4.0	0
2024-T351 Al alloy	[6]	360	248	100 [b]	4.4	-1
G40.11 steel	[6]	376	540	144	11.5	-1
SM41B steel	[13,21,22]	194	326	457	12.36	-1
	[13,21,22]	194	274	296	8.36	0
	[13,21,22]	194	244	218	6.38	0.4
Mild steel (0.15% C)	[23,18]	340	420	296	12.8	-1
NiCr steel	[24,18]	834	1000	52	12.8	-1
2.25Cr-1Mo steel	[25]	380	440	237	12.0	-1
304 stainless steel	[13,18]	222	720	88	12.0	-1

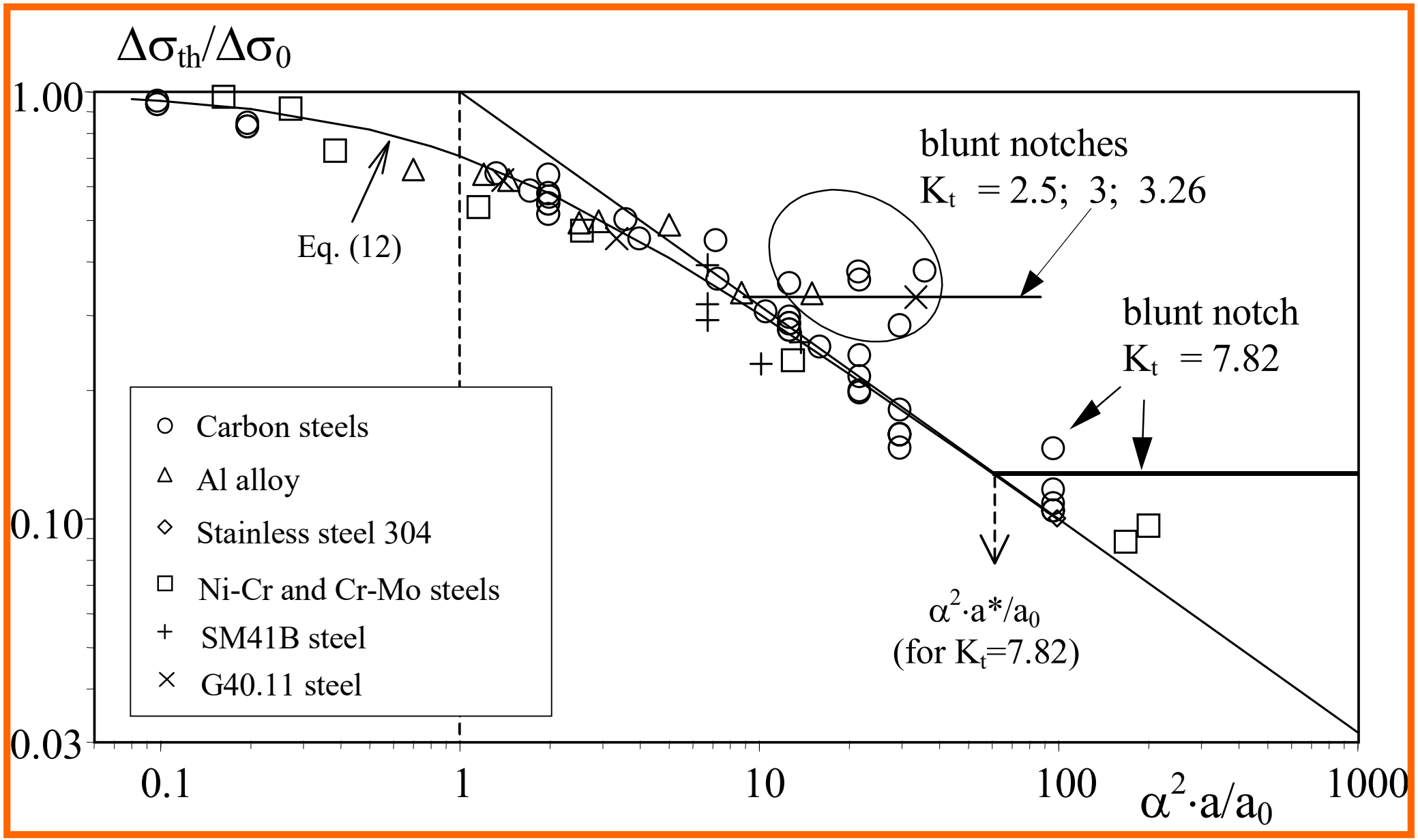

Fatigue strength of specimens containing defects and notches

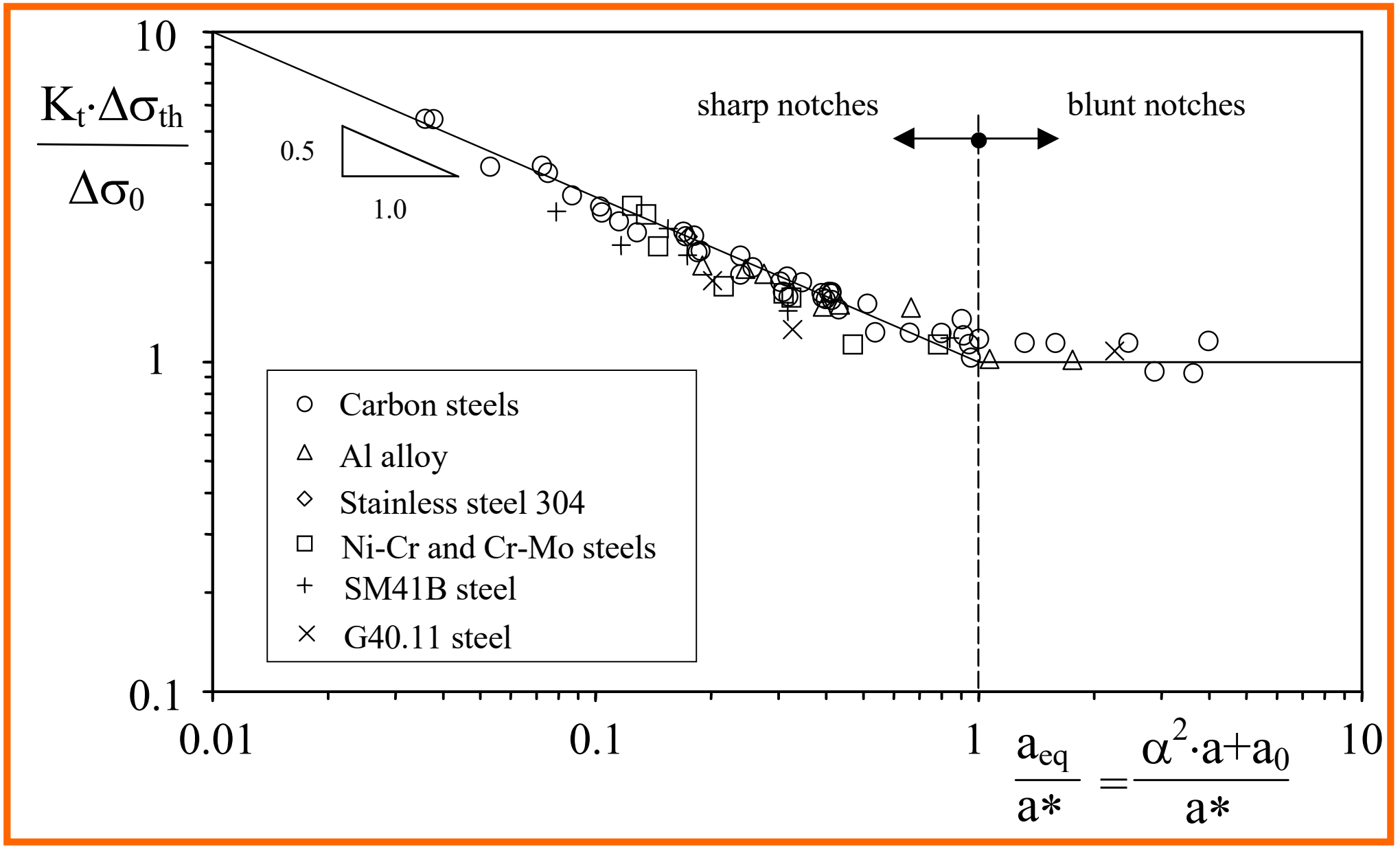

Transition between the fatigue behaviour of sharp and blunt notches versus the equivalent notch size normalised with respect to a*.

NOTCH STRESS DISTRIBUTIONS

For the linear elastic analysis of plane cases, conventional approaches have been soundly established since **Kolosov-Muskhelishvili (1909, 1953) and Neuber (1958), who used complex potential functions and bi-harmonic potential functions, respectively.**

As far as sharp notches are concerned, main contributions have been the crack solution due to **Westergaard (1939) and Irwin (1957) and the sharp V-shaped notch solution due to Williams (1952).**

Blunt cracks, i.e. slim parabolic notches, have been dealt with by **Creager and Paris (1967), and then by Glinka (1985),** who was able to give a closed-form expression to the generalised stress intensity factors in Creager-Paris' equations. In the close neighbourhood of the notch tip, where stress distributions mainly depend on the notch tip radius, such equations continue to be a very powerful tool.

COMPLEX POTENTIAL FUNCTIONS

$$\varphi(z) = a\,z^{\lambda} + d\,z^{\mu}$$

$$\psi(z) = b\,z^{\lambda} + c\,z^{\mu}$$

- coefficients a, b, c and d are complex,
- exponents λ and μ are real, with $\lambda > 0$ and $\lambda > \mu$.

When c and d are null, the approach matches Williams' solution (Williams, 1952, Carpenter, 1984).

Then, the general expressions of stress components turn out to be:

$$\begin{aligned}\sigma_\theta = {} & \lambda r^{\lambda-1}\left[a_1(1+\lambda)\cos(1-\lambda)\theta + b_1\cos(1+\lambda)\theta + a_2(1+\lambda)\sin(1-\lambda)\theta - b_2\sin(1+\lambda)\theta\right] + \\ & + \mu r^{\mu-1}\left[d_1(1+\mu)\cos(1-\mu)\theta + c_1\cos(1+\mu)\theta + d_2(1+\mu)\sin(1-\mu)\theta - c_2\sin(1+\mu)\theta\right]\end{aligned}$$

$$\begin{aligned}\sigma_r = {} & \lambda r^{\lambda-1}\left[a_1(3-\lambda)\cos(1-\lambda)\theta - b_1\cos(1+\lambda)\theta + a_2(3-\lambda)\sin(1-\lambda)\theta + b_2\sin(1+\lambda)\theta\right] \\ & + \mu r^{\mu-1}\left[d_1(3-\mu)\cos(1-\mu)\theta - c_1\cos(1+\mu)\theta + d_2(3-\mu)\sin(1-\mu)\theta + c_2\sin(1+\mu)\theta\right]\end{aligned}$$

$$\begin{aligned}\tau_{r\theta} = {} & \lambda r^{\lambda-1}\left[a_1(1-\lambda)\sin(1-\lambda)\theta + b_1\sin(1+\lambda)\theta - a_2(1-\lambda)\cos(1-\lambda)\theta + b_2\cos(1+\lambda)\theta\right] + \\ & + \mu r^{\mu-1}\left[d_1(1-\mu)\sin(1-\mu)\theta + c_1\sin(1+\mu)\theta - d_2(1-\mu)\cos(1-\mu)\theta + c_2\cos(1+\mu)\theta\right]\end{aligned}$$

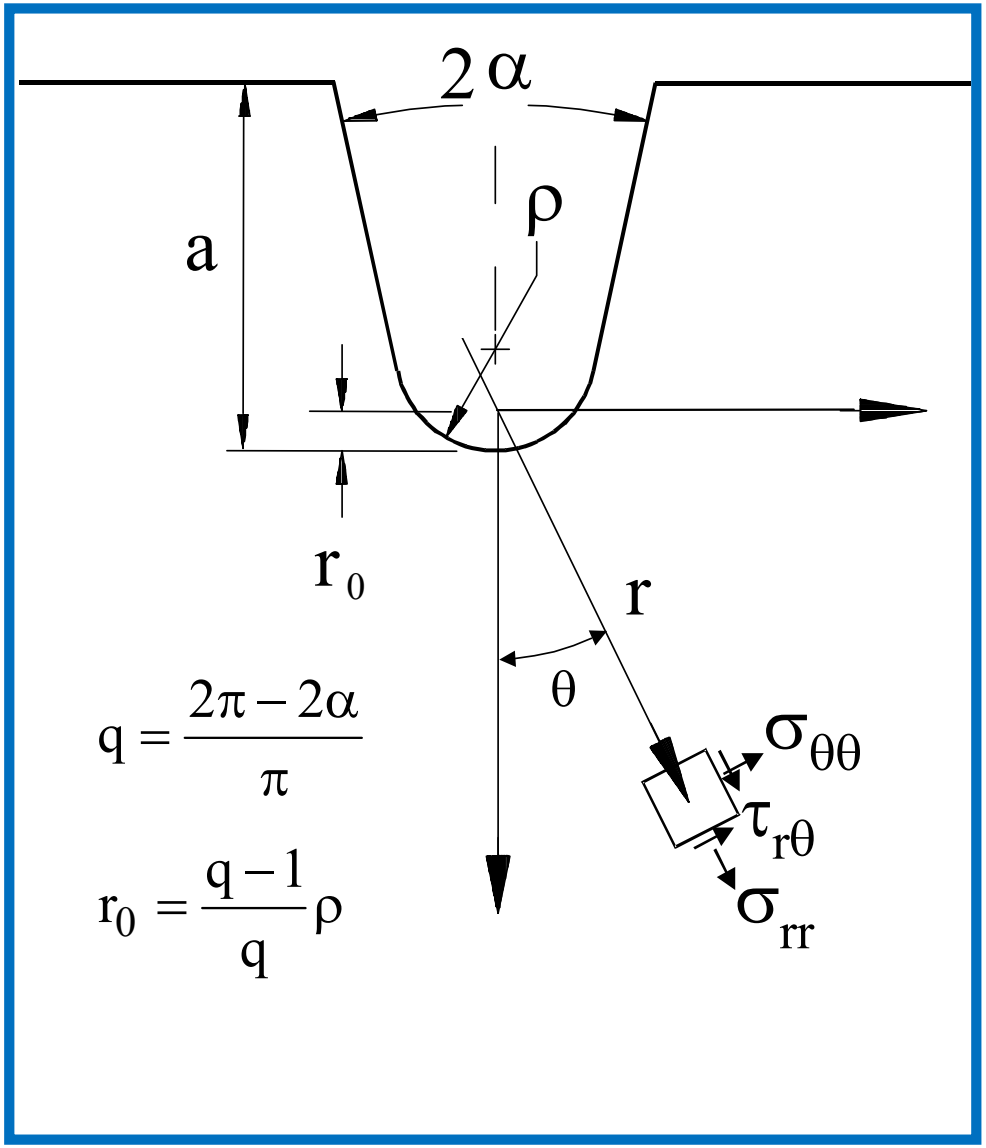

Coordinate system and symbols used for the stress field components.

Lazzarin and Tovo 1996

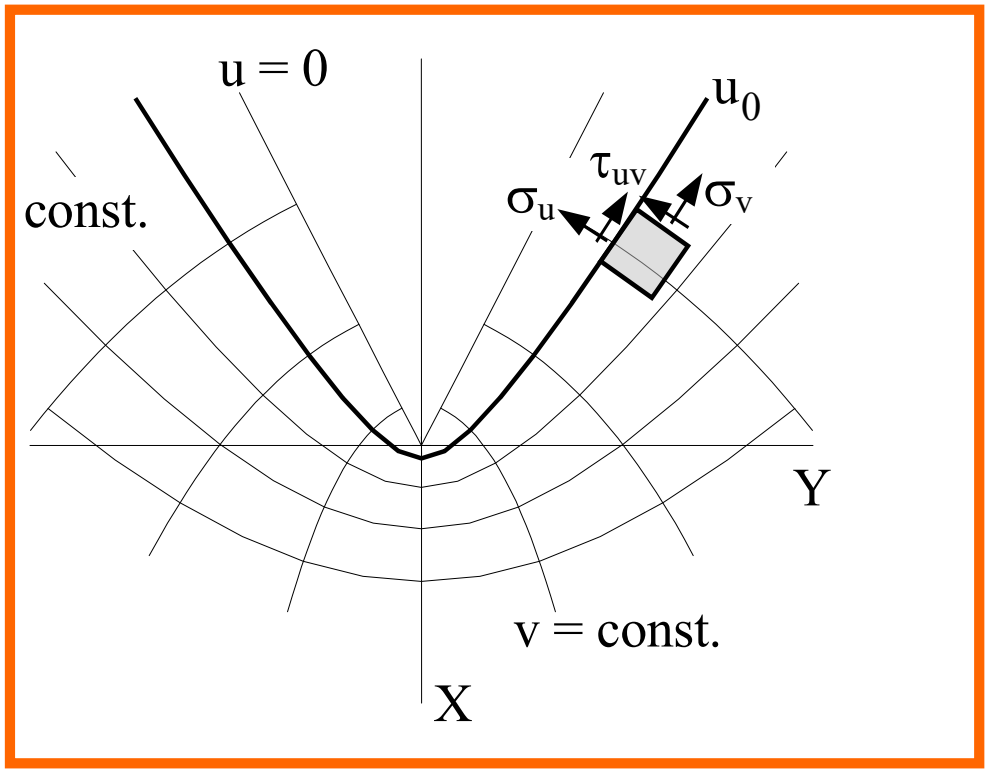

Auxiliary system based on curvilinear coordinates (u, v)

$$\left(\sigma_u\right)_{\substack{u=u_0\\v=0}} = \left(\sigma_r\right)_{\substack{r=r_0\\\theta=0}} = 0$$

$$\left(\tau_{uv}\right)_{\substack{u=u_0\\v=0}} = \left(\tau_{r\theta}\right)_{\substack{r=r_0\\\theta=0}} = 0$$

$$\left(\frac{\partial\sigma_u}{\partial v}\right)_{\substack{u=u_0\\v=0}} = \left(\frac{\partial\sigma_r}{\partial\theta} - \frac{2}{q}\tau_{r\theta}\right)_{\substack{r=r_0\\\theta=0}} = 0$$

$$\left(\frac{\partial\tau_{uv}}{\partial v}\right)_{\substack{u=u_o\\v=0}} = \left(\frac{\partial\tau_{r\theta}}{\partial\theta} - \frac{1}{q}\sigma_\theta\right)_{\substack{r=r_0\\\theta=0}} = 0$$

$$\left(\sigma_u\right)_{\substack{u=u_0\\v>>v_0}} = 0 \Rightarrow \lim_{\substack{r\to\infty\\\theta\to\pm q\frac{\pi}{2}}} \left(r^{1-\lambda}\,\sigma_\theta\right) = 0$$

$$\left(\tau_{uv}\right)_{\substack{u=u_0\\v>>v_0}} = 0 \Rightarrow \lim_{\substack{r\to\infty\\\theta\to\pm q\frac{\pi}{2}}} \left(r^{1-\lambda}\,\tau_{r\theta}\right) = 0$$

Conditions on the free edge, far away from the notch tip, lead to the following equations for

$$\sin(\lambda_1 q \pi) + \lambda_1 \sin(\pi q) = 0 \qquad \textbf{(Mode I)}$$

$$\sin(\lambda_2 q \pi) - \lambda_2 \sin(\pi q) = 0 \qquad \textbf{(Mode II)}$$

In general, Eqs. give n-solutions or eigenvalues.

The problem being linear, the general solution can be given as a linear combination of all particular solutions (Williams, 1957, Carpenter 1984, 1985).

However, the state of stress and displacement near the corner is dominated by the first eigenvector so that only the eigenvalue with the lowest modulus have been considered in our analyses.

Stresses due to Mode I loading

$$\begin{Bmatrix}\sigma_\theta\\ \sigma_r\\ \tau_{r\theta}\end{Bmatrix} = \lambda_1 r^{\lambda_1-1} a_1 \left[\begin{Bmatrix}(1+\lambda_1)\cos(1-\lambda_1)\theta\\ (3-\lambda_1)\cos(1-\lambda_1)\theta\\ (1-\lambda_1)\sin(1-\lambda_1)\theta\end{Bmatrix} + \chi_{b_1}(1-\lambda_1)\begin{Bmatrix}\cos(1+\lambda_1)\theta\\ -\cos(1+\lambda_1)\theta\\ \sin(1+\lambda_1)\theta\end{Bmatrix} + \right.$$

$$\left. + \frac{q}{4(q-1)}\left(\frac{r}{r_0}\right)^{\mu_1-\lambda_1}\left(\chi_{d_1}\begin{Bmatrix}(1+\mu_1)\cos(1-\mu_1)\theta\\ (3-\mu_1)\cos(1-\mu_1)\theta\\ (1-\mu_1)\sin(1-\mu_1)\theta\end{Bmatrix} + \chi_{c_1}\begin{Bmatrix}\cos(1+\mu_1)\theta\\ -\cos(1+\mu_1)\theta\\ \sin(1+\mu_1)\theta\end{Bmatrix}\right)\right]$$

Stresses due to Mode II loading

$$\begin{Bmatrix}\sigma_\theta\\ \sigma_r\\ \tau_{r\theta}\end{Bmatrix} = \lambda_2 r^{\lambda_2-1} a_2 \left[\begin{Bmatrix}(1+\lambda_2)\sin(1-\lambda_2)\theta\\ (3-\lambda_2)\sin(1-\lambda_2)\theta\\ (1-\lambda_2)\cos(1-\lambda_2)\theta\end{Bmatrix} + \chi_{b_2}(1+\lambda_2)\begin{Bmatrix}\sin(1+\lambda_2)\theta\\ -\sin(1+\lambda_2)\theta\\ \cos(1+\lambda_2)\theta\end{Bmatrix} + \right.$$

$$\left. + \frac{1}{4(\mu_2-1)}\left(\frac{r}{r_0}\right)^{\mu_2-\lambda_2}\left(\chi_{d_2}\begin{Bmatrix}(1+\mu_2)\sin(1-\mu_2)\theta\\ (3-\mu_2)\sin(1-\mu_2)\theta\\ (1-\mu_2)\cos(1-\mu_2)\theta\end{Bmatrix} + \chi_{c_2}\begin{Bmatrix}-\sin(1+\mu_2)\theta\\ \sin(1+\mu_2)\theta\\ -\cos(1+\mu_2)\theta\end{Bmatrix}\right)\right]$$

2α	λ_1	μ_1	χ_{b1}	χ_{c1}	χ_{d1}
0	0.5	-0.5	1	4	0
$\pi/4$	0.5050	-0.4319	1.1656	3.5721	0.0828
$\pi/3$	0.5122	-0.4057	1.3123	3.2832	0.0960
$\pi/2$	0.5448	-0.3449	1.8414	2.5057	0.1046
$2\pi/3$	0.6157	-0.2678	3.0027	1.5150	0.0871
$3\pi/4$	0.6736	-0.2198	4.1530	0.9933	0.0673
$5\pi/6$	0.7520	-0.1624	6.3617	0.5137	0.0413

Characteristic parameters for mode I loading.

2α	λ_2	μ_2	χ_{b2}	χ_{c2}	χ_{d2}
0	0.5	-0.5	1	-12	0
$\pi/4$	0.6597	-0.4118	0.8140	-10.1876	-0.4510
$\pi/3$	0.7309	-0.3731	0.6584	-8.3946	-0.4788
$\pi/2$	0.9085	-0.2882	0.2189	-2.9382	-0.2436
$2\pi/3$	1.1489	-0.1980	-0.3139	4.5604	0.5133
$3\pi/4$	1.3021	-0.1514	-0.5695	8.7371	1.1362
$5\pi/6$	1.4858	-0.1034	-0.7869	12.9161	1.9376

Characteristic parameters for mode II loading.

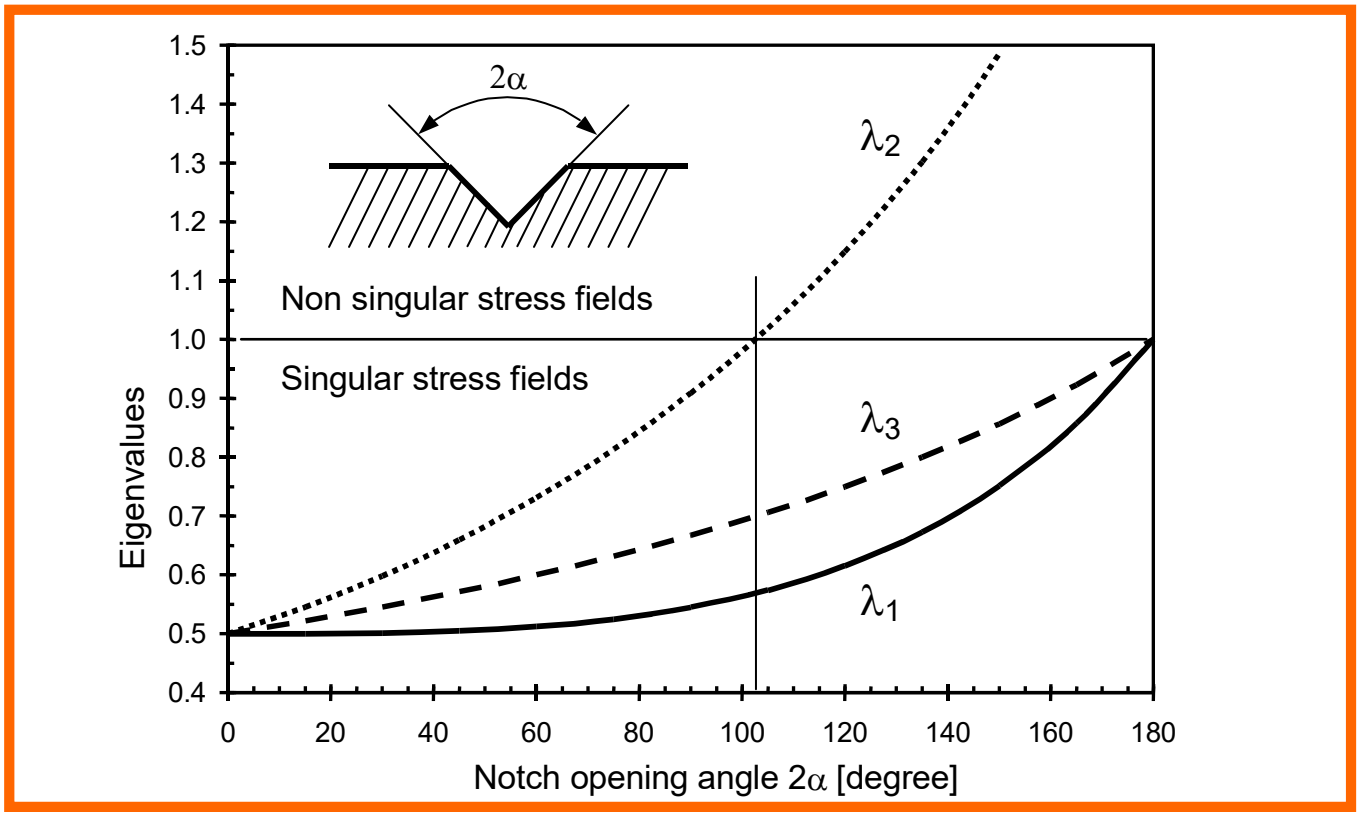

Eigenvalues λ_1, λ_2 and λ_3 against the notch opening angle 2α.

Evaluation of constant a_1

Relationship between constant a_1 and the maximum stress at the tip:

$$a_1 = \frac{\sigma_{max}}{\lambda_1 \, r_0^{\lambda_1 - 1} \left\{ 1 + \lambda_1 + \chi_{b_1} (1 - \lambda_1) + \left[(1 + \mu_1) \chi_{d_1} + \chi_{c_1} \right] \frac{q}{4(q-1)} \right\}}$$

2α=0°

$$\frac{\sigma_{max}}{2\sqrt{2}} \rho^{0.5} \left[(x + 0.5\rho)^{-0.5} + 0.5\rho (x + 0.5\rho)^{-1.5} \right]$$

2α=90°

$$\frac{\sigma_{max}}{3.874} \rho^{0.4555} \left[1.2976 (x + 0.3333\rho)^{-0.4555} + 0.3957 \rho^{0.8894} (x + 0.333\rho)^{-1.3449} \right]$$

2α=135°

$$\frac{\sigma_{max}}{4.940} \rho^{0.3264} \left[2.040 (x + 0.2\rho)^{-0.3264} + 0.2091 \rho^{0.8833} (x + 0.2\rho)^{-1.2197} \right]$$

The stress field in the neighbourhood of the notch tip can be expressed as a function of a stress field parameter, mode I N-SIF. Its definition is consistent with the usual Stress Intensity Factor definition if the notch radius and opening angle are both null.

Gross and Mendelsson (1972) definition:

$$K_I = \sqrt{2\pi} \lim_{r \to 0} (\sigma_\theta)_{\theta=0} \, r^{1-\lambda_1}$$

Smith and Miller (1978) were able to demonstrate that all notches with K_t greater than K_t^* behave identically and can be treated like cracks of the same depth. Under such conditions the choice more convenient is to define K_I on the basis of the stress term with exponent λ.

$$K_I = \lambda_1 \sqrt{2\pi} \left[1 + \lambda_1 + \chi_{b1} \left(1 - \lambda_1\right)\right] a_1$$

where the constant a_1 has to be determined at a convenient distance from the notch tip, where the stress fields of the rounded and sharp notch practically coincide

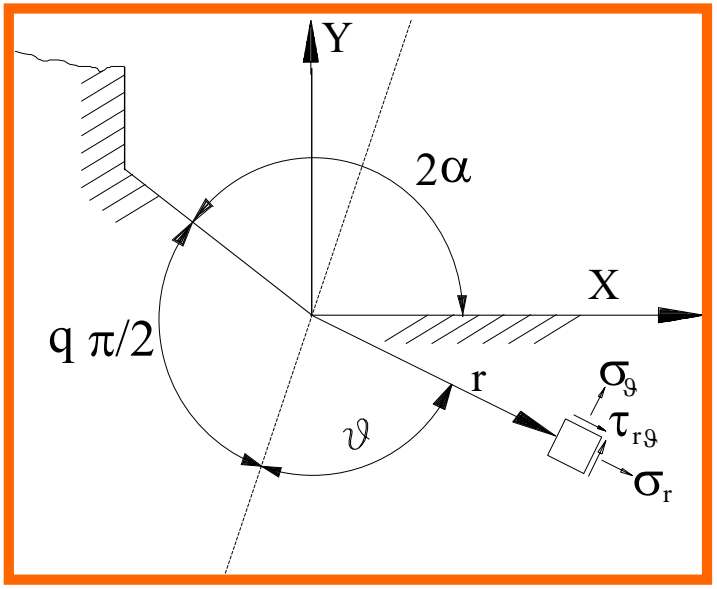

In the direction normal to the main plate ($\theta = 22.5°$)

$$\sigma_\theta = 0.361 \cdot r^{-0.326} \cdot K_1^N + 0.322 \cdot r^{0.302} \cdot K_2^N$$

Along the free edge ($\vartheta = 112.5°$)

$$\sigma_r = K_1 \cdot 0.423 \cdot r^{-0.326} + K_2 \cdot 0.553 \cdot r^{0.302}$$

For Mode I fracture

$$\begin{Bmatrix} \sigma_\vartheta \\ \sigma_r \\ \tau_{r\vartheta} \end{Bmatrix}_{\rho=0} = \frac{1}{\sqrt{2\pi}} \frac{r^{\lambda_1 - 1} K_1}{(1+\lambda_1) + \chi_1 (1-\lambda_1)} \left[\begin{Bmatrix} (1+\lambda_1)\cos(1-\lambda_1)\vartheta \\ (3-\lambda_1)\cos(1-\lambda_1)\vartheta \\ (1-\lambda_1)\sin(1-\lambda_1)\vartheta \end{Bmatrix} + \chi_1 (1-\lambda_1) \begin{Bmatrix} \cos(1+\lambda_1)\vartheta \\ -\cos(1+\lambda_1)\vartheta \\ \sin(1+\lambda_1)\vartheta \end{Bmatrix} \right]$$

For Mode II fracture,

$$\begin{Bmatrix} \sigma_\vartheta \\ \sigma_r \\ \tau_{r\vartheta} \end{Bmatrix}_{\rho=0} = \frac{1}{\sqrt{2\pi}} \frac{r^{\lambda_2 - 1} K_2}{(1-\lambda_2) + \chi_2 (1+\lambda_2)} \left[\begin{Bmatrix} -(1+\lambda_2)\sin(1-\lambda_2)\vartheta \\ -(3-\lambda_2)\sin(1-\lambda_2)\vartheta \\ (1-\lambda_2)\cos(1-\lambda_2)\vartheta \end{Bmatrix} + \chi_2 (1+\lambda_2) \begin{Bmatrix} -\sin(1+\lambda_2)\vartheta \\ \sin(1+\lambda_2)\vartheta \\ \cos(1+\lambda_2)\vartheta \end{Bmatrix} \right]$$

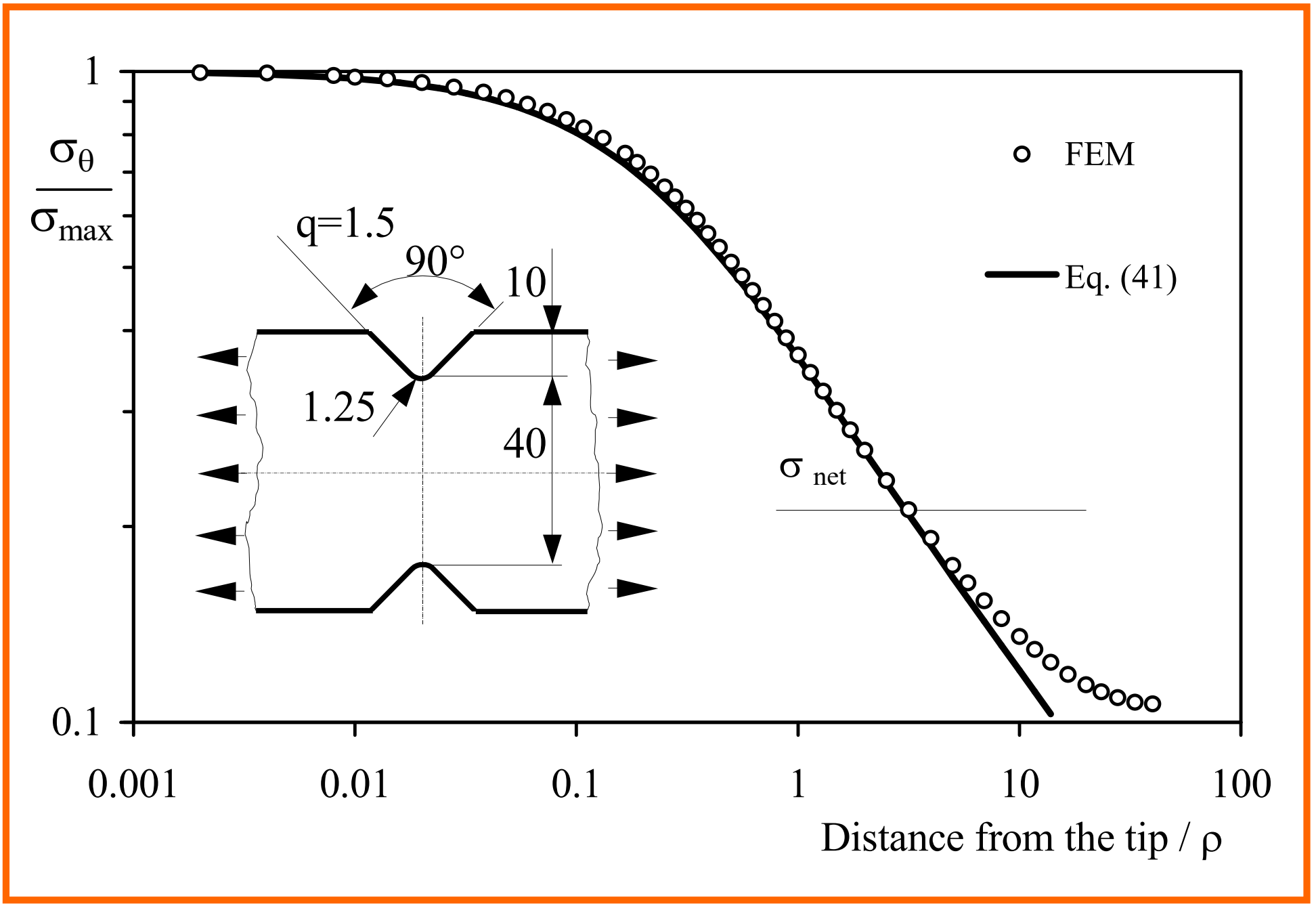

A comparison between numerical data and analytical predictions

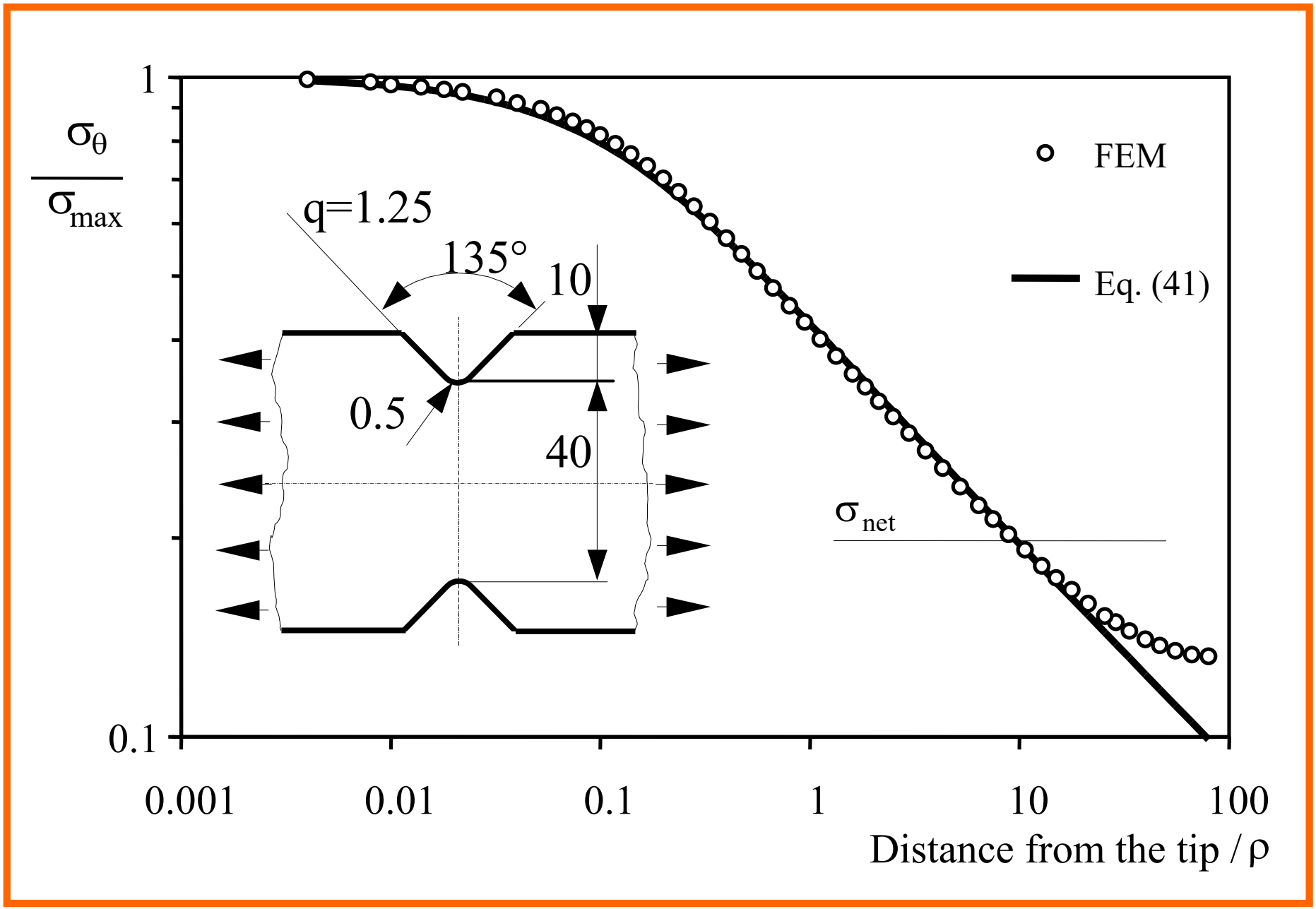

A comparison between numerical data and analytical predictions

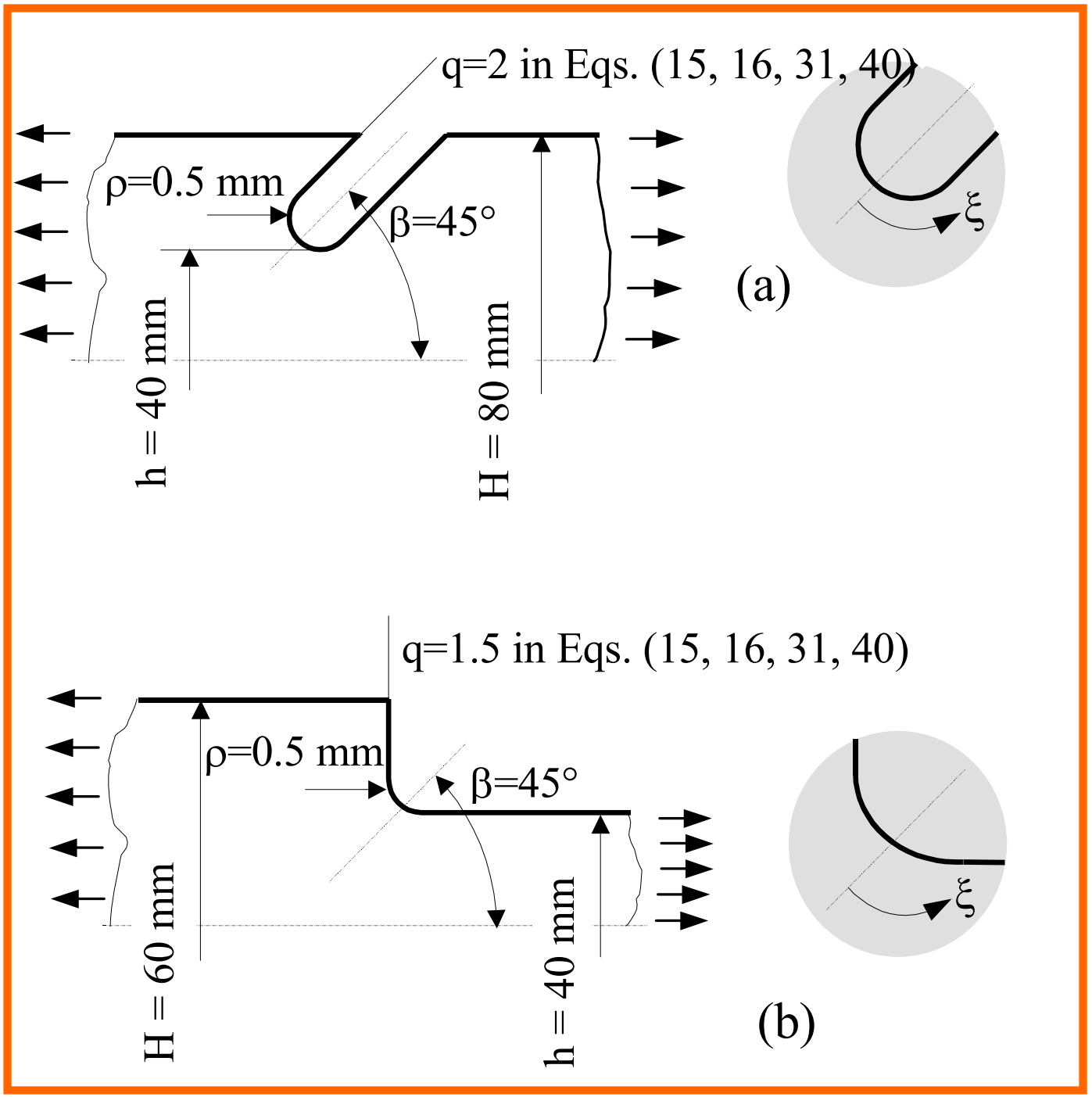

Shoulder fillet and slanted notches

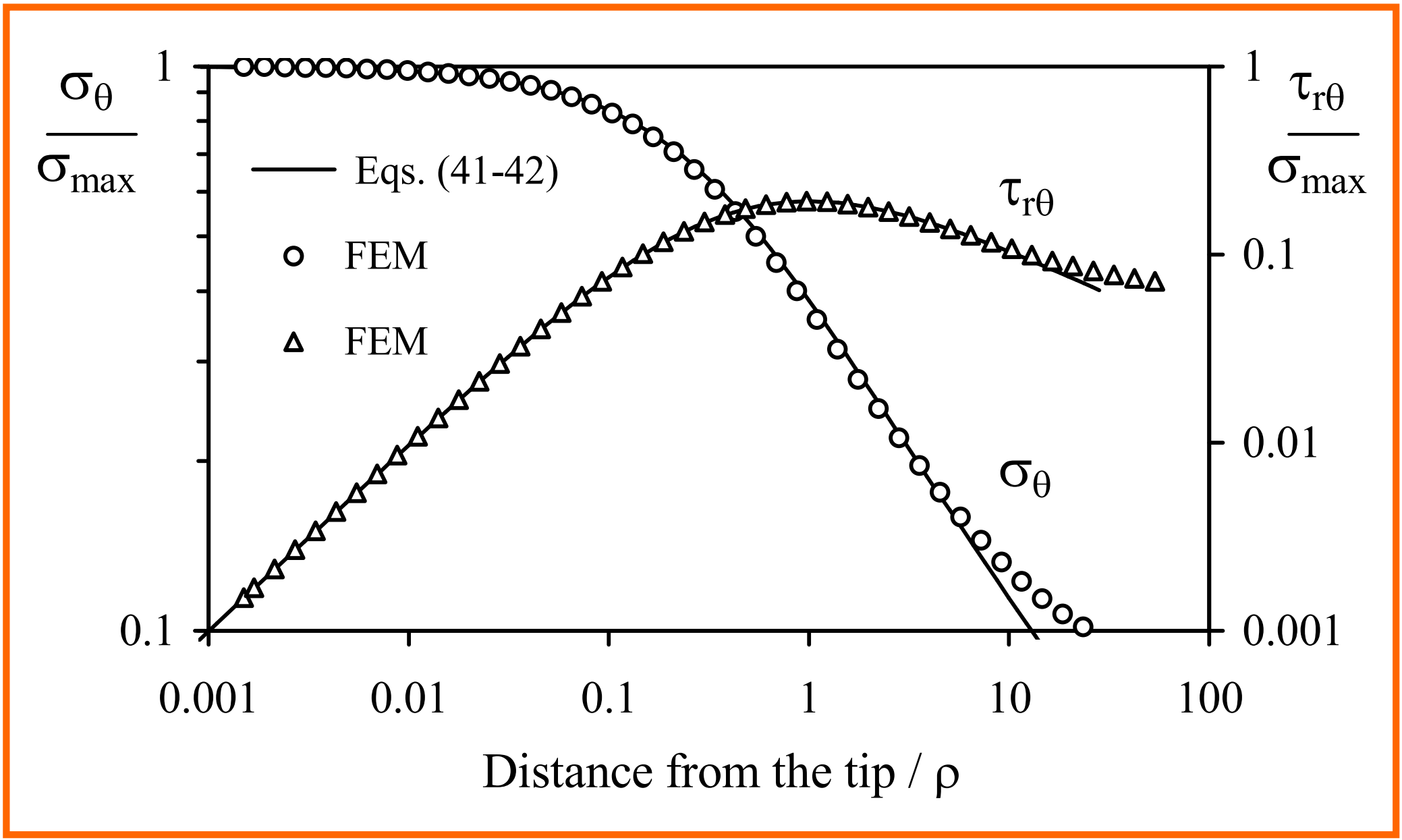

Stress fields along the bisector of the asymmetric notches

Section 3:

Strain Energy Density

STRAIN ENERGY DENSITY

- **Beltrami E** (1885) Sulle condizioni di resistenza dei corpi elastici, Rend. R. Ist. Lombardo di Scienze, Lettere e Arti, **18**, 704 (in Italian)
- **Gillemot L** (1965) Brittle fracture of welded materials. Commonwealth Welding Conference C.7.353-358.
- **Gillemot L** (1976) Criterion of crack initiation and spreading, Engng Fract Mech **8** 239-253.
- **Gillemot L, Czoboly E and Havas I** (1985) Fracture mechanics applications of absorbed specific fracture energy: Notch and unnotched specimens Theor Appl Fract Mech **4** 39-45
- **Sih GC** (1974) Strain-energy-density factor applied to mixed mode crack problems.Int J Fract **10** 305-321.
- **Sih GC** (1991) Mechanics of Fracture Initiation and Propagation: Surface and volume energy density applied as failure criterion, Kluwer Academic Publisher, Dordrecht
- **Sih GC, Tang XS** (2005) Scaling of volume energy density function reflecting damage by singularities at macro-, meso- and microscopic level. Theor Appl Fract Mech **43** 211–231.
- **Sih GC** (2007) *Multiscaling in molecular and continuum mechanics: interaction of time and size from macro to nano*. Dordrecht: Springer.
- **Sih G.C.** (2011) *Pseudo global energy released locally by crack extension involving multiscale reliability*

  Theoretical and Applied Fracture Mechanics 55 (2011) 52–59
- **Ellyin F., Kujawski D** (1989) Generalization of notch analysis and its extension to cyclic loading. Engineering Fracture Mechanics **32** 819-826
- **Ellyin F** (1997) *Fatigue Damage, Crack Growth and Life Prediction*, Chapman & Hall, London
- **Glinka G** (1985) Energy density approach to calculation of inelastic strain-stress near notches and cracks Engng Fract Mech **22** 485-508.
- **Gdoutos EE** (1990) *Fracture Mechanics Criteria and Applications*, Dodrecht: Kluwer Academic Publishers; 1990.
- **Park J, Nelson D** (2000) Evaluation of an energy-based approach and a critical plane approach for predicting constant amplitude multiaxial fatigue life. Int J Fatigue **22** 23-39.

ADVANTAGES OF A LOCAL-ENERGY APPROACH BASED ON NSIFs

- Permits consideration of the scale effect.
- Permits consideration of the contribution of different Modes.
- Permits consideration of the cycle nominal load ratio.
- Overcomes the complex problem tied to the different NSIF units of measure in the case of crack initiation at the toe ($2\alpha=135°$) or root ($2\alpha=0°$).
- Overcomes the problem of multiple crack initiation and their interaction.
- SED can be evaluated with coarse meshes
- It directly takes into account the T-stress
- It directly includes three-dimensional effects

SHARP NOTCHES AND THE SED APPROACH

$$W(r,\theta) = W_1(r,\theta) + W_2(r,\theta) + W_{12}(r,\theta)$$

$$W_1(r,\theta) = \frac{1}{2E} r^{2(\lambda_1 - 1)} \cdot \left(K_1^N\right)^2 \left[\tilde{\sigma}_{\theta\theta}^{(1)2} + \tilde{\sigma}_{rr}^{(1)2} + \tilde{\sigma}_{zz}^{(1)2} - 2\nu\left(\tilde{\sigma}_{\theta\theta}^{(1)}\tilde{\sigma}_{rr}^{(1)} + \tilde{\sigma}_{\theta\theta}^{(1)}\tilde{\sigma}_{zz}^{(1)} + \tilde{\sigma}_{rr}^{(1)}\tilde{\sigma}_{zz}^{(1)}\right) + 2(1+\nu)\tilde{\sigma}_{r\theta}^{(1)2} \right]$$

$$W_2(r,\theta) = \frac{1}{2E} r^{2(\lambda_2 - 1)} \cdot \left(K_2^N\right)^2 \left[\tilde{\sigma}_{\theta\theta}^{(2)2} + \tilde{\sigma}_{rr}^{(2)2} + \tilde{\sigma}_{zz}^{(2)2} - 2\nu\left(\tilde{\sigma}_{\theta\theta}^{(2)}\tilde{\sigma}_{rr}^{(2)} + \tilde{\sigma}_{\theta\theta}^{(2)}\tilde{\sigma}_{zz}^{(2)} + \tilde{\sigma}_{rr}^{(2)}\tilde{\sigma}_{zz}^{(2)}\right) + 2(1+\nu)\tilde{\sigma}_{r\theta}^{(2)2} \right]$$

Since the integration field is symmetric with respect to the notch bisector the contribution of W_{12}=0

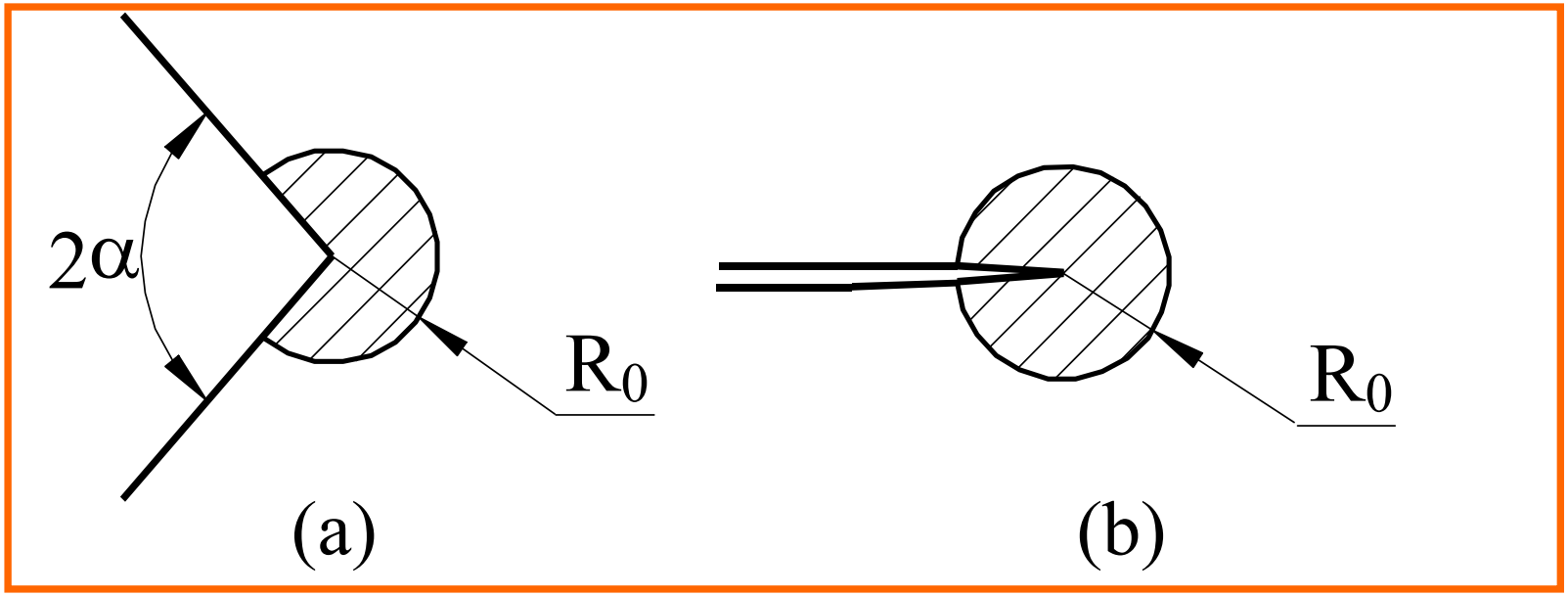

Lazzarin, P., Zambardi R. (2001). International Journal of Fracture

SHARP NOTCHES AND THE SED APPROACH

$$E(R) = \int_A W \cdot dA = \int_0^R \int_{-\gamma}^{+\gamma} \left[W_1(r,\theta) + W_2(r,\theta) \right] \cdot r dr d\theta$$

$$E(R) = E_1(R) + E_2(R)$$

$$= \frac{1}{E} \frac{I_1(\gamma)}{4\lambda_1} \cdot \left(K_1^N \right)^2 \cdot R^{2\lambda_1} + \frac{1}{E} \frac{I_2(\gamma)}{4\lambda_2} \cdot \left(K_2^N \right)^2 \cdot R^{2\lambda_2}$$

$$A(R) = \int_0^R \int_{-\gamma}^{+\gamma} r dr d\theta = R^2 \gamma$$

$$\overline{W} = \frac{E(R)}{A(R)} = \frac{1}{E} \cdot e_1 \cdot \left(K_1^N \right)^2 \cdot R^{2(\lambda_1 - 1)} + \frac{1}{E} \cdot e_2 \cdot \left(K_2^N \right)^2 \cdot R^{2(\lambda_2 - 1)}$$

MEAN VALUE OF THE STRAIN ENERGY DENSITY V-SHARP NOTCHES (mode I+ II)

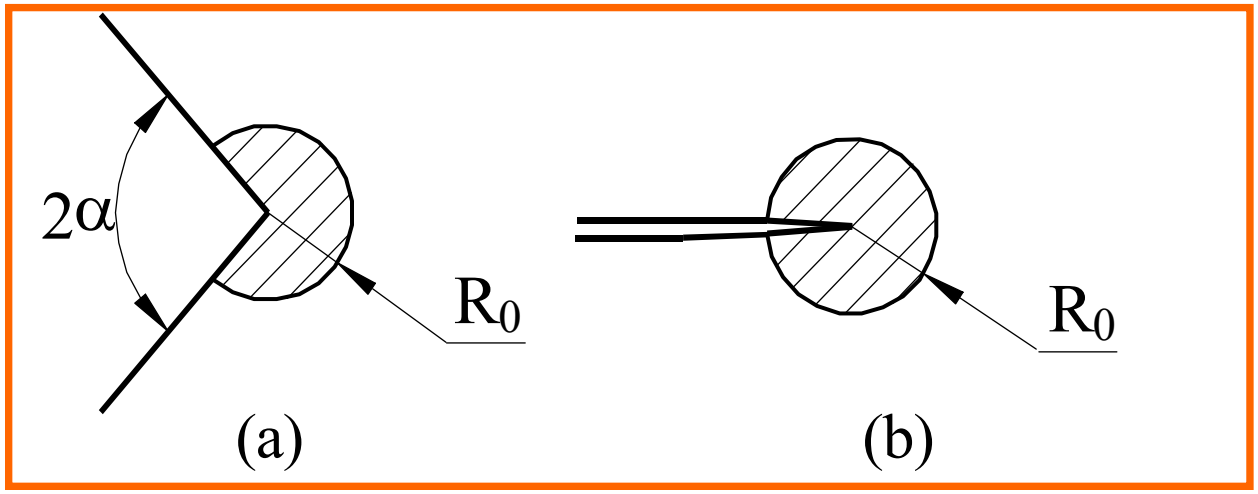

$$\Delta\overline{W} = \frac{e_1}{E}\left[\frac{\Delta K_1^N}{R_0^{1-\lambda_1}}\right]^2 + \frac{e_2}{E}\left[\frac{\Delta K_2^N}{R_0^{1-\lambda_2}}\right]^2$$

$$e_1 = -5.373\cdot 10^{-6}(2\alpha)^2 + 6.151\cdot 10^{-4}(2\alpha) + 0.1330$$

$$e_2 = 4.809\cdot 10^{-6}(2\alpha)^2 - 2.346\cdot 10^{-3}(2\alpha) + 0.3400$$

R_0: control volume radius

$e_{1,2}$: shape functions, which depend on the notch angle and Poisson's ratio

BLUNT NOTCHES AND THE SED APPROACH UNDER MODE I LOADING

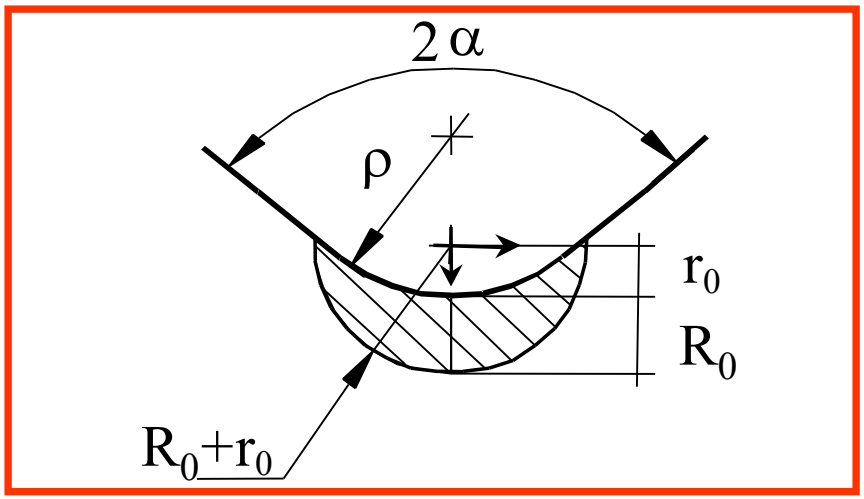

The criterion based on the local energy and valid for brittle or quasi-brittle material considers that the strain energy averaged over a control volume is critical for notched components

$$\overline{W}_1^{(e)} = H(2\alpha, R_0/\rho) \left(\frac{q-1}{q}\right)^{2(1-\lambda_1)} \left[\frac{\sqrt{2\pi}}{1+\widetilde{\omega}_1}\right]^2 \frac{\sigma^2{}_{\max}}{E}$$

$$\overline{W}_1^{(e)} = H(2\alpha, R_0/\rho) \frac{(K_{1\rho}^V)^2}{E} \frac{1}{\rho^{2(1-\lambda_1)}}$$

Lazzarin P., Berto F. 2005, International Journal of Fracture

SHAPE OF THE VOLUME

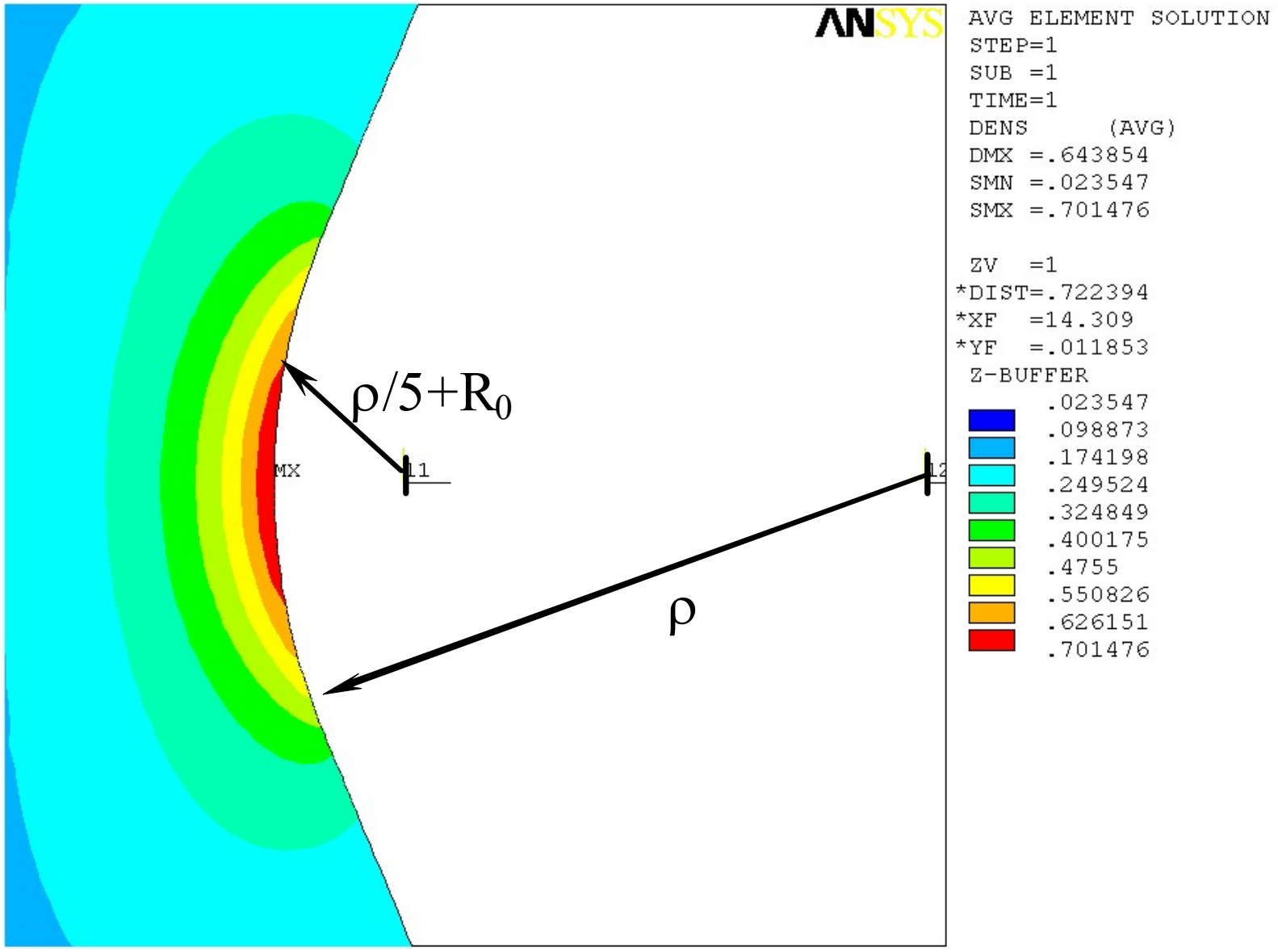

The SED contour lines are parallel to the volume perimeter

2α (rad)	R_0/ρ	H ν=0.3	ν=0.35	ν=0.4
0	0.01	0.5638	0.5432	0.5194
	0.05	0.5086	0.4884	0.4652
	0.1	0.4518	0.4322	0.4099
	1	0.1314	0.1217	0.1110
$\pi/3$	0.01	0.6678	0.6436	0.6157
	0.05	0.5998	0.5769	0.5506
	0.1	0.5302	0.5087	0.4842
	1	0.1435	0.1349	0.1252
$\pi/2$	0.01	0.6290	0.6063	0.5801
	0.05	0.5627	0.5415	0.5172
	0.1	0.4955	0.4759	0.4535
	1	0.1328	0.1256	0.1174
$3\pi/4$	0.01	0.4114	0.3966	0.3795
	0.05	0.3652	0.3516	0.3359
	0.1	0.3206	0.3082	0.2938
	1	0.1037	0.0988	0.0932

BLUNT NOTCHES AND THE SED APPROACH: MODE I AND U NOTCHES

R_0/ρ	H			R_0/ρ	H		
	ν=0.3	ν=0.35	ν=0.4		ν=0.3	ν=0.35	ν=0.4
0.001	0.5777	0.5570	0.5332	0.05	0.5086	0.4884	0.4652
0.002	0.5761	0.5555	0.5316	0.06	0.4962	0.4761	0.4531
0.003	0.5746	0.5539	0.5300	0.070	0.4844	0.4645	0.4416°
0.004	0.5730	0.5524	0.5285	0.08	0.4731	0.4533	0.4306
0.005	0.5715	0.5508	0.5270	0.1	0.4518	0.4322	0.4099
0.006	0.5699	0.5493	0.5255	0.117	0.4354	0.4161	0.3940°
0.008	0.5668	0.5462	0.5225	0.175	0.3855	0.3669	0.3459°
0.0088	0.5657	0.5451	0.5213°	0.2	0.3670	0.3488	0.3283
0.01	0.5638	0.5432	0.5194	0.3	0.3069	0.2902	0.2713
0.0175	0.5527	0.5321	0.5085°	0.4	0.2622	0.2468	0.2295
0.02	0.5490	0.5285	0.5049	0.5	0.2276	0.2135	0.1976
0.03	0.5349	0.5145	0.4910	0.6	0.2000	0.1870	0.1725
0.035	0.5281	0.5077	0.4843°	0.7	0.1775	0.1655	0.1522
0.04	0.5214	0.5011	0.4778	0.8	0.1591	0.1480	0.1357

The strain energy density averaged over the control volume can be evaluated as a function of the peak stress:

$$\overline{W}_1^{(e)} = H(R_0/\rho)\frac{\left(K_{\rho,I}^{V}\right)^2}{E\,\rho}$$

$$\overline{W}_1^{(e)} = H(R_0/\rho)\frac{\pi\,\sigma^2{}_{\max}}{4E}$$

MIXED MODE: BLUNT NOTCHES

It is possible in the presence of mode II to express the mode I stress intensity factor as a function of the stress at the notch tip, $\sigma_{\theta\theta}^*$. In this case the stress along the bisector line is no longer the maximum stress:

$$K_{\rho,I}^{V} = \sqrt{2\pi}\ \sigma_{\theta\theta}^{*}\ \frac{r_0^{1-\lambda_1}}{1+\tilde{\omega}_1} = \sqrt{2\pi}\ \frac{\sigma_{\theta\theta}^{*}}{1+\tilde{\omega}_1}\left(\frac{q-1}{q}\rho\right)^{1-\lambda_1}$$

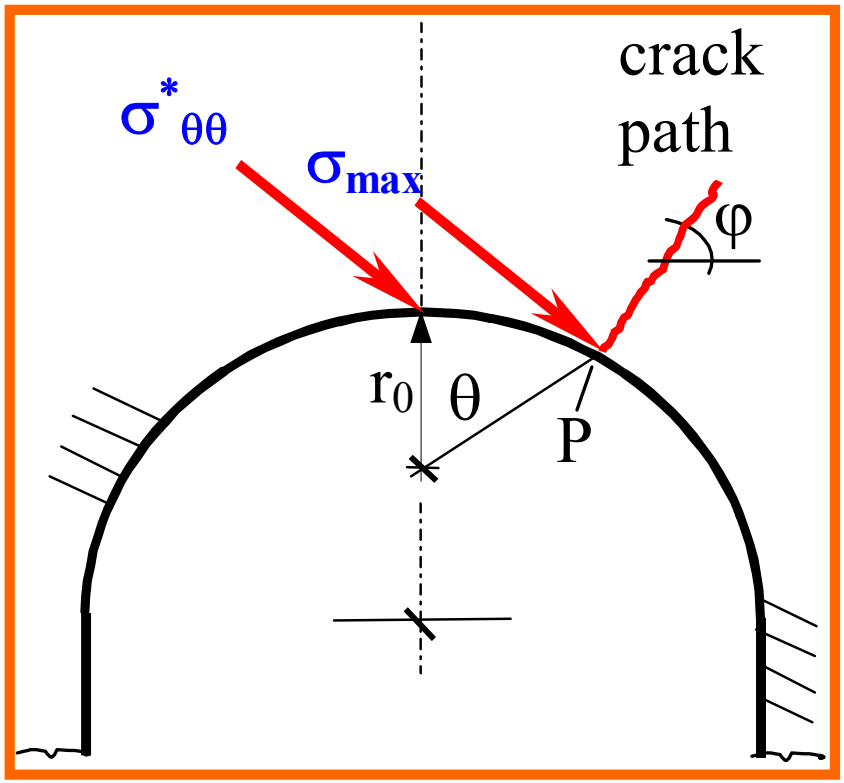

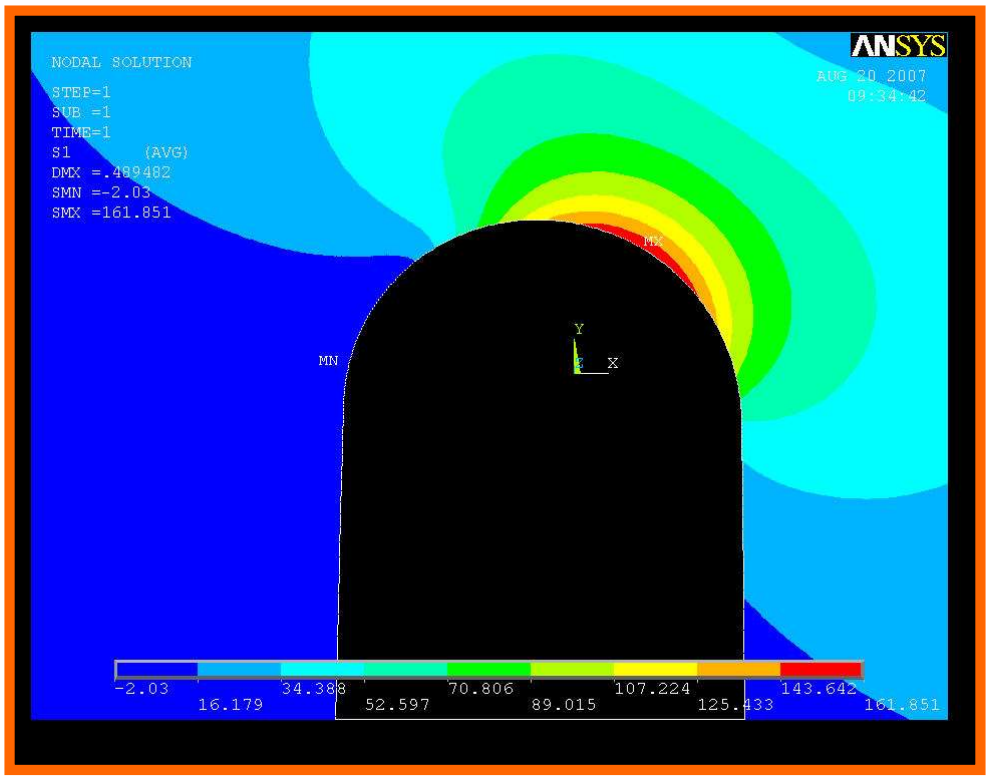

Gómez F.J., Elices M., Berto F., Lazzarin P. (2007) International Journal of Fracture

Berto F., Lazzarin P., Gómez F.J., Elices M., (2007) International Journal of Fracture

EXTENSION OF THE SED APPROACH TO MIXED MODE: AN EQUATION FOR U NOTCHES

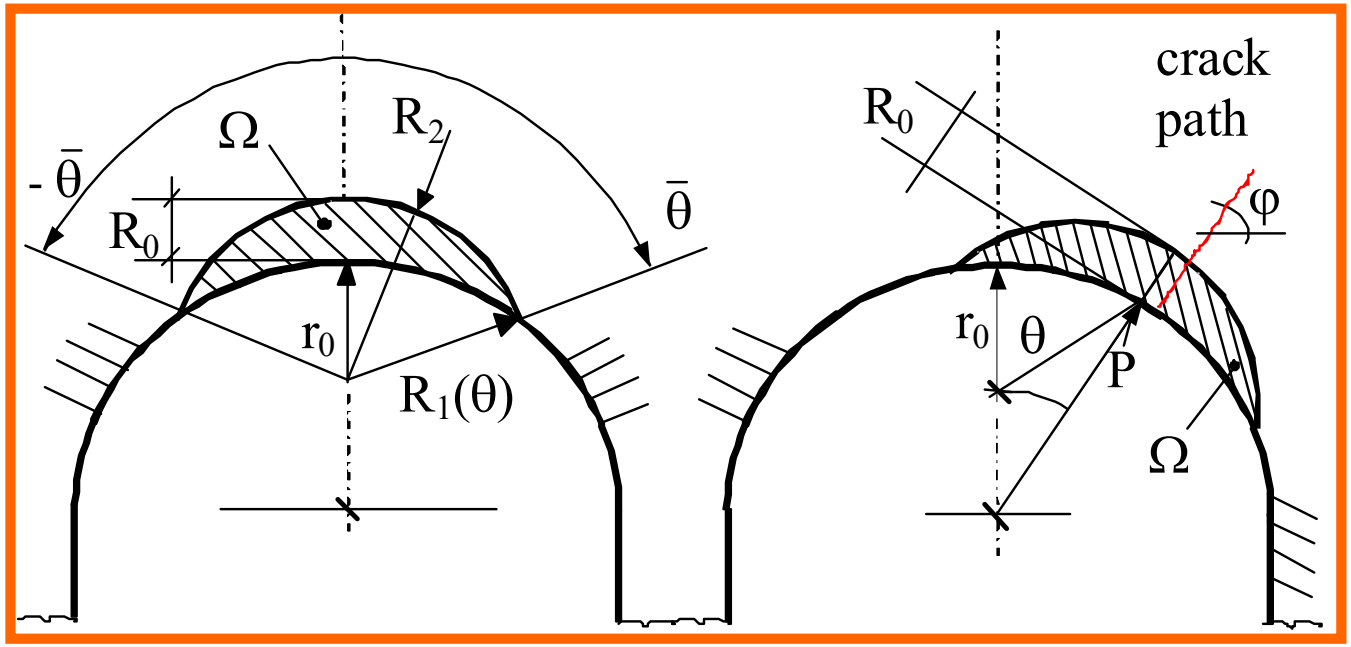

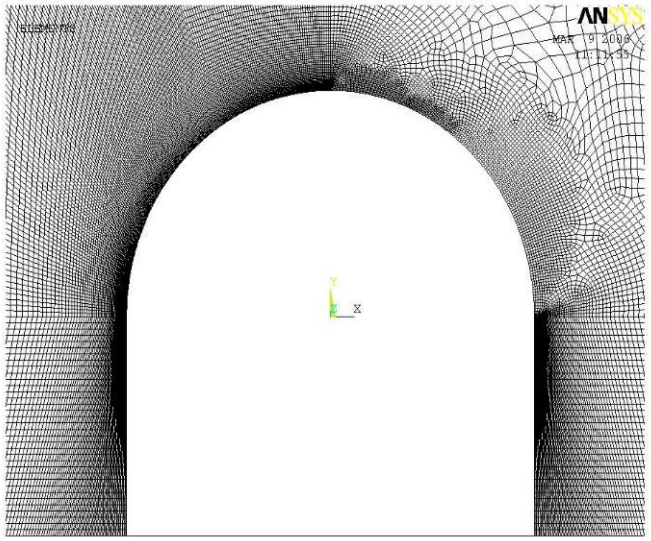

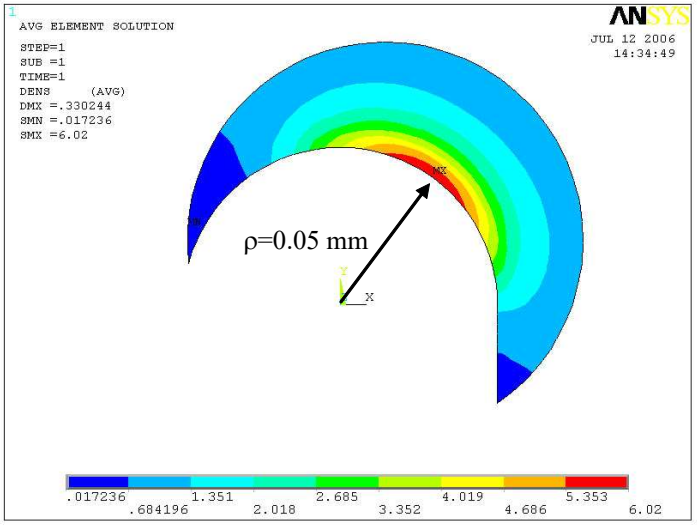

$$\overline{W}_1^{(e)} = H(R_0/\rho)\,\frac{\pi\,\sigma^2_{\max}}{4E}$$

CONTROL VOLUME DEFINITION UNDER STATIC LOADIG

$$\overline{W} = \frac{E(R)}{A(R)} = \frac{1}{E}\cdot e_1 \cdot \left(K_1^N\right)^2 \cdot R^{2(\lambda_1 - 1)} + \frac{1}{E}\cdot e_2 \cdot \left(K_2^N\right)^2 \cdot R^{2(\lambda_2 - 1)}$$

The critical energy

$$W_C = \sigma_t^2 / 2E$$ **Unnotched material**

$$\overline{W}_1^{(e)} = \frac{E_1^{(e)}}{A} = \frac{I_1}{4\,E\,\lambda_1\,\pi}\left(\frac{K_{IC}}{R_0^{0.5}}\right)^2$$ **cracked material**

$$\overline{W} = W_C$$

$$R_0 = \frac{(1+\nu)(5-8\nu)}{4\pi}\left(\frac{K_{IC}}{\sigma_t}\right)^2$$

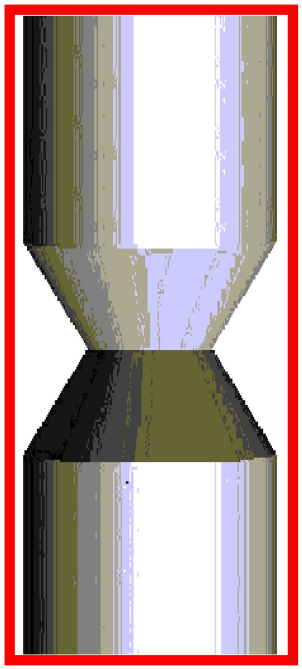

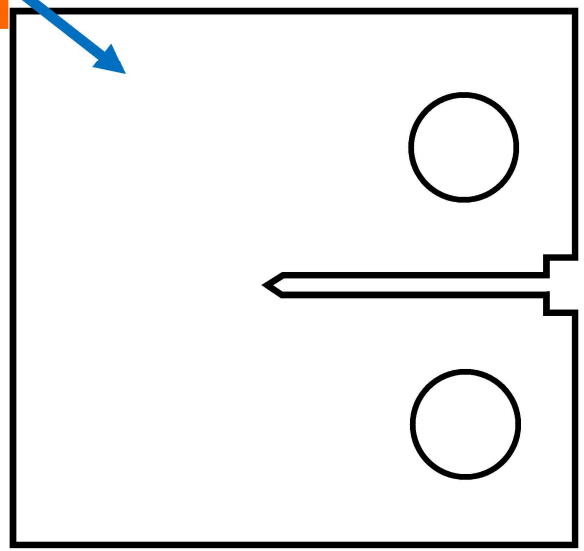

THE INFLUENCE OF POISSON'S RATIO

$$R_0 = \frac{(1+\nu)(5-8\nu)}{4\pi}\left(\frac{K_{IC}}{\sigma_t}\right)^2$$

2α (gradi)	γ/π rad	λ_1	I_1 ν=0.3	I_1 ν=0.35	I_1 ν=0.4
0	1	0.5000	0.8450	0.7425	0.6300
30	11/12	0.5014	0.8366	0.7382	0.6301
60	5/6	0.5122	0.8066	0.7194	0.6235
90	3/4	0.5445	0.7504	0.6801	0.6024
120	2/3	0.6157	0.6687	0.6184	0.5624
135	5/8	0.6736	0.6201	0.5796	0.5344
140	11/18	0.6972	0.6030	0.5657	0.5239
150	7/12	0.7520	0.5678	0.5366	0.5013

NOTCHED SAMPLES UNDER STATIC LOADING

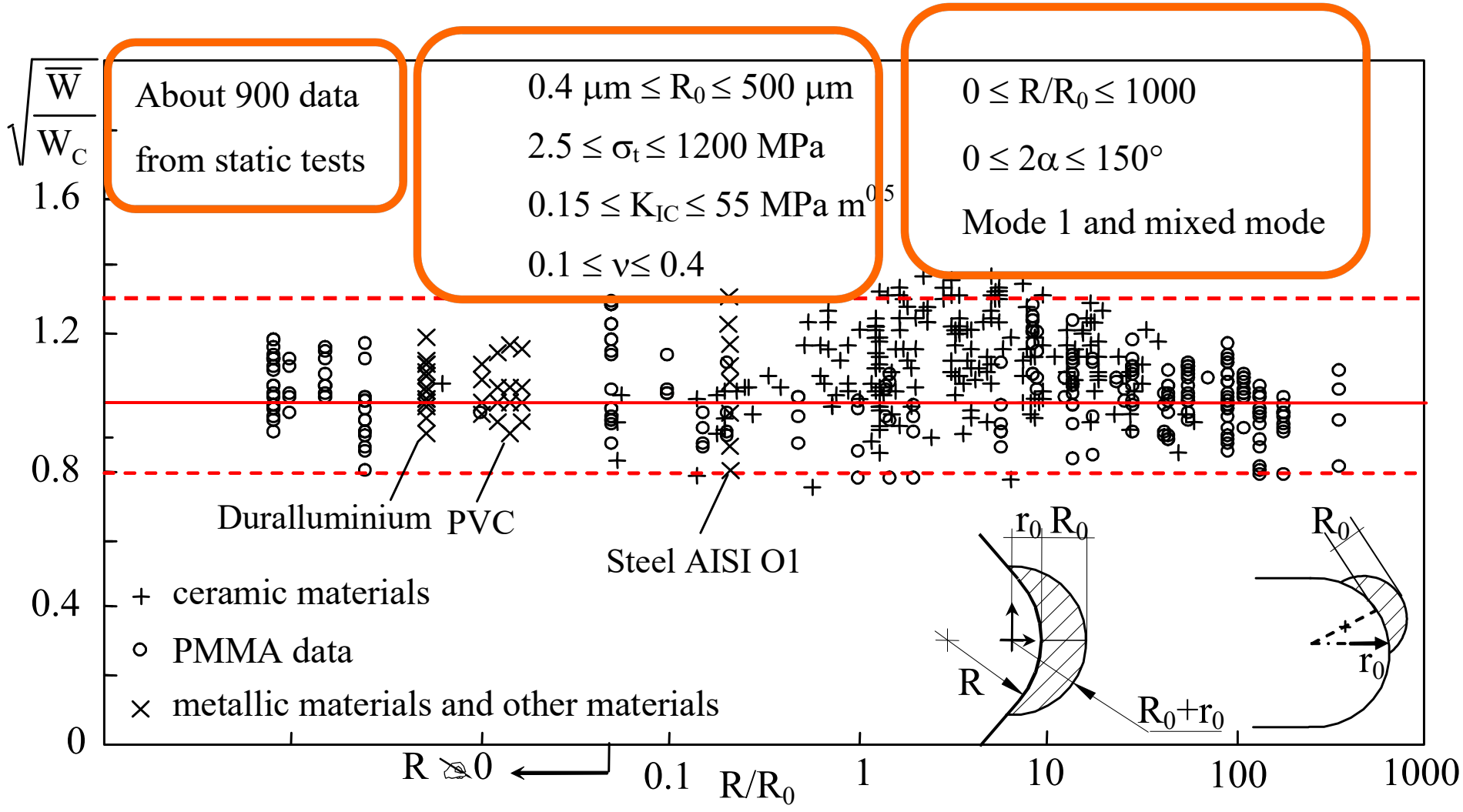

Synthesis of data taken from the literature. Different materials are summarised, among the others AISI O1 and duralluminium

NOTCHED SAMPLES UNDER STATIC LOADING

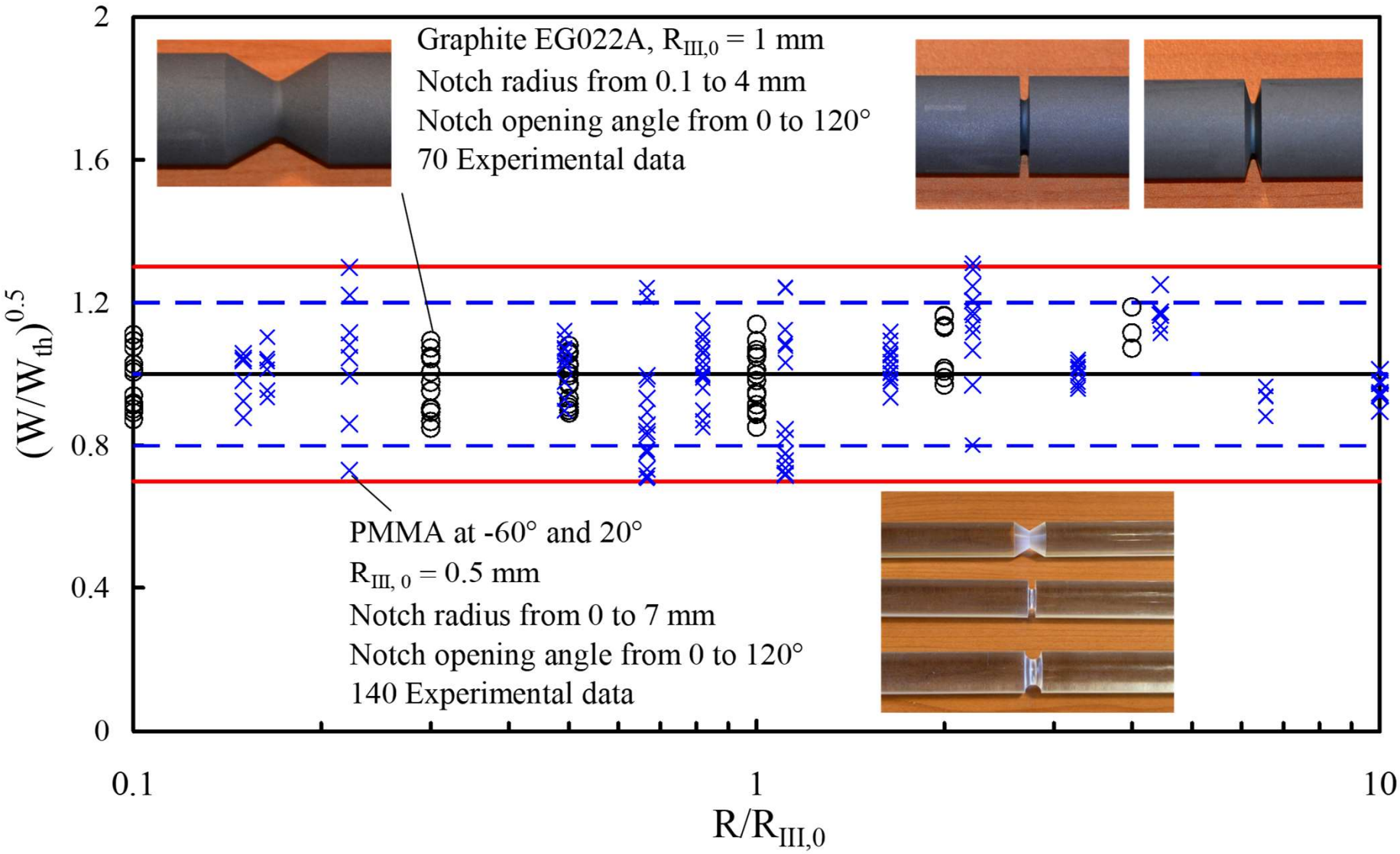

Synthesis of 210 new data from notched specimens under torsion

STRAIN ENERGY DENSITY AT THE NOTCH TIP FATIGUE

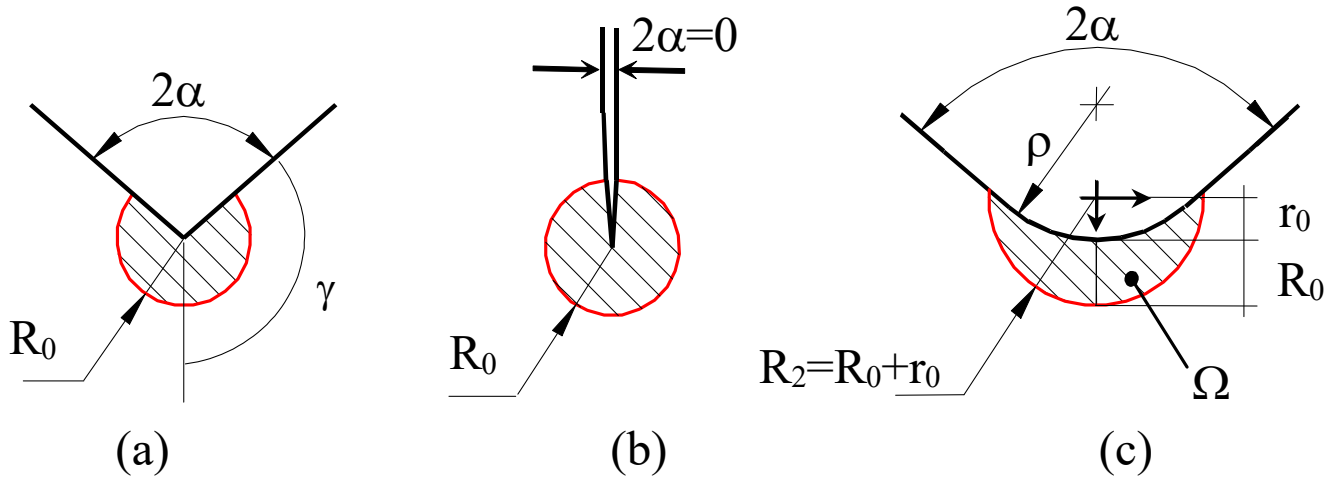

$$R_0 = \left(\sqrt{2\, e_1} \times \frac{\Delta K_{1A}}{\Delta \sigma_{1A}} \right)^{\frac{1}{1-\lambda_1}}$$

Plain (unnotched specimens): Beltrami's expressions

$$\Delta \overline{W} = c_w \frac{\Delta \sigma_{nom}^2}{2E}$$

V-notched specimens: SED in a control volume

$$\Delta \overline{W} = \frac{1}{E} \left[e_1 \times \frac{\Delta K_1^{\,2}}{R_1^{2(1-\lambda_1)}} \right]$$

STRAIN ENERGY DENSITY AT THE NOTCH TIP FATIGUE

$$R_0 = \frac{(1+\nu)(5-8\nu)}{4\pi}\left(\frac{\Delta K_{th}}{\Delta\sigma_0}\right)^2$$

$$R_0 = \frac{(5-3\nu)}{4\pi}\left(\frac{\Delta K_{th}}{\Delta\sigma_0}\right)^2$$

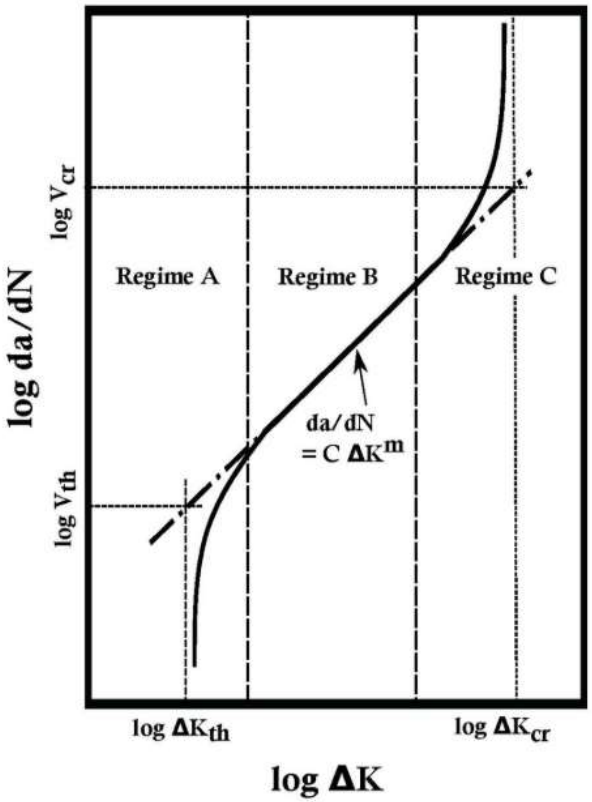

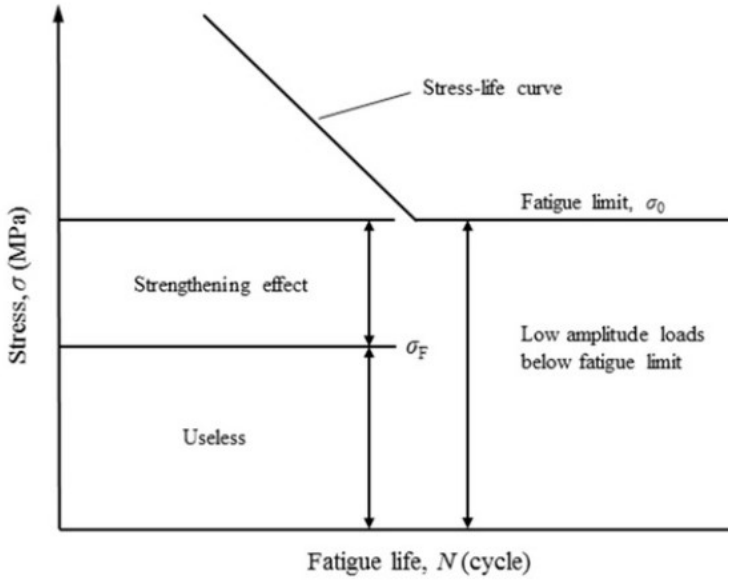

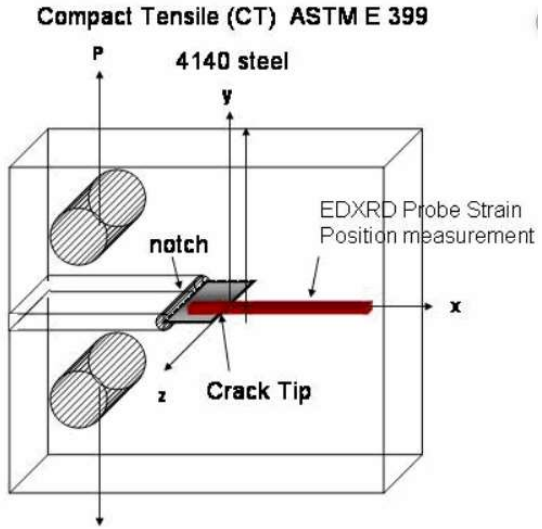

NEW BOOK (2013)

Advanced Methods of Fatigue Assessment (Hardcover)

by Dieter Radaj, Michael Vormwald